Robust Energy Management Systems for Isolated Microgrids Under Uncertainty

by

Jose Daniel Lara

A thesis
presented to the University of Waterloo
in fulfillment of the
thesis requirement for the degree of
Master of Applied Science
in
Electrical and Computer Engineering

Waterloo, Ontario, Canada, 2014

Author's Declaration

I hereby declare that I am the sole author of this thesis. This is a true copy of the thesis, including any required final revisions, as accepted by my examiners.

I understand that my thesis may be made electronically available to the public.

Abstract

Microgrids are small and local clusters of generation and load operated in a coordinated manner. These systems are being enhanced with Smart Grid technologies in order to better integrate more Renewable Energy (RE) sources and thus reduce dependency on fossil fuels. This thesis focuses on isolated microgrids, which are characterized by low inertia Distributed Energy Resources (DERs), limited availability of resources, and high correlation of RE sources of the same type, where, variability and uncertainty become significant issues.

In order to enhance the operation of microgrids, a mathematical formulation and architecture of a robust Energy Management System (EMS) for isolated microgrids is proposed in this thesis. The developed algorithm is able to manage the uncertainty of RE sources and hedge the system against uncertainty in RE forecast. The proposed strategy addresses uncertainty using Receding Horizon Control (RHC), combined with a two-stage decision-making process with recourse. The first-stage decisions are the Unit Commitment (UC) variables, determined using a Robust Optimization (RO)-based formulation, and solved using a primal cutting-planes algorithm. Also a method based on the historical performance of the forecasting system is presented for the selection of the uncertainty policy, which represents the decision maker's risk preference. The second stage refines the dispatch commands using an Optimal Power Flow (OPF) calculation with a rather detailed model of the microgrid considering relevant system dynamic constraints. The proposed architecture is based on different look-ahead windows to better account for uncertainty, and obtain a feasible dispatch solution within reasonable computational times.

The EMS is tested on a modified CIGRE test system for different configurations, comparing the results with respect to deterministic and Stochastic Optimization (SO)-based formulations. The results reflect the effectiveness of the proposed EMS to hedge the system against uncertainties, improving the system's level of reserves, and dispatching Energy Storage Systems (ESSs) appropriately, so that the operational costs are reduced. The improvements are achieved without requiring probabilistic information from the forecasting system, and based on an appropriate definition of the uncertainty set. The results show that the developed architecture and algorithm are compatible with real-time applications.

Dedication

This thesis is dedicated to Leon K. Kirchmayer, for pioneering the mathematical bases to develop this thesis.

Table of Contents

List of Tables

List of Figures

List of Acronyms

ACO	Ant Colony Optimization
CCO	Chance Constrained Optimization
CDF	Cumulative Probability Distribution Function
CHP	Combined Heat and Power
DER	Distributed Energy Resource
DG	Distributed Generator
DSM	Demand Side Management
EMS	Energy Management System
ESS	Energy Storage System
GHG	Green-House Gas
LP	Linear Programming
MILP	Mixed-Integer Linear Programming
MINLP	Mixed-Integer Nonlinear Programming
MPEC	Mathematical Program with Equilibrium Constraints
MPC	Model Predictive Control
MT	Micro-Turbine
NEA	Niching Evolutionary Algorithm

NLP Nonlinear Programming

OPF Optimal Power Flow

PEC Power Electronics Converter

PDF Probability Density Function

PSO Particle Swarm Optimization

PV Photovoltaic

RE Renewable Energy

RHC Receding Horizon Control

RHOPF Receding Horizon Optimal Power Flow

RO Robust Optimization

RUC Robust Unit Commitment

SO Stochastic Optimization

SoC State-of-Charge

SUC Stochastic Unit Commitment

UC Unit Commitment

WT Wind Turbine

Nomenclature

Functions

ϵ	Cutting-planes algorithm tolerance
$\mathcal{J}$	RHC function to determine z_{t+1}
$\mathcal{J}_1$	First stage vector function
$\mathcal{J}_2$	Recourse vector function.
H	System constraints vector function on the RHC model
H_1	First stage constraints vector function on recourse model
H_2	Second stage constraints vector function on recourse model
H_3	Coupling constraints vector function on recourse model
J	Cost function of the RHC model for each time step
J_1	First stage cost function on recourse model for each time-step
J_2	Second stage cost function on recourse model for each time-step

Indices

ω	Non-dispatchable generation units.
g	Dispatchable generation units.
k	Iteration count.

kt	Time step for the three-phase OPF.
l	Load.
s	ESS units
t	Time step for the RUC.
i	Index of scenarios for the two-stage SO formulation

Sets

$\mathcal{F}_{kt}$	Realization of the forecast.
$\mathcal{H}$	Feasibility set of the RO-based recourse model.
$\mathcal{U}$	Uncertainty set.

Parameters

Γ	Budget of uncertainty.
${\Delta P_{\omega,t}}^{max}$	Max forecast mismatch, unit ω, at time t, [p.u.]
δ_t^{max}	Uncertain variable maximum limit, at time t
η_s^{in}	ESS in efficiency for unit s, [%].
η_s^{out}	ESS out efficiency for unit s, [%].
$\mathcal{F}^*$	Input forecast available at time t
$\mathcal{F}^i$	Forecast scenario at time t with probability i
π_i	Probability of scenario i
ρ	Model parameters in the RHC model.
$\widetilde{\mathcal{F}}^*$	Input forecast available at time t, subject to uncertainty.
$\widetilde{\rho}$	Model parameters subject to uncertainty.
C_g^P	Power cost for g, [\$/kW]

C_g^u	Start-up cost for generator g, [$].
C_g^v	Shut-down cost for generator g, [$].
C_g^w	Commitment cost for generator g, [$].
C_c	Power curtailment cost, [$/kW].
C_{sh}	Load shed cost, [$/kW].
E_s	Parameter matrix of master problem dual variables, unit s.
M	Constant for the disjunctive constraints.
MD_g	Min-down time for unit g, [h]
MU_g	Min-up time for unit g, [h]
P_g^{max}	Max power limit for unit g, [Kw]
P_g^{min}	Min power limit for unit g, [Kw]
$P_{\omega,t}^*$	Forecast for unit ω, at time time t, [kW]
$P_{\omega,t}^i$	Power output, unit ω, at time t of scenario with probability i, [kW]
$P_{l,t}$	Power for load l, at time t, [kW]
RD_g	Ramp-down limit for unit g, [Kw/h]
RU_g	Ramp-up limit for unit g, [Kw/h]
SOC_s^{max}	Max SoC limit for storage s, [kWh].
SOC_s^{min}	Min SoC limit for storage s, [kWh].
$SOC_{s,kt_{15}}$	Frontier condition at the end obtained from the RUC, [kWh].
SOC_{s,kt_1}	Initial SoC in the three-phase OPF look-ahead window, [kWh].
$SOC_{s,t+1}^{MP}$	Target frontier SoC level for unit s in the OPF, [kWh].

Variables

$\alpha 1_{\omega,t}$	Dual variable of (3.3k), at time t.
$\alpha 2_{\omega,t}$	Dual variable of (3.3l), at time t.
$\alpha 3_{\omega,t}$	Dual variable of (3.3m), at time t.
$\alpha 4_{\omega}$	Dual variable of (3.3n)
$\beta 1_{g,t}$	Dual variable of (3.3d), at time t.
$\beta 2_{g,t}$	Dual variable of (3.3e), at time t.
$\Delta P_{\omega,t}$	Forecast mismatch, for source ω, at time t, [p.u.]
$\Delta {P_{\omega,t}}^{+}$	Upward power mismatch variable, for source ω, at time t [p.u.]
$\Delta {P_{\omega,t}}^{-}$	Downward power mismatch variable, for source ω, at time t, [p.u.]
δ	Vector of uncertain variables in the RO recourse model
λ_t	Dual variable of (3.3g), at time t.
$\mu 1_{g,t}, \mu 2_{g,t}$	Dual variables of (3.3c), at time t.
θ	Auxiliary variable for the adversarial problem.
$\varepsilon 1_{s,t}$	Dual variable (3.3f), at time t.
$\varepsilon 2_{s,t}$,$\varepsilon 3_{g,t}$	Dual variables (3.3i), at time t.
$\varepsilon 4_{s,t}$	Dual variable (3.3j), at time t.
$\varepsilon 5_{s,t}$	Dual variable (3.3g), at time t.
$\varepsilon 6_{s,t}$	Dual variable (3.3h), at time t.
$b1_{\omega,t}$-$b4_{\omega,t}$, $b5_{\omega}$	Disjunctive constraints binary variables.
ESS_s^{shed}	SOC shedding, storage unit s, [kWh].
LB^k	Lower boundary at iteration k
$P_{c,t}$	Power curtailed, at time t, [kW].
$P_{g,t}$	Power output for unit g, at time t, [kW].

$P_{s,t}$	Power output for unit s, at time t, [kW].
$P_{s,t}^{in}$	ESS input power, at time t, [kW].
$P_{s,t}^{out}$	ESS output power, at time t, [kW].
$P_{sh,t}$	Load shed, at time t, [kW].
$SOC_{s,t}$	SoC of storage unit s, at time t, [kWh].
SOC_s^{fix}	Variable to fix $SOC_{s,t+1}$ to first stage.
t_u	Time step the unit starts or shuts down.
$u_{g,t}$	Start-up decision variable for generator g, time t.
UB^k	Upper boundary at iteration k
$v_{g,t}$	Shut-down decision variable for generator g, time t.
$w_{g,t}$	Commitment status variable for generator g, time t.
y	Vector of variables of the system states $\{y_t, \ldots, y_{t+n}\}$
y_t	System variables at time t on the RHC and recourse model
z_1	Vector of variables of the first stage $\{z_{1t}, \ldots, z_{1t+n}\}$
z_2	Vector of variables of the second stage $\{z_{2t}, \ldots, z_{2t+n}\}$
z_{1t}	First variables on the recourse model, at time t
z_{2t}	Second variables on the recourse model, at time t
z_t	Control variable at time t on the RHC model

Chapter 1

Introduction

1.1 Motivation

Electric power systems have long been operated under the paradigm of bulk, dispatchable power generation transported through high-voltage long transmission lines, and delivered to end users through low- and medium-voltage distribution networks. With the introduction of novel automation and control techniques, communication mechanisms, and compact Distributed Energy Resources (DERs), the concept of "Smart Grid" was developed [1]. The means to realize this concept have been the focus of research and development in power systems for several years now.

Despite the advances in Smart Grid technologies, their rate of adoption has been slow. Nevertheless, policies towards reducing Green-House Gas (GHG) emissions in the electric power sector [2], addressing energy poverty [3], and increasing the reliability of the electric grid to weather climate related disasters [4] have particularly fostered the interest for the adoption of Smart Grid technologies in microgrids. Among the main drivers for a faster uptake and the incentive to develop market-ready technologies in microgrids are the growing interest in increasing deployment of renewable generation on military installations [5], remote communities [6, 7], and critical facilities such as university campuses, hospitals and mines [8].

Microgrids are systems for electric power generation, distribution, and consumption that build on a locally integrated grid, in some cases abating the need to extend transmission systems or bulk power generation (e.g., isolated microgrids). When combined with Smart Grid technologies, these grids are able to integrate DERs more effectively,

creating an enhanced distribution network, improving the service delivered to costumers, and improving the efficiency of the energy allocation when combined with Demand Side Management (DSM) schemes and Energy Storage Systems (ESSs). Microgrids provide a framework to address modern challenges of the electric power sector and are posed to become mainstream in terms of electric power generation and distribution.

Exploiting all the opportunities that microgrids present is a main focus of current research in power systems [9]. In spite of the advantages microgrids possess, there are major challenges when it comes to the integration of Renewable Energy (RE) sources, which is one of the main motivations to pursue their development. Regardless of the type of microgrid, i.e., isolated or grid-connected, dealing with the technical challenges posed by these grids is imperative in order to maximize their benefits. The challenges are [10]:

- Reliable and economic operation of microgrids with high penetration of intermittent RE. Particularly in isolated microgrids, the negative effect of this intermittence is more significant due to the high levels of correlation between the DERs powered by the same sources and the limited generation reserves.
- Schedule and dispatch of controllable demand and generation with uncertainty considerations. Since an adequate operation of the microgrid requires a certain level of coordination between the assets, this is more challenging if the information from forecasts and their inherent uncertainties are not taken into account.
- Proper reserve management in a low-inertia, resource-constrained environment. Unlike bulk power systems, microgrids operating in stand-alone mode do not have large amounts of conventional generation that can provide spinning reserve to perform the required regulation tasks.
- Optimal management of ESSs to cope with uncertainty, so that storage technologies enable higher penetration of integration of RE-sources. When dispatching ESSs, the State-of-Charge (SoC) levels must be accounted for to maintain a tradeoff between providing balancing capacity to the system and the cost minimization.

The main interest of this research is the management of uncertainty with a focus on isolated microgrid dispatch or Energy Management System (EMS). This is a challenging problem from the point of view of microgrid operation. Given the inherent resource limitation in isolated microgrids, failing to hedge the system against uncertainty can result in loss of load, power curtailment, or system collapse. Thus, this research focuses on the application of Robust Optimization (RO)-based techniques to produce uncertainty

immunized dispatch in real-time, combining recourse actions and Receding Horizon Control (RHC). These techniques are tested on a CIGRE test system under different configurations, comparing the results with respect to a deterministic and stochastic formulations , and demonstrating the ways and benefits of considering uncertainty in EMS applications.

1.2 Literature Review

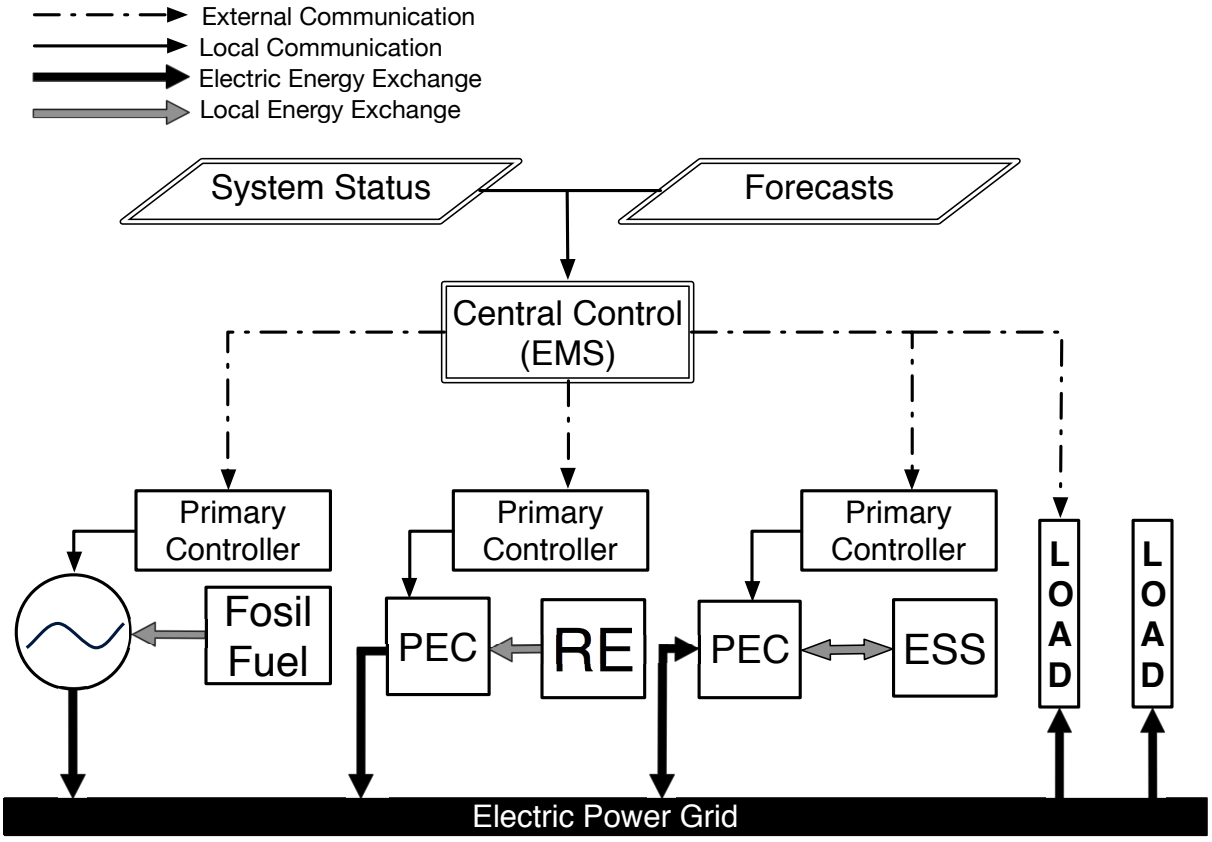

Figure 1.1: Centralized control structure of a microgrid.

The idea of isolated networks that combine diesel fleets and some level of RE-sources has been around for a while. The first coordinated efforts to develop isolated wind-diesel technology were in 1985 and since then, their control has been a challenge [11]. However, there seems to be a consensus in the research community, from the early wind-diesel

systems (e.g., [11]) to the latest authoritative reports on microgrid control, that centralized architectures are the best options to address the control challenges when it comes to dispatch control or EMS in isolated microgrids [10].

A centralized EMS determines the optimal operation point of every DER and uses the results as set points for each device, as shown un Figure 1.1 where both synchronous generator and Power Electronics Converter (PEC) interfaced units are shown. Increased computational capabilities in modern controller hardware allows the EMS to perform more sophisticated calculations, particularly optimization algorithms, and incorporate system information, forecast data, and real-time measurements in its decision making process. The dispatch computation in the EMS is a combination of the scheduling of the units, obtained from the Unit Commitment (UC), and their optimal dispatch. The combination of integer variables and non-linear models makes the mathematical formulation of the EMS a Mixed-Integer Nonlinear Programming (MINLP) problem, which result in computationally challenging formulations due the lack of appropriate algorithms for real-time applications [12].

In order to deal with the complexities in the mathematical modeling, a common approach is to use meta-heuristic methods to solve the optimization problem. For example, in [13], the challenges associated with making on-line calculations to coordinate the generation units are discussed, and a Particle Swarm Optimization (PSO) and Ant Colony Optimization (ACO) based solution technique for a simplified dispatch problems is proposed. A more detailed mathematical model that includes commitment and dispatch calculation is presented in [14]; using a microgrid that includes detailed models of storage units, the authors propose a Niching Evolutionary Algorithm (NEA) to deal with the complexities of the formulation. However, the aforementioned approaches present complications, since they do not always guarantee appropriate convergence and there is little experience using them for real-time applications.

Reduction and simplification of the problem is another way to cope with the intricacies of microgrid scheduling and dispatch. This can mean converting the problem to a Mixed-Integer Linear Programming (MILP) problem by using dc approximation of the power flow equations and avoiding reactive power representation in the problem, as proposed in [15], where the authors recognize the importance of reactive power and the complexity of considering it in the calculations. In [16], a dynamic programming approach is proposed to solve the allocation of resources in a simplified representation of the system, not including UC modeling; however, the authors highlight the relevance of optimizing over a look-ahead window, to determine the least-cost dispatch.

An optimization algorithm aimed at reducing the fuel consumption considering system

constraints is presented in [17], where the authors optimize the power sharing characteristic of the thermal units in real-time, and point out that implementing the solution of the optimization problem requires having a communication infrastructure between the generators and the controller to achieve real-time operation. The paper discusses the simplifications possible in order to make the mathematical problem tractable and useful for real-time applications.

The technique that seems to deliver the best results is decomposing the problem into an integer linear problem and a non-linear problem, emulating the approach used in electricity markets. Thus, first the UC is determined using a multi-period linearized optimization model, and then the Nonlinear Programming (NLP) Optimal Power Flow (OPF) is implemented based on the committed units for that particular time-step obtained from the UC solution. This approach has been proposed for microgrid control in [18], where there is a two-layer control with a multi-step optimization in each layer, and the authors exploit the benefits of RHC (or Model Predictive Control (MPC)) in order to properly coordinate the allocation of ESS to smooth fluctuations. However, despite the benefits of the proposed decomposition approach, the system modeling is incomplete and there is no coordination between the layers.

The deficiencies in the aforementioned proposal are addressed in [19], where an improved two-layer scheme is introduced, using a multi-step scheduling-layer to optimize an MILP equivalent of the system, and later refine the dispatch in real-time with a single-step OPF. A feedback loop is included to coordinate the layers in cases where the dispatch is infeasible, but without considering the effect of three-phase unbalance. A penalty is introduced in the OPF layer to reduce deviations of the ESS from the scheduled value. A more sophisticated version is introduced in [12], where the authors include the effect of unbalance by using a RHC three-phase OPF for the second stage calculation, among other improvements, thus addressing previous shortcomings regarding system modeling.

The aforementioned research use an arbitrary proportional rule in order to provide the system with adequate reserves, and do not consider the uncertainties associated with the forecasts used in the multi-stage dispatches. Hence, papers that discuss the hedging in power systems and microgrids against RE uncertainty are discussed next.

1.2.1 Uncertainty in Power System Dispatch

The issue of uncertainty in the context of bulk power systems operation has been widely studied. Classically, the spinning reserves are determined by proportional rules based on deterministic criteria [20]. However, with the inclusion of RE sources in the system, more

uncertainty is present in power systems due to the stochastic nature of these resources, and hence increasing the complexity of system operations. Researchers applied various stochastic approaches in order to develop more sophisticated techniques to optimally allocate reserves. Thus, Chance Constrained Optimization (CCO), RO and Stochastic Optimization (SO) are the common techniques prorposed to manage uncertainty, with several mathematical formulations being available in the literature.

Chance Constrained Techniques

Chance constrained approaches minimize the dispatch cost by representing uncertainty in the form of probability attainment, implying that one or a set of constraints have a desired probability of satisfaction, where the random variables have a known Probability Density Functions (PDFs) or Cumulative Probability Distribution Functions (CDFs). In [21], the authors propose a dispatch model using a two-stage CCO that ensures, given a probability measure, a large portion of the wind power output at each operating hour is utilized. The first stage yields the UC decisions and the dispatch, and a second stage determines the expected value of the load shedding at each bus. The problem is solved using a sample average approximation to estimate the PDF of the wind power; wherein the forecast is replaced by an empirical distribution assuming wind power is subject to multivariate normal distribution. The result is a formulation that uses a discrete representation of the PDF in the constraints. A chance constrained OPF is also proposed in [22], where the aim is to obtain optimal commitment decisions in the presence of uncertainty, so that the expected value of the objective function is minimized and simultaneously satisfies the constraints with a predefined probability level. This approach combines a stochastic approach with a chance constrained one, resulting in a multivariate non-linear problem which however, requires too many approximations to make it tractable, making the reliability of the result questionable.

The principal drawback of the CCO approaches from the operative point of view is that they require a known PDF which, in the case of RE-sourced power assuming parametric forecast, may result in a poor representation of the uncertainty [23]. Furthermore, in probabilistic constrained formulations the PDFs have to be approximated again to make the optimization problem tractable. Also, the computational challenges and simplifications required to develop CCO-based dispatch algorithms renders them unsuitable for practical, real-time applications in microgrids, considering the inherent modeling complexities mentioned in Section 1.1.

Stochastic Programming Techniques

Stochastic programming is a very common tool used to build decision-making models for the efficient management of uncertainties. The objective is to find an optimal solution that minimizes the expected cost of a stochastic variable [24], which can be represented by a continuous non-linear function or, more commonly, through a set of scenarios. A stochastic version of UC problem is proposed in [25], where Lagrangian relaxation techniques are used to solve the Stochastic Unit Commitment (SUC) and simplify the representation of the constraints in the problem. Due to its computational complexity, this technique was rarely applied initially; however, this has changed recently due to availability of parallel computing tools, more powerful solution algorithms, and the application of scenario reduction techniques.

In [26], the authors formulate a two-stage stochastic programming model for reserve commissioning using weighted scenarios and employing a Lagrangian relaxation. The proposed algorithm schedules the "slow" generation units using a first stage sub-problem, and later, a second stage is used to commit the "fast" generation units and dispatching all of the resources. An emphasis is placed on the advantages of the proposed decomposition for implementation in parallel computing architectures, and the results show that the stochastic approach is superior to the deterministic reserve rules that are commonly used in practice.

A different approach is shown in [27], where a short-term market clearing algorithm is developed that accounts for variations from power forecasts. The authors highlight that the technique is able to manage not only spinning reserve, but also ramping reserves. The problem is solved directly by an MILP solver without the application of any simplification or decomposition, showing that current preprocessing techniques in commercial solvers can manage large scale problems. The same direct calculation approach is used in [28] to allocate DSM reserves using a two-stage SO formulation of the security constrained SUC.

Another example is the security constrained SUC presented in [29], which considers uncertainties such as outages and load forecast inaccuracies, generating scenarios based on Monte Carlo simulations. The authors highlight the convenience of decomposition techniques, based on a long-term SUC master-problem and short-term sub-problems being solved separately leading to reduced need for computational resources. The two-stage SUC is also used in [30] for the management of uncertainty of load and generator outages in a hydro-thermal power system; the scenarios are solved using a decomposition method for stochastic integer programming with a combination of Lagrangian relaxation and branch-and-bound solution techniques.

A large-scale SUC model that incorporates additional constraints in order to limit the

probability of loss of load is proposed in [31]. The unavailability of generation is expressed by a discrete set of outage scenarios in the first stage, while load uncertainty is represented as a continuous random variable in the second stage. The objective is to minimize the overall operation cost given reliability constraints that limit the energy delivery and may cause load shedding. The proposal combines system uncertainties in terms of generator unavailability and load fluctuations with a discrete set of scenarios in a single optimization formulation. The results show the benefits of recourse models to deal with different sources of uncertainty in power systems, reducing load shedding in this particular case.

Based upon the aforementioned discussions, it can be concluded that the following are some of the main challenges of the SO approach:

- Scenario generation: Even though several apporaches to relate forecasts of wind power to credible scenarios have been proposed (e.g.[32]), the appropriate number of scenarios required to achieve a good representation of the uncertainty, is still not clear. Furthermore, there is not much research on scenario generation methods for other sources of uncertainty.
- Large problem size: As a result of the scenario-based representation which reproduces the constraints, the problem can become large scale. Although some authors argue that modern solvers can handle the large scale problems (e.g. [27, 28]), this conclusion is derived from small academic test case studies and not from practical applications. A detailed review of solution algorithms is presented in [33], showing the benefits of parallelization, which is a promising computational approach to handle large-size problems.

Despite these challenges, the application of SO techniques to microgrid EMS development is feasible, given the reduced size of the dispatch problem. However, the challenges regarding scenario generation remain, especially if there is a need for modeling various sources of uncertainty, resulting in a rapid increase in problem scale, making this approach becomes infeasible.

Robust Optimization Techniques

Given the random nature of RE sources and the challenges to define appropriate probabilistic models for them, robust optimization has become very popular since it can be applied without requiring many assumptions about probability. The robust optimization methodology obtains an optimal solution that hedges the system against any outcome within a given uncertainty set [34].

In the context of bulk power systems, several approximations of the robust counterparts of the UC using a DC-OPF framework have been proposed, depending on the source of the uncertainty. In [35], the authors propose a generalized two-stage Robust Unit Commitment (RUC) model, where nodal current injections are considered to be uncertain; the resulting model is able to represent uncertainties from both load and RE sources. In the context of this paper, the budget of uncertainty represents the number of nodes subject to a uncertain injections. The problem is solved using a Benders' decomposition approach, combined with an outer approximation algorithm to manage bi-linear terms, and the results are compared with a reserve adjustment methodology used by the New England ISO.

Other approaches model uncertainty as an "affine policy" [36], which means that the focus is not on the value of the variable but rather on its deviation from the forecasted value. The author solve a multi-stage RUC problem, modeling uncertainties corresponding to price-responsive demand and RE sources in an open market, using an L-shaped method, given the complexity and scale of the formulation. This type of formulations can be regarded as too conservative, as it solves a combination of the two worst outcomes of the uncertainty sets. In order to overcome this issue, in [37] an RUC model using a robust-regret formulation, to adjust the conservatism, is proposed, where the forecast error is separated by percentiles, and used to determine the bounds of the uncertainty set. The algorithm is benchmarked against SUC and RUC approaches, delivering results with a smaller expected cost and is less conservative than RUC. However, the "regret model" requires the application of heuristics, with too much dependance on the decider preferences.

One of the main advantages of RO for dispatch applications under uncertainty is its flexibility to represent unknowns, unlike CCO and SO which require probability information in order to develop the models, resulting in intractable formulations or large-scale problems. For this reason, RO has been proposed for several applications in power systems; for example, in [38] RUC is used to address the $N-k$ operational security problem. Also, the authors in [39] propose a bidding technique to build hourly offer curves for a price-taker producer participating in a generation pool. Other applications of RO to power system operations are discussed in [40], where several examples of their application to reserve procurement, demand response, etc., are introduced.

The flexibility of RO-based dispatch makes them very appealing for microgrid applications, given the aforementioned adaptability to model several sources of uncertainty without requiring probabilistic information. However, the complexities arising from the min-max structures, common in this type of mathematical formulation, can hinder their use [41] with approximations of the bi-linear terms possibly being required. Nonetheless, given that the solution is located at the extreme points of a polyhedron [36], these one is not detrimental to the quality of the solution, unlike the CCO formulations.

1.2.2 Uncertainty in Microgrids

Management of uncertainty in generation dispatch is a challenging problem and requires the application of mathematical techniques that incorporate more information into an automated decision making process. In the context of isolated microgrids, this is paramount given the critical demand-supply balance, the low inertia of the generation fleet, and the high correlation of RE sources. Thus, work on EMS has primarily concentrated on RHC strategies for energy management in microgrids [12, 18, 19], since these allow implementing dispatch actions that anticipate future events such as variations in power outputs from DERs and demand, and also account for the effect of present actions into future time steps, which is particularly important in the presence of ESS.

In addition to [12, 18, 19], in [42], an RHC dispatch control is presented and tested on a grid-connected single-bus microgrid model; the mathematical model is a classical OPF with constraints on device currents, to avoid overloading. The control is tested with a time step of 1-hour and prediction horizon of 4-hours, and the results show a slight reduction in the system dispatch cost primarily due to a better allocation of the ESS energy. However, the device models are simple, and better performance can be obtained if forecasting techniques are used instead of historical information. A more refined approach is presented in [43], where the dispatch of the microgrid is calculated every hour considering a longer optimization horizon of 48 hours, to capture long-term load and generation patterns. The objective function includes non-linear costs approximated with piece-wise functions, some start-up/shut-down decisions, resulting in an MILP formulation. The proposed EMS is applied to the dispatch of load, a diesel generator, and ESS in a microgrid with the presence of photovoltaic panels and two wind turbines. It demonstrates the economic benefits of using the RHC compared to a single step methodology, particularly when dealing with updated forecast. Even though these RHC-based algorithms improve the handling of RE sources, information about the uncertainty inherent in the forecasts is not properly incorporated, thus the implicit consideration is that a prediction will hold for a given time step, but the realization often does not necessarily match the forecast. Hence, a better approach to handle these mismatches is needed.

A dispatch strategy for RE sources in electricity markets has been proposed in [44], using the concept of risk-limiting dispatch, which considers the probability of not being able to supply the load; to solve the proposed optimization problem, uncertain variables are assumed to be uniformly distributed. A similar approach using probabilistic constraints is used in [45], where the authors propose a DC-OPF model with line flow constraints, using a scenario approximation approach to address computational issues associated with the PDFs. In [46], the uncertainty is modeled in the form of independent forecast errors

represented by normally distributed random variables; the proposed method uses a CCO approach by modeling energy-balance equation as a probabilistic constraint. The problem is converted to an equivalent deterministic form by direct substitution of the GaussianPDF and solved using gradient-based algorithms. These papers propose methods that do not allow to properly account for the time-dependency of the random variables; furthermore, the complexity of the proposed formulations rule out the possibility of modeling the UC, given the need to consider the integer variables, that results in a complex MINLP problem.

Another approach presented in [47] considers the RE sources as a disturbance with Gaussian PDF in the nodal power balance equations, approximating the probabilistic constraint using empirical mean based on a large number of samples. The resulting equivalent deterministic optimization problem is then solved using dynamic programming over 24-hours, with a 4-hour look-ahead window. However, the forecast is not updated at every step, and the objective function includes a penalty to maintain the ESS SoC as close as possible to its maximum capacity. This approach has the drawback of not allowing the EMS to allocate the ESS in a way that improves system efficiency, enforcing a fixed level of SoC. Furthermore, the uncertainty representation is weak, since as shown in [48, 49] Gaussian assumptions about the forecasting error PDF are not necessarily adequate.

As previously stated, assumptions regarding representation of PDFs associated with RE-sources may help to simplify the formulations to be able to solve the problems efficiently; however, this may lead to weak representations of uncertainty [23]. In order to address this shortcoming, approaches using scenario-based SO have been proposed, as in the case of [50], where a heuristic logic that combines a master SUC with a slave distribution system OPF is presented, in order to generate a more accurate dispatch; historical samples are used as scenarios for both solar and wind power. A more detailed model is presented in [51], where the authors combine the SUC with the detailed three-phase Receding Horizon Optimal Power Flow (RHOPF) presented in [12]. Generating the dispatch commands directly from the three-phase OPF, instead of using them to adjust the SUC results, the proposed EMS is tested with different configurations and the results are compared to a proper scenario generation technique with the historical data approach.

Even though the preceding papers propose the application of scenario based stochastic EMS, reasoning that for small-scale systems, like an isolated microgrid, the computational effort is not critical; the challenges regarding the uncertainty representation and generation are still present. The inherent requirement of probabilistic information to generate the scenarios, and the weak assumption that historical information represents the uncertainty reliably are some of the weaknesses of the approach. Furthermore, the scenario-based representation does not allow the decision maker to include preferences about the uncertainty representation, thus making it inflexible.

In light of the aforementioned limitations of probabilistic and stochastic approaches, RO offers an attractive framework for dispatch formulations, with adequate accounting of the uncertainties without requiring probabilistic assumptions. Given these advantages, papers addressing uncertainty in RE sources using RO frameworks in the context of microgrid applications have been published. For example, in [52], the authors present a robust wind dispatch and bidding algorithm with independent uncertainty sets for prices and available generation; this approach relates a financial risk-measure with the uncertainty set for price and using a cardinal uncertainty set for the wind power forecast. A proposal that combines RHC and a robust counterpart of the dispatch problem is presented in [53], in order to produce safe intervals for the operation of wind power facilities, avoid infeasible operating points, and reduce curtailment. The resulting model is a single-stage bilevel mathematical program able to obtain intervals of operation for wind power, reducing the violations of the required spinning reserves in the system. This papers show that the application of RO in real-time applications in the context of Smart Grid is possible with an appropriate mathematical model, however, they do not address the problem of dispatch in microgrids, and do not combine the concept of recourse with the RHC.

As just mentioned, in the field of EMS, the application of RO is still limited. For example, the controller proposed in [54], exploits the decomposable structure of the simplified economic dispatch in dc power flow model, resulting in an "affinely adjustable robust counterpart" problem that can be solved in a distributed fashion, and that is guaranteed to converge under heterogeneous and asynchronous communications. Similarly, in [55], the authors propose a distributed RO algorithm considering a central hub that exchanges information with all DER units, aiming at maximizing the social welfare in a grid-connected microgrid. A polyhedral representation of the uncertainty set is used, with a novel definition using various non-overlaping horizons assuming different models depending how the uncertainties relate to the assets. These two papers, feature system models with many simplifications, which limit their practical application, particularly for isolated microgrids, since only grid-connected microgrids are considered. Furthermore, the rationale behind a distributed optimization approach is not clear, given the limited size of the microgrid dispatch problem being addressed.

1.3 Research Objectives

Based on the techniques proposed so far to manage uncertainty in microgrid dispatch, and the need to properly embed them in EMS for isolated microgrids, the main research objectives of this thesis are the following:

- Propose a mathematical model for microgrid EMS using an RO approach, suitable for the operation of isolated microgrids, with and without ESS.
- Provide an improved and appropriate EMS architecture suitable for real-time applications, based on a two-stage recourse model, and demonstrate its application on a realistic microgrid.
- Investigate the differences between the robust and stochastic approaches to consider uncertainty in the dispatch of isolated microgrids.

1.4 Thesis Outline

This thesis is structured as follows:

- Chapter 2 presents the relevant background to the thesis, such as the EMS requirements for isolated microgrids, Stochastic Optimization (SO) and Robust Optimization (RO) principles, and the conceptual framework of recourse and RHC.
- Chapter 3 presents the architecture, the mathematical models of the proposed RUC, and the criteria to select the uncertainty set.
- In Chapter 4, the results of several case studies are presented and discussed for two different configurations of a microgrid, and comparing them for stochastic, robust, and deterministic variants of the algorithm.
- Finally, in Chapter 5, the main conclusions and contributions of this work are presented, along with future work recommendations.

Chapter 2

Background Review

In this chapter, a general overview of the concepts, models, tools and techniques used in the development of the thesis work are presented. Thus, first a summary on microgrids is introduced, describing some of its key features and control requirements. Next, various mathematical tools to account for uncertainty in the EMS problem are examined. Finally, the primal cutting-planes algorithm used to solve the proposed RUC, along with its advantages is explained, and its connection with the SO-based recourse model is examined.

2.1 Microgrids

The definition of microgrids is a subject of discussion in the electric power sector, considering that small-scale networks have existed for a long time, plus the recent advent of communications and enhanced control techniques. According to the latest authoritative report [10], a microgrid can be described as a cluster of loads, Distributed Generator (DG) units, and ESSs operated in coordination to reliably supply electricity, which can be connected to the host power system at the distribution level at a single point of connection or operated in an isolated fashion.

The focus of this research is microgrids not connected to the bulk power system, such as the case of remote communities [6] or remote temporary sites like military bases [5]. These isolated microgrids are the best candidates for the implementation of Smart Grid technologies, given that they benefit the most from the penetration of RE and the performance improvements. Thus, there is an increased interest in improved control techniques; actually, advanced control technologies are proposed and applied in isolated networks around

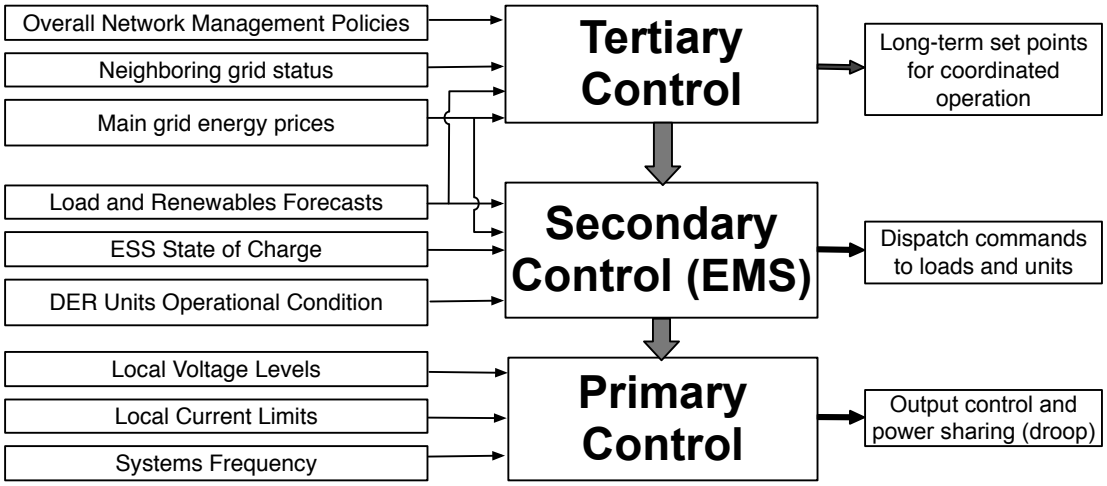

Figure 2.1: Hierarchical approach to control of microgrids.

the world. There are many successful cases in practical applications that result in improvements to existing microgrids operation, such as the case presented in [56], located in Bella Coola, BC. Other countries like United States [5], Portugal [56], and Chile [43] have isolated microgrid projects in remote locations, with Smart Grid technologies being applied in its operation.

2.1.1 Control Definitions and Operational Requirements

In order to provide energy efficiently with the required quality and security, the distinct DER units within the microgrid must be operated in a coordinated and coherent way. This requires the combination of many control techniques at different levels [57], with multiple control requirements, where a hierarchical structure is the natural choice for the adequate operation and control [58]. A central controller also allows the microgrid to operate as a single entity able to optimize its operation continuously [59]. Figure 2.1 shows the different control actions and variables assigned to each layer for a centralized hierarchical control; in this structure, the time frames associated with the tasks in each layer must be spaced in order to prevent interference [58]. The primary control operates at the device level; system-wise control is performed at the secondary level, and can operate either in a distributed or centralized fashion; and the tertiary control operates outside the microgrid boundaries [10].

The present work concentrates on the secondary control level, also referred to as the

microgrid EMS, and the requirements to manage uncertainty in dispatch applications for isolated microgrids. Given the special technical requirements of these types of microgrids, the EMS should be able to account for the uncertainty associated with intermittent energy sources and model the system components properly, in order to efficiently dispatch the available ESSs and DGs automatically and in real-time.

2.1.2 Microgrid EMS

Several contributions to EMS controls in microgrids have been presented in the literature, ranging from decentralized approaches mainly focused on grid-connected microgrids, to centralized approaches that are more suitable for isolated microgrids [60]. The architecture of the EMS must be selected according to its operational characteristics, starting with the type of connection to the grid. Decentralized approaches are more appropriate for grid-connected microgrids since their aim is to allocate the energy sources economically meeting certain power quality standards. In such systems, the main grid provides the frequency reference, balancing out any surplus or shortfall of energy; the same applies to voltage profiles, since the main grid can provide a constant voltage at the point of common coupling. In contrast, in stand-alone microgrids, keeping the generation-load balance requires the DER units to control the system voltage and frequency, while simultaneously allocating the resources efficiently and securely as the main task. Moreover, from the control point of view, isolated topologies require different considerations regarding the control architecture, with preference to centralized approaches.

For EMS design, the following considerations are required in order to properly define the control requirements: Frequency and voltage regulation should be performed at the device level using local information at each unit; droop control is considered to be part of the primary control, since it relies only on local frequency measurements without information from other units or the system state. Ultimately, from the stability and security points of view, the EMS is mainly concerned with providing the system with enough reactive and active power capabilities to perform the required regulation tasks. Hence, the objective of considering uncertainty is the need for system security, i.e., having enough capacity in the system to perform the frequency and voltage regulation when changes in the RE sources arise.

In the context of microgrids, some of the classical assumptions of conventional power systems modeling have to be revised and modified [10]; the most relevant are: high R/X in lines, variable power loads, unbalanced operation, and the presence of ESSs. Hence, in general, proper models for most microgrid components are based on those used in distribution systems analysis rather than bulk power systems. The resulting EMS mathematical

formulation is then based on the types of DERs, presence of ESSs in the microgrid, various objectives such as cost and/or environmental impact and the network model, among others. The EMS blocks represent various components with different level of detail, depending on the requirements of system modeling at each decision stage (i.e., linear models for the UC, and detailed non-linear models for the OPF).

The EMS model used throughout this work is as follows:

- *Cost Function:* The most common cost function to be minimized is the actual cost of operating the generation units, including fuel and commitment costs. The cost function should also include slack variables for load shedding and power curtailment, in order to provide sufficiently large recourse and avoid unfeasibility; thus, this can be represented as follows:

$$\sum_t \sum_g \Bigg[\underbrace{C_g^u u_{g,t} + C_g^v v_{g,t} + C_g^w w_{g,t}}_{\text{Commitment cost}} + \underbrace{C_g^P P_{g,t}}_{\text{Linear fuel cost.}} + \underbrace{C_c P_{c,t}}_{\substack{\text{Power curtail} \\ \text{cost.}}} + \underbrace{C_{sh} P_{sh,t}}_{\substack{\text{Load shed} \\ \text{cost.}}} \Bigg] \tag{2.1}$$

  In general the fuel cost as a function of the output power is a non-linear equation; however, to keep the model linear in the proposed RUC formulation, the fuel cost function is considered to be linear using a constant coefficient C_g^P representing the cost in \$/kW that depends on the price of fuel.

- *System Operational Constraints:* These correspond to the operation of the microgrid, provide the coupling between the DG models in the system, and also ensure that solution of the commitment variables $u_{g,t}$, $v_{g,t}$, $w_{g,t}$ follow the start-up and shut-down constraints for each unit, these constraints are as follows:

$$u_{g,t} - v_{g,t} = w_{g,t} - w_{g,t+1} \qquad \forall t,\ g \tag{2.2a}$$

$$v_{g,t} + u_{g,t} \leq 1 \qquad \forall t,\ g \tag{2.2b}$$

$$\sum_g P_{g,t} + \sum_\omega P^*_{\omega,t} - P_{c,t} = \sum_l P_{l,t} - P_{sh,t} \qquad \forall t \tag{2.2c}$$

  These constraints are required regardless of the types of units used in the microgrids, like (2.2c) is required to guarantee that total demand $\sum_l P_{l,t}$ is met at all times by the available generation units. Also includes the load shedding $P_{sh,t}$ and power curtailment $P_{c,t}$ terms to guarantee feasibility. In some cases, a proportional reserve equation can be

included; however, in the developed RUC, it was not included, since the main interest in this research is determining the system reserves through the RO formulation, and not through a proportional rule.

- *DER Operational Constraints:* The following DER output and ramping limits must be included, and the output must be forced to zero if the unit is not committed:

$$P_g^{min} w_{g,t} \leq P_{g,t} \leq P_g^{max} w_{g,t} \qquad \forall t,\ g \qquad (2.3a)$$
$$P_{g,t} - P_{g,t-1} - u_{g,t} P_g^{max} \leq RU_g \qquad \forall t,\ g \qquad (2.3b)$$
$$P_{g,t-1} - P_{g,t} - v_{g,t} P_g^{max} \leq RD_g \qquad \forall t,\ g \qquad (2.3c)$$

The capacity constraints related to the minimum and maximum output power P_g^{min} P_g^{max} are of particular importance in microgrid operation with small- and medium-size diesel fleets, in order to avoid carbon build-up or overload [6]. Ramping limits RU_g and RD_g must be modeled according to each diesel unit characteristics to reduce pulsations and meet operational limits related to the thermal capabilities of the reciprocating engine [61].

Minimum-up and -down constraints are also required as follows:

$$w_{g,t} - w_{g,t-1} - w_{g,t_u} \leq 0 \qquad \forall t_u : 1 \leq t_u - (t-1) \leq MU_g,\ t,\ g \qquad (2.3d)$$
$$w_{g,t-1} - w_{g,t} + w_{g,t_u} \leq 1 \qquad \forall t_u : 1 \leq t_u - (t-1) \leq MD_g,\ t,\ g \qquad (2.3e)$$

Even though DER units in microgrids are highly flexible, (2.3d) and (2.3e) are still necessary to impose MU_g and MD_g in cases where Combined Heat and Power (CHP) units are included [62], when the units require warming up, or when commitment decisions are revised to account for required reactive power support [12].

- *ESS Operational Constraints:* In addition to (2.3a)-(2.3c), the ESS SoC balance constraints and limits are modeled by including the following constraints:

$$P_{s,t}^{in} \leq P_s^{max} \qquad \forall t,\ s \qquad (2.4a)$$

$$P_{s,t}^{out} \leq P_s^{max} \qquad \forall t,\ s \qquad (2.4b)$$

$$P_{s,t} = P_{s,t}^{out} - P_{s,t}^{in} \qquad \forall t,\ s \qquad (2.4c)$$

$$SOC_s^{min} \leq SOC_{s,t} \leq SOC_s^{max} \qquad \forall t,\ s \qquad (2.4d)$$

$$SOC_{s,t+1} = SOC_{s,t} + \left(P_{s,t}^{in} \eta_s^{in} - \frac{P_{s,t}^{out}}{\eta_s^{out}} \right) \Delta t \qquad \forall t,\ s \qquad (2.4e)$$

These equations constrain the maximum output and input power $P_{s,t}^{out}$, $P_{s,t}^{in}$ and the ESS storage capacity limits SOC_s^{min} and SOC_s^{max} to ensure that there the equipment doesn't operate outside safe ranges. Additionally, () models the charging and discharging cycles of the ESS units. This model can be used to represent a wide range of devices such as batteries and hydrogen-storage sets, and is known as the SoC book-keeping model, which is widely used for these types of applications (e.g., [63, 64]).

2.2 Uncertainty in Energy Management Systems

The main principle to account for uncertainty in control tasks affected by random inputs is to include as much information as possible into the mathematical formulation. Having a successful management of RE uncertainty in the EMS problem requires the combination of two different tools: RHC to incorporate forecasts, and recourse actions to hedge the controller against the uncertainties in the forecast. The mathematical formulations to realize this are explained next.

2.2.1 Receding Horizon Control

RHC is an optimization-based strategy for automatic control of processes that is widely used in a range of engineering applications, such as chemical processes, power systems control and aviation [65]. The technique is based on the premise that control set-points can be defined as an open-loop finite-horizon mathematical problem as follows:

$$z_{t+1} = \mathcal{J}\left(\{z_t, z_{t+1}, \ldots, z_{t+n}\}, \{y_t, y_{t+1}, \ldots, y_{t+n}\}, \rho, \mathcal{F}^* | t\right) \qquad (2.5)$$

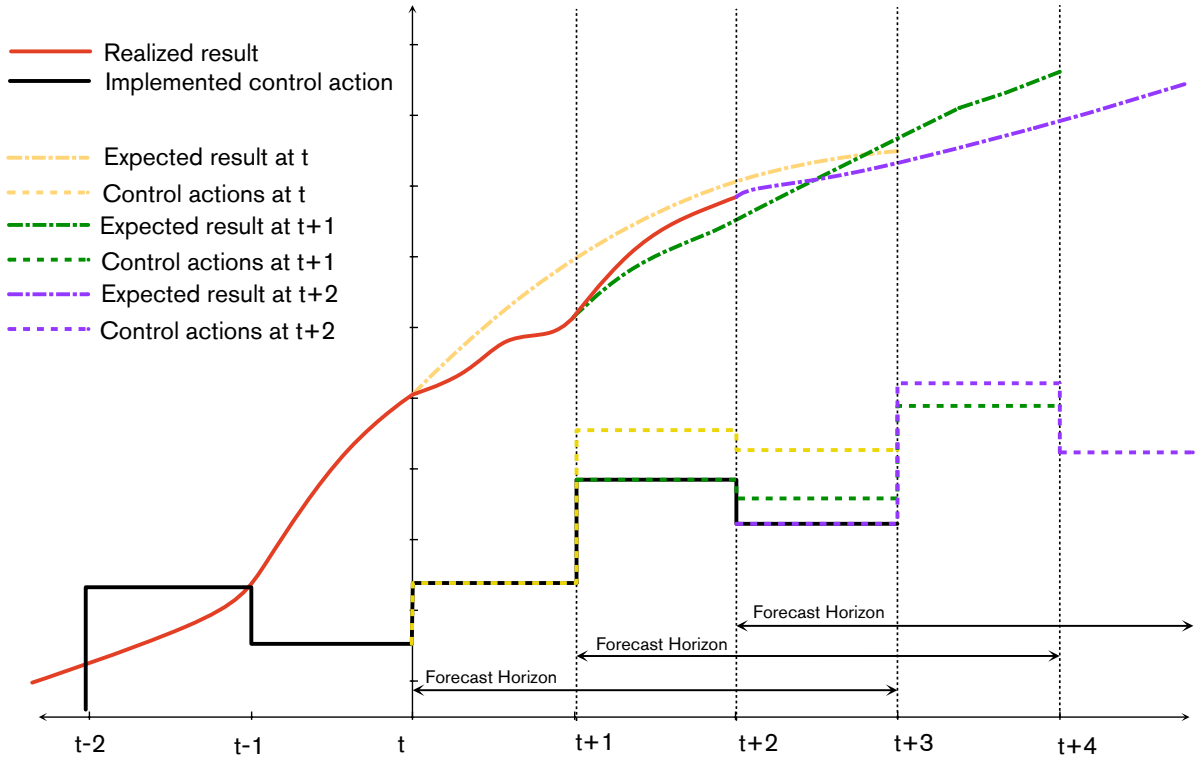

Figure 2.2: RHC calculation steps.

Figure 2.2 illustrates the approach: at the current time t, the optimal control actions of the next time step z_{t+1} are a function $\mathcal{J}(\cdot)$ of the control variables z and system states y over the n-step time horizon, time-invariant system parameters ρ and forecasted input variables available at the particular time t $\mathcal{F}^*|t$.

The optimization problem is solved for a sequence of control actions over the whole finite horizon $\{t, t+1, \ldots, t+n\}$ at each time-step, so that a selected performance criteria (e.g., square root of the error, cost, emissions, energy) are optimized; however, only the command for the next time-step $(t+1)$ is implemented. The mathematical program takes into account estimates of future system states and control actions based on available information at time

t. This finite-horizon optimal control problem can be formulated as follows:

$$\mathcal{J}(\cdot) = \min_{\{z_t,\ldots,z_{t+n}\}} \sum_{t}^{t+n} J(z_t, y_t) \tag{2.6a}$$

$$\text{s.t.} \quad H\left(z_t, y_t, \rho, \mathcal{F}^*|t\right) \leq 0 \qquad \forall t \tag{2.6b}$$

A system performance function for each time step is given by $J(\cdot)$, which is minimized for the entire look-ahead window, defined as the sum of $J(\cdot)$ from time t to $t+n$ as per (2.6a). RHC minimizes the deviations from a given set-point over the look-ahead window; for dispatch applications, the objective can be the minimization of total energy costs given the heat rate information of the thermal units. The operational constraints are modeled by the vector function H, which represent the limits on the control variables and depends on the devices to be managed (e.g.,valves, motors, pumps). Likewise, system variables are also bounded in order to avoid equipment damage or to comply with a particular operational standard; for example, in microgrid dispatch, changes in output power from thermal units must not violate ramping constraints, as in (2.3b), and the SoC limits of the storage cannot be exceeded, as in (2.4d).

The application of RHC control technique presents some disadvantages given possible problems with the mathematical model, particularly in the case of complex systems such as electric power grids. Thus, the main drawbacks for the EMS problem are [66]:

- Longer calculation times: Compared with non-optimal controls, such as heuristic rule setting, the total computation time of RHC may be longer, particularly for nonlinear systems. Therefore, RHC may not be fast enough for real-time applications under various circumstances; however, this problem can be overcome with improvements in optimization algorithms, parallelization, and the application of appropriate control architectures, such as the decomposition approach used in general in power systems and in this thesis.

- Uncertainty-aware RHC: For many applications, SO enables the inclusion of uncertainty under an expected-value framework and in RO, using a minimax framework; however, the repeated computation requirement of RHC makes it difficult to incorporate stochastic or robust mathematical models. Nevertheless, the complexity depends on the source of uncertainty and its modeling.

Despite the possible challenges RHC presents for dispatch processes, there are advantages when considering its application to microgrid EMS. The most relevant are [66]:

- The RHC systematic approach produces an optimal control signal for every time step over the finite horizon, providing superior handling for processes with large number of set points and controlled variables. Moreover, this technique is particularly beneficial when variables have strong time-coupling constraints like ramping and ESS charging.
- RHC enhances system stability by predicting weak conditions within the look-ahead window before these actually arise, as for example, in the case of the reactive power management in the RHOPF proposed in [12].
- Adaptability to future system parameter changes that can be estimated before-hand. Since only finite future system states are needed for the computation of the current control actions, the control can adapt to changing parameters in time-varying systems with predictable behavior.

Developing appropriate system models combined with addequate optimization algorithms, enables the application of RHC to complex systems such as microgrids. Furthermore, as discussed in the literature review, RHC is a proven technique that provides solutions to some of the microgrid control challenges, particularly those related to the integration of RE.

2.2.2 Recourse Actions

The concept of recourse was introduced in [67] as a mathematical framework for sequential decision making under uncertainty, and in the optimization literature refers to the ability to adapt the solution of a mathematical program to a specific outcome [68]. Thus, given an optimization problem that can be divided in two stages, one that must be realized before the uncertainty unveils and another one once the uncertainty is revealed; the objective is to obtain a solution for the first-stage decision variables such that the second-stage variables can accommodate the uncertain outcomes. Hence, applying recourse actions can hedge the system against uncertainties in the look-ahead window of the RHC formulation.

The general two-stage RHC problem with recourse can be formulated as follows:

$$\mathcal{J}(\cdot) = \min_{\substack{\{z_{1t},\ldots,z_{1t+n},\\ z_{2t},\ldots,z_{2t+n}\}}} \sum_{t}^{t+n} \left[J_1(z_{1t}, y_t) + J_2(z_{2t}, y_t)\right] \tag{2.7a}$$

$$\text{s.t.} \quad H_1\left(z_{1t}, y_t, \rho\right) \leq 0 \qquad \forall t \tag{2.7b}$$

$$H_2\left(z_{2t}, y_t, \rho, \mathcal{F}^*|t\right) \leq 0 \qquad \forall t \tag{2.7c}$$

$$H_3\left(z_{1t}, z_{2t}, y_t, \rho, \mathcal{F}^*|t\right) \leq 0 \qquad \forall t \tag{2.7d}$$

where z_{1t} is a subset of the control variables z_t named first-stage variables, and represents decisions that must be made "here and now". In the case of the EMS, these can be the commitment, the spinning reserve calculation, or ESS SoC, which are control actions that need to be calculated before the uncertainty is resolved. $J_1(\cdot)$ is the function that evaluates the performance in terms of the control action variables z_{1t} and system states y_t, and the vector function H_1 represents the constraints specific to this stage and variables at each time step, following the same model described for the RHC.

The goal of the mathematical model (2.7) is to obtain an optimal solution for z_{1t+1} that guarantees the feasibility of the subset of the control variables z_{2t} after the uncertainty is revealed, which are known as recourse actions or "wait-and-see" actions. The cost function $J_2(\cdot)$ is used to evaluate the system performance at each time step and determine the expected outcome or worst case depending on the type of formulation used. Hence, the recourse actions are defined after the first-stage has been implemented, enabling the decision maker to adapt to the actual outcomes [40]. The recourse mathematical problem is then defined as follows:

$$\min_{\{z_{2t},\ldots,z_{2t+n}\}} \mathcal{J}_2 = \sum_{t}^{t+n} J_2(z_{2t}, y_{1t}) \tag{2.8a}$$

$$\text{s.t.} \quad H_2\left(z_{2t}, y_t, \widetilde{\rho}, \widetilde{\mathcal{F}}^*|t\right) \leq 0 \qquad \forall t \tag{2.8b}$$

$$H_3\left(z_{1t}, z_{2t}, y_t, \widetilde{\rho}, \widetilde{\mathcal{F}}^*|t\right) \leq 0 \qquad \forall t \tag{2.8c}$$

where vector functions H_2 and H_3 are relevant to the recourse, and include the possible uncertain variables $\widetilde{\rho}$ and $\widetilde{\mathcal{F}}^*|t$. Vector function H_3 is of particular importance, since it

defines the coupling between the two stages, as shown in (2.8c), which includes all the system states y_t and the solution of z_{1t} and z_{2t}. The optimization problem is solved over z_{2t}, where z_{1t} is fixed and defined by the first stage.

There are two general types of mathematical problems that can be designed to support decision making considering uncertainty with a recourse model, and have been applied to power system applications: stochastic programming, which can be further separated into approaches that use PDFs or a finite discrete set of scenarios (e.g., [27]); and robust optimization (e.g., [53]). The resulting formulations provide a hedged or uncertainty immunized solution of the first stage variables, and their solutions vis-a-vis the solution of the deterministic equivalent produce higher cost first-stage variables, but at the same time it reduces the use of expensive recourse actions (e.g., load shedding or power curtailment in the dispatch problem) to manage the effect of an uncertain outcome; on the other hand, an uncertainty measure that is too conservative may result in a solution where the cost of the hedged commitment is larger than the value added, thus making ineffective the hedging strategy. This is known as the difference between the price of perfect information and the value of the stochastic or robust solution discussed extensively in [24, 40, 69].

Depending on the type of formulation i.e.,stochastic or robust, there is mathematical guarantee that the resulting commitment provides to the system enough capacity to respond to variations in the RE sources, depending on the representation of the uncertainty. In the forthcoming sections, scenario based SO and RO recourse formulations are presented in order to explore the conceptual differences between the two approaches.

2.3 Stochastic Optimization

The two-stage SO problems are formulated on the basis of expected cost of the recourse, which can be defined using a continuos PDF; however, the difficulty of estimating accurate PDFs for RE and the introduction of non-linear functions hinders the use of this type of techniques. On the other hand, SO-based two-stage recourse problems can also be formulated on a discrete representation of the uncertainty using a finite set of scenarios as depicted in Figure 2.3. In this case, the equivalent deterministic problem of the stochastic dispatch problem using a discrete representation of the uncertainty can be defined as follows:

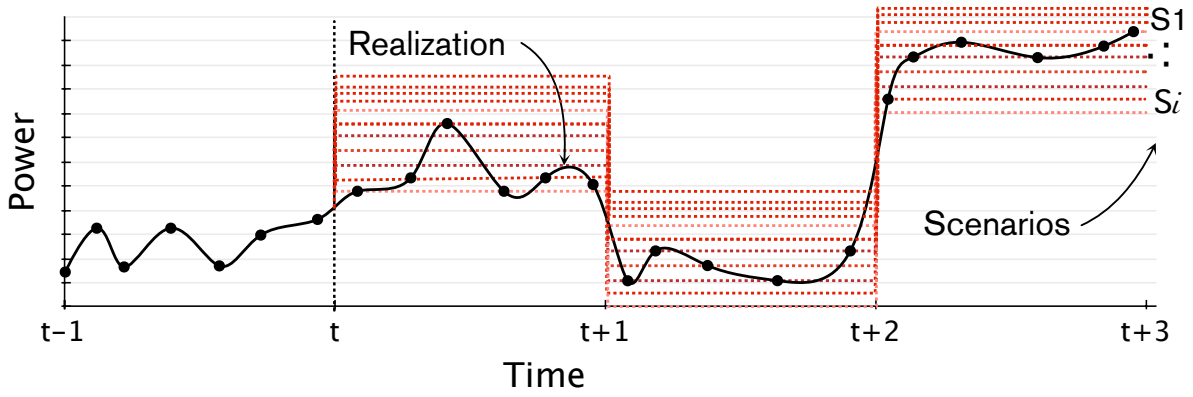

Figure 2.3: SO uncertainty representation

$$\min_{z_1, z_2^i} \sum_{t}^{t+n} \left[J_1(z_{1t}, y_t) + \underbrace{\sum_i \pi_i \cdot J_2(z_{2t}^i, y_t^i)}_{\text{Expected value of the recourse}} \right] \tag{2.9a}$$

$$\text{s.t.} \quad H_1\left(z_{1t}, y_t, \rho\right) \leq 0 \qquad \forall t \tag{2.9b}$$

$$H_2\left(z_{2t}^i, y_t^i, \rho, \mathcal{F}^i|t\right) \leq 0 \qquad \forall t,\ i \tag{2.9c}$$

$$H_3\left(z_{1t}, z_{2t}^i, y_t^i, \rho, \mathcal{F}^i|t\right) \leq 0 \qquad \forall t,\ i \tag{2.9d}$$

This SO-problem calculates the solution of the first-stage variables $z_1 = \{z_{1t}, \ldots, z_{1t+n}\}$, taking into account the interaction with the entire set of scenarios. Each recourse scenario is defined by the pair $\{z_2^i, \pi_i\}$, where the resulting recourse action $z_2^i = \{z_{2t}^i, \ldots, z_{2t+n}^i\}$ is determined by the solution of the second-stage problem for a sequence of input vectors $\mathcal{F}^i|t$ representing scenario i, obtained using the forecast information available at time t.

Using a discrete representation of the uncertainty requires to solve all the scenarios simultaneously leading to large-scale problems, since constraints H_2, H_3, and their respective variables have to be duplicated for each scenario, which hinders its application in real-time dispatch [29, 20]. For this reason, special techniques such as Monte Carlo simulations or decomposition approaches like the L-shaped method are required in order to find a solution [24]. On the other hand, the scenario-based SUC formulation has the advantage that

the solution of the binary variables must guarantee feasibility at the lowest cost for every scenario yielding the optimal solution for the expected outcome.

The quality of the decision making process from an scenario-based SO program is highly dependent on the characterization of the uncertainty probability space. Some techniques to generate credible RE power scenarios are moment matching techniques [70], where some measure of distance between the statistical properties of the generated outcomes is minimized according to the decision maker specified properties. Internal sampling is another method to produce scenarios, as presented in [71], where the authors embed the Monte Carlo in the optimization algorithm to estimate function values and gradients. Another technique is statistic ensemble generation using interval forecasting information and historical error, as presented in [32] and applied to microgrid dispatch in [51].

2.3.1 Stochastic EMS approach

The aforementioned SO-based can be implemented as a SUC problem and applied to isolated microgrids, as proposed in [51], where the authors combine it with an RHOPF to develop an uncertainty-aware EMS. The model exploits the decomposition concept described in section 2.2.2, using a linear simplification of the system to solve the SUC, to refine it afterwards based on three-phase OPF. The stochastic-predictive formulation is a two-stage decision-making procedure, where the commitment variables $u_{g,t}$, $v_{g,t}$, $w_{g,t}$ introduced in section 2.1.2 are calculated prior to the realization of system uncertainties.

The SUC model proposed in [51] assumes that the system parameters are not affected by the outcomes of the random variables, thus making it a fixed recourse model [72]. The formulation of the scenario-based SUC for isolated microgrids considering storage is as follows:

$$\min_{\substack{u_{g,t},v_{g,t}\\ w_{g,t},P^i_{g,t}}} \sum_t \sum_g \left[C^u_g u_{g,t} + C^v_g v_{g,t} + C^w_g w_{g,t} + \underbrace{\sum_i \pi_i \left(C^P_g P^i_{g,t} + C_{sh} P^i_{sh,t} + C_c P^i_{c,t} \right)}_{\text{Cost of the expected recourse}} \right] \tag{2.10a}$$

$$\text{s.t. } SOC^i_{s,t+1} = SOC^{fix}_s \qquad \forall i \tag{2.10b}$$

$$u_{g,t} - v_{g,t} = w_{g,t} - w_{g,t+1} \qquad \forall t,\ g \tag{2.10c}$$

$$v_{g,t} + u_{g,t} \leq 1 \qquad \forall t,\ g \quad (2.10d)$$

$$w_{g,t} - w_{g,t-1} - w_{g,t_u} \leq 0 \qquad \forall t_u : 1 \leq t_u - (t-1) \leq MU_g,\ t,\ g \quad (2.10e)$$

$$w_{g,t-1} - w_{g,t} + w_{g,t_u} \leq 1 \qquad \forall t_u : 1 \leq t_u - (t-1) \leq MD_g,\ t,\ g \quad (2.10f)$$

$$\sum_g {P_{g,t}}^i + \sum_\omega P^i_{\omega,t} - {P_{c,t}}^i = \sum_l P_{l,t} - {P_{sh,t}}^i \qquad \forall t,\ i \quad (2.10g)$$

$$P_g^{min} \cdot w_{g,t} \leq {P_g}^i \leq P_g^{max} \cdot w_{g,t} \qquad \forall t,\ i,\ g \quad (2.10h)$$

$${P_{g,t}}^i - {P_{g,t-1}}^i - u_{g,t} \cdot P_g^{max} \leq RU_g \qquad \forall t,\ i,\ g \quad (2.10i)$$

$${P_{g,t-1}}^i - {P_{g,t}}^i - v_{g,t} \cdot P_g^{max} \leq RD_g \qquad \forall t,\ i,\ g \quad (2.10j)$$

$${P_{s,t}}^i = P_{s,t}^{out\,i} - P_{s,t}^{in\,i} \qquad \forall t,\ i,\ s \quad (2.10k)$$

$$P_{s,t}^{in\,i} \leq P_s^{max} \qquad \forall t,\ i,\ s \quad (2.10l)$$

$$P_{s,t}^{out\,i} \leq P_s^{max} \qquad \forall t,\ i,\ s \quad (2.10m)$$

$$SOC_s^{min} \leq {SOC_{s,t}}^i \leq SOC_s^{max} \qquad \forall t,\ i,\ s \quad (2.10n)$$

$${SOC_{s,t+1}}^i = {SOC_{s,t}}^i + \left(P_{s,t}^{in\,i} \eta_s^{in} - \frac{P_{s,t}^{out\,i}}{\eta_s^{out}} \right) \Delta t \qquad \forall t,\ i,\ s \quad (2.10o)$$

This model consists of the minimum-up/minimum-down constraints and the start-up/shut-down logic of the UC decision variables, represented by (2.10c)-(2.10f). Equations (2.10g)-(2.10o) are the DG and ESS constraints describing different types of units in the system, and must be feasible for each scenario. Each scenario is optimized simultaneously using the same set of first-stage solutions, thus guaranteeing the minimum cost solution of the binary variables for a feasible recourse. Finally, in order to maintain the SOC_{t+1} as a first-stage variable in the SUC model, equation (2.10b) fixes the value of this variable for all scenarios.

The source of uncertainty in the proposed EMS for each scenario is defined by the pair $\{P^i_{\omega,t}, \pi_i\}$, where $P^i_{\omega,t}$ is a possible RE profile of the power output for unit ω at time t. Each scenario i is also characterized by its probability π_i, which is also the probability of a given recourse solution $\{P^i_{g,t}, P^i_{sh}, P^i_c\}$; both values are used to calculate the expected value of the recourse in (2.10a). Each scenario is considered to be indistinguishable from others from the first-stage point-of-view.

Statistic ensembles is the preferred technique to generate the scenarios, given that the approach intrinsically incorporates the accuracy of the forecasting algorithm into the calculations. The method also respects the temporal correlation of forecast errors by embedding them in all the scenarios for the horizon of interest [23]. This technique is not

computationally expensive; thus, once a forecast is issued, it can be immediately applied.

The stochastic approach detailed in (2.10), combined the advantages of the detailed mathematical formulations proposed in [12] is able to produce a reliable microgrid EMS with a probabilistic immunity to the uncertainties, as explained in [51]. In this paper, the uncertainty-aware EMS was tested under different configurations in order to obtain the most suitable combination of parameters; the best results were obtained when used with a 24 hour look-ahead window, and scenarios generated with a technique that best represented the uncertainty.

2.4 Robust Optimization

Robust two-stage recourse models are a suitable alternative for decision making under uncertainty, since recourse decisions are made representing random variables using uncertainty sets rather than probabilistic models [34]. This feature has made RO a popular approach, as it requires few or no assumptions on probability information, thus abating the difficulties related to identification of PDFs for RE sources. The concept was first proposed by Soyster in [73], who developed a linear optimization model employing the least favorable realization of the uncertainty; however, issues related to overconservatism and computational tractability discouraged its application until more recently. Thus, recent work has promoted the use of this technique in several engineering applications; for example, in [74] the authors propose efficient algorithms to solve robust counterparts of problems with ellipsoidal uncertainty sets; also, [75] exploited the characteristics of polyhedral uncertainty formulations by proposing a measure of robustness referred to as uncertainty budget, to manage the trade-off between efficiency and reliability.

Two-stage RO has a higher flexibility when compared with other techniques, given the feature of RO to model uncertainty by a deterministic set [76]. In this model, the first-stage decisions are determined after the worst case of the uncertain variables is known, which is referred to as adjustable or robust optimization. The definitions and mathematical properties of the robust adaptable problem are presented in [77], where the authors detail the advantages of these models and discuss the computational tractability of different formulations.

The two-stage RO mathematical model for the multi-period RHC (2.6a) can be stab-

lished as follows:

$$\min_{z_1,z_2} \sum_{t}^{t+n} \left[J_1(z_{1t}, y_t) + \underbrace{\max_{\delta} \quad J_2(z_{2t}, y_t)}_{\text{Worst-case realization of the recourse}} \right] \tag{2.11a}$$

$$\text{s.t.} \quad H_1\left(z_{1t}, y_t, \rho\right) \leq 0 \qquad \forall t \tag{2.11b}$$

$$H_2\left(z_{2t}, y_t, \rho, \mathcal{F}^*|t, \delta\right) \leq 0 \qquad \forall t \tag{2.11c}$$

$$H_3\left(z_{1t}, z_{2t}, y_t, \rho, \mathcal{F}^*|t, \delta\right) \leq 0 \qquad \forall t \tag{2.11d}$$

$$\delta \in \mathcal{U} \tag{2.11e}$$

This formulation determines the least-cost feasible solution of the first-stage variables z_1 considering the least favorable recourse. Conceptually, the recourse is the optimal solution of the control variables z_2 to the worst-case realization of the uncertainty represented by the vector of uncertain variables δ, which can be interpreted as a mismatch in the information from the forecasted input $\mathcal{F}^*|t$, the system parameters ρ, or both. The uncertain variables must be bounded to a set $\mathcal{U}$ according to their characteristics. If the model parameters are not affected by the uncertainty and only the forecast input has uncertainty, the problem is considered to have fixed recourse, given that the available system resources to manage the uncertainty are fixed. This type of modeling of the uncertainty is called "affine adaptability", as per [77], where the author provides mathematical proofs that for certain structures of the uncertainty set, the mathematical problem can be solved efficiently and in polynomial time. Moreover, the theoretical bases are presented to demonstrate that in a system with linear constraints affine rules lead to optimal results, defining the "worst case" of the uncertainty as the largest value of the objective function over all the realizations of the variables in the uncertainty set, i.e.,

$$z_{2\text{worst case}} = \min_{z_2} \quad \left\{ \sup_{\delta \in \mathcal{U}} \mathcal{J}_2(z_2, y) \middle| z_2 \in \mathcal{H}, y \in \mathcal{H} \right\} \tag{2.12}$$

which corresponds to the minimal cost solution of the supremum of the values within the uncertainty set, such that the solutions for z_2 and y are within the feasibility set $\mathcal{H}$ defined by (2.8b)-(2.8c) [74].

A detailed analysis of different uncertainty set models and their computational tractability is discussed in [78], where the authors prove that in order to maintain a linear tractability, the uncertainty set must be defined as a polyhedron, such that the additional equations

in the mathematical program can be modeled as a "simplex". This is particularly important for the RUC formulation in order to avoid introducing non-linearities and maintain the problem as an MILP. Furthermore, the hedging level of the first-stage decisions is controlled by the parameters of the uncertainty set, given that the levels of conversativism are directly related to the definition of $\mathcal{U}$. There are major challenges related to the structure and description of the uncertainty set and its relationship with RE power forecast accuracy; if the structure of the uncertainty set is not appropriately defined, it may lead to non-convex problem formulations. Hence when using polyhedral sets, the decision maker assumes that the uncertain variable is bounded by a symmetric range known as variation distance, i.e., at each time step, the realization $\mathcal{F}_{kt}$ belongs to an interval $[\delta_t - \mathcal{F}_t^*|_t, \mathcal{F}_t^*|_t + \delta_t]$, as shown in Figure 2.4. In this context, $\mathcal{U}$ can be mathematically defined as follows:

$$\mathcal{U} = \left\{ \delta \middle| \ |\delta_t| \leq \delta_t^{max} \wedge \sum_{t}^{t+n} \frac{|\delta_t|}{\delta_t^{max}} \leq \Gamma \quad \forall t \right\} \tag{2.13}$$

where Γ is referred to as the budget of uncertainty, and characterizes the relationship among the individual uncertainty variables. An extensive discussion about the significance of Γ for different RO models is presented in [75]. This type of uncertainty sets are known as cardinal uncertainty sets, and the decision-maker risk preference is represented by the selection of Γ and δ_t^{max}, with different interpretations used in the literature according to the modeling interest and the problem at hand, for example:

- The maximum number of variables that can be at their least-favorable values simultaneously (e.g.,[35]).
- The correlation between uncertain variables of different natures or physical locations (e.g.,[79]).
- The maximum number of periods the variables can reach the worst value in a look-ahead window (e.g., [52]).

In the context of this research, δ_t^{max} is the maximum value of this mismatch at time t, and Γ corresponds to the number of periods a mismatch happens.

Relationship between SO and RO

As discussed in [76] and detailed in Figure 2.5, there is a relationship between the SO and RO approaches. The stochastic approach solves the two-stage problem (2.7) for all

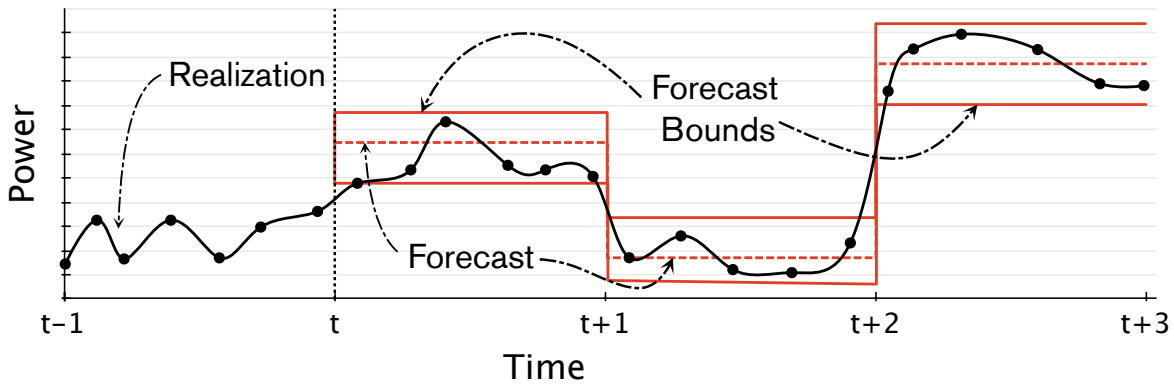

Figure 2.4: RO uncertainty representation

the scenarios that define the uncertainty space (depicted as dots in Figure 2.5), assigning some probability to each one; however, only a few scenarios play a relevant role in the hedging of the first stage variables due to their effect on the recourse actions. Conversely, a robust approach with a polyhedral uncertainty set solves for the vertices of the simplex model (represented as crosses in Figure 2.5), where one of those vertices is regarded as the worst-case realization, defining the most pessimistic recourse without any regards for the probability of that outcome. Moreover, if the uncertainty set is expanded or reduced, it can include more or less scenarios, and some may be left out, changing the size of the uncertainty space.

The RO-based approach operates with the underlying assumption that the uncertainty set is capable of providing a continuos representation of the uncertain space, and that is accurately characterized by the least favorable outcome of the recourse. In the other hand, SO-based approaches solve for the expected value of the recourse, represented as the weighted sum of uncertain outcomes given their probabilities. For SO the calculation is done for the entire space that represents the uncertain variable, while in RO the interest is only for the result of the worst outcome.

The aforementioned discussion portraits the conceptual difference between the two approaches to hedge the system. SO is based on the expected recourse and assumes that the i scenarios are enough to represent the uncertainty. On the other hand RO's objective is to find, within the continuos representation of the uncertainty, the scenario that is more detrimental to the system's performance, and assumes that by guarantying feasibility for that scenario any other one will be also be feasible.

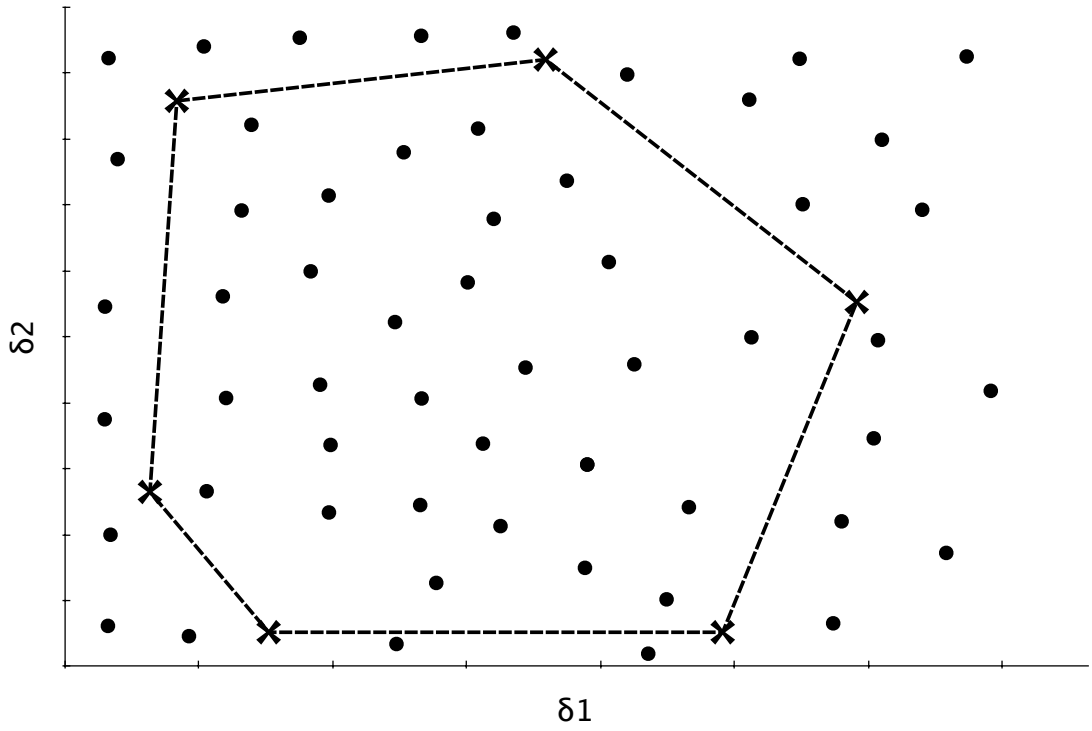

Figure 2.5: Comparison between RO and SO approaches

2.4.1 Primal cutting-planes Algorithm

Optimization algorithms based on the concept of cutting-planes is a very mature area of study, with a wide range of applications. Such algorithms include the Benders' decomposition approach [80], Dantzing-Wolfe decomposition [81], and others widely discussed in [82]. In this section, the interest is to describe the algorithm used to solve the RUC problem within the microgrid EMS, known as the primal cut decomposition algorithm proposed in [83]. The primal cutting-planes is based on Kelley's algorithm, originally presented in [84], to solve optimization problems with linear objective functions over a convex non-linear set of constraints. The author in [84] proposes that the convex optimization problem can be solved employing an outer approximation of the convex area using an adversarial problem, and mentions that this problem is easy to solve when the convex approximation is defined by a finite set of constraints, thus making it appropriate for the RUC problem.

The inclusion of primal cutting-planes is regarded as a constraint-and-column generation strategy [85]. In this context, the formulation of the two-stage RO exploits the struc-

ture of the recourse approach discussed in section 2.2.2. Other cutting-planes methods generate the cuts using the information from the dual problem, following the mathematical idea behind Benders' decomposition such as [41]. The primal cutting-plane algorithm is theoretically able to handle any structure of the uncertainty set, and given the assumption of complete recourse with a polyhedral uncertainty set, the adversarial maximization problem over the uncertain variables is a Linear Programming (LP) problem. Hence, for the RUC application, a finite set of constraints primal to the first stage are defined at each iteration by the solution of the recourse problem (2.8) [76].

Similar to other decomposition techniques, the primal cut is solved using a master- sub-problem framework. The sub-problem is defined using the formulation of the worst-case recourse (2.12) as follows:

$$\min_{z_2^{k+1}} \max_{\delta^{k+1}} \quad \mathcal{J}_2(z_2^{k+1}, y^{k+1}) \tag{2.14a}$$

$$\text{s.t.} \quad H_2\left(z_{2t}^{k+1}, y_t^{k+1}, \rho, \mathcal{F}^* | t, \delta^{k+1}\right) \leq 0 \qquad \forall t \tag{2.14b}$$

$$H_3\left(z_{1t}^{k}, z_{2t}^{k+1}, y_t^{k+1}, \rho, \mathcal{F}^* | t, \delta^{k+1}\right) \leq 0 \qquad \forall t \tag{2.14c}$$

$$\delta^{k+1} \in \mathcal{U} \tag{2.14d}$$

This mathematical model provides the optimal solution for z_2^{k+1} to handle the least favorable realization of the uncertain variables δ^{k+1} for iteration k starting at $k = 0$. In the developed RUC, the formulation includes a sufficiently large recourse, given by the load shedding and power curtailment variables, thus always guaranteeing a feasible solution.

After solving for the uncertain variables in the sub-problem (2.14), the resulting δ^{k+1} is used to generate the cuts in the master problem at each iteration k, leading to the following mathematical formulation:

$$\min_{z_1^{k+1}, \theta^{k+1}} \quad \mathcal{J}_1(z_1^{k+1}, y^{k+1}) + \theta^{k+1} \tag{2.15a}$$

$$\text{s.t.} \quad \mathcal{J}_2(z_2^{k+1}, y^{k+1}) \leq \theta^{k+1} \qquad \forall k \tag{2.15b}$$

$$H_1\left(z_{1t}^{k+1}, y_t^{k+1}, \rho\right) \leq 0 \qquad \forall t \tag{2.15c}$$

$$H_2\left(z_{2t}^{k+1}, y_t^{k+1}, \rho, \mathcal{F}^* | t, \delta^{k+1}\right) \leq 0 \qquad \forall t,\ k \tag{2.15d}$$

$$H_3\left(z_{1t}^{k+1}, z_{2t}^{k+1}, y_t^{k+1}, \rho, \mathcal{F}^* | t, \delta^{k+1}\right) \leq 0 \qquad \forall t,\ k \tag{2.15e}$$

The algorithm dynamically creates the cuts by replicating the set of constraints (2.15b)-(2.15e) from the primal of the problem, after the solution from the recourse is obtained. For the proposed RUC, when the model has fixed recourse, the algorithm can obtain the

optimal solution in a finite number of iterations [76], which is important, since this allows its application to real-time dispatch. The iterative algorithm process of the primal cutting-planes can be generalized as follows:

set $k = 0$, $UB^k = +\infty$, $LB^k = -\infty$, $z_1 = z_1^0$
while $k \leq$ *Max Iter.* **do**
  while $UB^k - LB^k \geq \epsilon$ **do**
    solve *Sub-problem (2.14)* **return**
      Sub-problem solution: $\{z_2^{k+1}, \delta^{k+1}\}$
    end
    update $UB^{k+1} = \min\left\{UB^k, \mathcal{J}_1(z_1^k) + \mathcal{J}_2(z_2^{k+1})\right\}$;
    Introduce primal cuts (2.15b)-(2.15e) for kth iteration
    solve *Master-problem (2.15)* **return**
      Master-problem solution: $\{z_1^1, \ldots, z_1^{k+1}, y^{k+1}, \theta^{k+1}\}$
    end
    update $LB^{k+1} = \mathcal{J}_1(z_1^{k+1}) + \theta^{k+1}$;
    update $k = k + 1$
  end
  Optimal solution: z_1^{k+1}
end
Most recent solution: z_1^{k+1}

As discussed in [76], this algorithm posseses a better performance than the dual-based approaches, provided that the sub-problem is able to identify a "significant" scenario at each iteration, thus decreasing the convergence rates (i.e, reducing the $UB^k - LB^k$ gap). Moreover, the primal cut introduces more variables and constraints than the dual-decomposition approaches, and thus maintains the structure of the problem improving the overall performance.

2.5 Summary

This chapter reviewed various concepts and mathematical tools used throughout this thesis in order to accomplish the research objectives. The microgrid concept was first introduced, and providing an overview of the control requirements and structure appropriate for isolated microgrids. Afterwards, the RHC technique was introduced and formalized, including a discussion on its implementation, as well as advantages and disadvantages of its application to EMS. Also, the recourse formulation of problems under uncertainty was then

discussed along with the general mathematical model for SO. The SUC model applied to microgrid EMS was also presented. Finally, the RO-based recourse model was presented including a detailed description of the algorithm used to solve the RUC problem.

Chapter 3

Robust EMS Approach

This chapter presents the application of the theoretical foundations of system modeling, RHC, two-stage actions and RO to the problem of isolated microgrid dispatch. First, the RUC model for microgrid EMS is presented, including the master-, sub-problem decomposition formulation to solve the RUC by means of the primal cutting-planes algorithm; a unique trait of the proposed RUC model is the inclusion of ESS modeling for the first time. Second, a framework to define the parameters of the uncertainty set based on historic information is proposed and applied to select the uncertainty policies used throughout this thesis. Finally, the EMS architecture is presented and relevant implementation considerations are discussed, including the solution procedure and an enhancement of the previously-proposed three-phase OPF ESS model.

3.1 Primal cutting-planes Formulation of RUC

The RUC mathematical model objective is to yield the least-cost uncertainty-immune solution for the UC variables given a bounded uncertainty set. This approach is quite appealing given that, for the RE-based DERs, the probabilistic information cannot be estimated appropriately or in some cases is unavailable. In the proposed RUC model for isolated microgrids, the binary variables of the UC problem are determined assuming that the uncertainty is in the dispatch variables, and the uncertainty only affects the forecasted power output of the RE and not other system parameters.

The proposed microgrid EMS employs the RUC to hedge the system against uncertainty by committing enough units to perform the dispatch reliably; consequently, the variables

$w_{g,t}, u_{g,t}$ and $v_{g,t}$ are defined as part of the master-problem. Furthermore, in the presence of storage, the EMS should be able to maintain the SoC of the ESS at a level that enables the system to cope with the RE variability; this is accomplished by including the SoC at time step $t+1$ as a master-problem variable. This inclusion of the ESS has not been considered in the classical RUC models for bulk power systems. Hence, the RUC problem for the microgrid with storage can be formulated as follows:

$$\min_{\substack{u_{g,t},v_{g,t}\\ w_{g,t},P^k_{g,t}}} \max_{\Delta P_{w,t}} \sum_t \sum_g \left[C^u_g u_{g,t} + C^v_g v_{g,t} + C^w_g w_{g,t} + \underbrace{C^P_g P_{g,t} + C_{sh} P_{sh,t} + C_c P_{c,t}}_{\text{Recourse}} \right] \tag{3.1a}$$

$$\text{s.t.} \quad u_{g,t} - v_{g,t} = w_{g,t} - w_{g,t+1} \qquad \forall t,\ g \tag{3.1b}$$

$$v_{g,t} + u_{g,t} \leq 1 \qquad \forall t,\ g \tag{3.1c}$$

$$w_{g,t} - w_{g,t-1} - w_{g,t_u} \leq 0 \qquad \forall t_u : 1 \leq t_u - (t-1) \leq MU_g,\ t,\ g \tag{3.1d}$$

$$w_{g,t-1} - w_{g,t} + w_{g,t_u} \leq 1 \qquad \forall t_u : 1 \leq t_u - (t-1) \leq MD_g,\ t,\ g \tag{3.1e}$$

$$\sum_g P_{g,t} + \sum_\omega P^*_{\omega,t}(1 - \Delta P_{\omega,t}) - P_{c,t} = \sum_l P_{l,t} - P_{sh,t} \qquad \forall t \tag{3.1f}$$

$$P^{min}_g \cdot w_{g,t} \leq P_g \leq P^{max}_g \cdot w_{g,t} \qquad \forall t,\ g \tag{3.1g}$$

$$P_{g,t} - P_{g,t-1} - u_{g,t} \cdot P^{max}_g \leq RP_g \qquad \forall t,\ g \tag{3.1h}$$

$$P_{g,t-1} - P_{g,t} - v_{g,t} \cdot P^{max}_g \leq RD_g \qquad \forall t,\ g \tag{3.1i}$$

$$P_{s,t} = P^{out}_{s,t} - P^{in}_{s,t} \qquad \forall t,\ s \tag{3.1j}$$

$$P^{in}_{s,t} \leq P^{max}_s \qquad \forall t,\ s \tag{3.1k}$$

$$P^{out}_{s,t} \leq P^{max}_s \qquad \forall t,\ s \tag{3.1l}$$

$$SOC^{min}_s \leq SOC_{s,t} \leq SOC^{max}_s \qquad \forall t,\ s \tag{3.1m}$$

$$SOC_{s,t+1} = SOC_{s,t} + \left(P^{in}_{s,t}\eta^{in}_s - \frac{P^{out}_{s,t}}{\eta^{out}_s} \right) \Delta t \qquad \forall t,\ s \tag{3.1n}$$

$$\Delta P_{\omega,t} \in \mathcal{U} \qquad \forall t,\ \omega \tag{3.1o}$$

where the cost function and constraints follow the system modeling approach discussed in Chapter 2. The objective function (3.1a) accounts for the commitment costs and the cost of the least-favorable recourse; the constraints (3.1b)-(3.1e) are H_1 in the recourse model

(2.7), since they are relevant only to the commitment variables; and H_2 is characterized by (3.1g)-(3.1l) and (3.1m)-(3.1n) for $t > t+1$, which model the system constraints, such as the DERs and ESS operating characteristics. Finally, the coupling constraints H_3 are given by (3.1f) and (3.1m)-(3.1n) for $t = t+1$, as variables from both stages are present in these equations.

Uncertainty Set

Since the uncertain variables in the proposed model are time-related, as discussed in Section 2.4, the uncertainty vector is defined by (2.13). Hence, given a power forecast $P^*_{\omega,t}$ for an RE source ω at time t, the uncertainty corresponds to the mismatch $\Delta P_{\omega,t}$ between the forecast and the actual power output; thus, the uncertainty vector for each RE source ω is defined as $\delta_\omega = [\Delta P_{\omega,t} \ \dots \ \Delta P_{\omega,t+n}]^T$.

The mismatch is accounted for in the power balance equation following an affine robust model, complying with the requirements to maintain tractability discussed in Section 2.4. Also, the uncertainty set must be defined as a simplex, such that the RUC is kept as an MILP problem. In order to meet these modeling requirements, the definition of the uncertainty set for each RE source ω, which is based on absolute values, can be transformed into a set of linear constraints by including the positive variables ${\Delta P_{\omega,t}}^+$ and ${\Delta P_{\omega,t}}^-$ as follows:

$$\Delta P_{w,t} = {\Delta P_{\omega,t}}^+ - \Delta P^-_{w,t} \qquad \forall t \qquad (3.2a)$$

$${\Delta P_{\omega,t}}^+ - {\Delta P_{\omega,t}}^{max} \leq 0 \qquad \forall t \qquad (3.2b)$$

$${\Delta P_{\omega,t}}^- - {\Delta P_{\omega,t}}^{max} \leq 0 \qquad \forall t \qquad (3.2c)$$

$$\sum_t \left[\frac{{\Delta P_{\omega,t}}^+ + {\Delta P_{\omega,t}}^-}{{\Delta P_{\omega,t}}^{max}} \right] - \Gamma \leq 0 \qquad (3.2d)$$

This set of equations is included in the mathematical model described by (3.1) substituting (3.1o) with (3.2) for each RE source, with the decision-maker risk preference being represented by the selection of the pair $(\Gamma, {\Delta P_{\omega,t}}^{max})$. The budget of uncertainty Γ corresponds to the number of periods in which the RE source power deviates from the forecasted value, and the value of ${\Delta P_{\omega,t}}^{max}$ is the maximum value of the mismatch from the forecast as per (3.2). These values are calculated from the historical performance of the forecasting system, as discussed in the forthcoming sections. Note that, in the context of isolated

microgrids, the uncertainty of similar RE sources (e.g., solar or wind) is bundled into one variable $\Delta P_{\omega,t}$ for each time step, given the limited physical dispersion.

The solution algorithm for (3.1) is based on the separable problems described in Section 2.4.1, where the uncertainty δ^{k+1} is considered as a variable only in the sub-problem, such that the sub-problem is solved independently from the master-problem. Following the definitions of "wait-and-see" and "here-and-now" actions detailed in Section 2.2.2, the next subsections discuss the sub- and master-problem mathematical model of the RUC.

Sub-problem

The sub-problem is the equivalent of the mathematical formulation defined by (2.14) applied to the UC problem including storage. Hence, the optimization problem is solved assuming fix values for the first stage variables $z_{1t}^k = [w_{1,t}^k \dots w_{g,t}^k u_{1,t}^k \dots u_{g,t}^k v_{1,t}^k \dots v_{g,t}^k SOC_{1,t+1}^k \dots SOC_{s,t+1}^k]^T$, which are obtained from the current system state for iteration $k = 0$, and from the master-problem for every other iteration k . Hence, the RUC sub-problem mathematical model can be defined as follows:

$$\min_{{P_{g,t}}^{k+1}} \max_{{\Delta P_{\omega,t}}^{k+1}} \sum_t \left[C_{sh} P_{sh,t}^{k+1} + C_c P_{c,t}^{k+1} + \sum_g C_g^P P_{g,t}^{k+1} \right] \tag{3.3a}$$

$$\text{s.t.} \sum_g P_{g,t}^{k+1} + \sum_\omega P_{\omega,t}^* (1 - \Delta P_{\omega,t}^{k+1}) - P_{c,t}^{k+1} = \sum_l P_{l,t} - P_{sh,t}^{k+1} \qquad \forall t \tag{3.3b}$$

$$P_g^{min} \cdot w_{g,t}^k \le P_g^{k+1} \le P_g^{max} \cdot w_{g,t}^k \qquad \forall t,\ g \tag{3.3c}$$

$$P_{g,t}^{k+1} - P_{g,t-1}^{k+1} - u_{g,t}^k \cdot P_g^{max} \le RU_g \qquad \forall t,\ g \tag{3.3d}$$

$$P_{g,t-1}^{k+1} - P_{g,t}^{k+1} - v_{g,t}^k \cdot P_g^{max} \le RD_g \qquad \forall t,\ g \tag{3.3e}$$

$$P_{s,t}^{k+1} = P_{s,t}^{outk+1} - P_{s,t}^{ink+1} \qquad \forall t,\ s \tag{3.3f}$$

$$P_{s,t}^{ink+1} \le P_s^{max} \qquad \forall t,\ s \tag{3.3g}$$

$$P_{s,t}^{outk+1} \le P_s^{max} \qquad \forall t,\ s \tag{3.3h}$$

$$SOC_s^{min} \le SOC_{s,t}^{k+1} \le SOC_s^{max} \qquad \forall t > t+1,\ s \tag{3.3i}$$

$${SOC_{s,t+1}}^{k+1} = {SOC_{s,t}}^{k+1} + \left({P_{s,t}^{in}}^{k+1} \eta_s^{in} - \frac{P_{s,t}^{outk+1}}{\eta_s^{out}} \right) \Delta t \qquad \forall t > t+1,\ s \tag{3.3j}$$

$$\Delta P_{w,t}^{k+1} = \Delta P_{\omega,t}^{+\ k+1} - \Delta P_{\omega,t}^{-\ k+1} \qquad \forall t,\ \omega \qquad (3.3k)$$

$$\Delta P_{\omega,t}^{+\ k+1} - \Delta P_{\omega,t}{}^{max} \leq 0 \qquad \forall t,\ \omega \qquad (3.3l)$$

$$\Delta P_{\omega,t}^{-\ k+1} - \Delta P_{\omega,t}{}^{max} \leq 0 \qquad \forall t,\ \omega \qquad (3.3m)$$

$$\sum_{t} \left[\frac{\Delta P_{\omega,t}^{+\ k+1} + \Delta P_{\omega,t}^{-\ k+1}}{\Delta P_{\omega,t}{}^{max}} \right] - \Gamma \leq 0 \qquad \forall \omega \qquad (3.3n)$$

where system state variables correspond to the ESS model variables $y_t^{k+1} = [P_{1,t}^{out\,k+1} \ \ldots \ P_{s,t}^{out\,k+1} \ P_{1,t}^{in\,k+1} \ \ldots \ P_{s,t}^{in\,k+1} \ SOC_{1,t}{}^{k+1} \ \ldots \ SOC_{s,t}{}^{k+1}]^T$, considering that in order to maintain $SOC_{s,t+1}$ as a first-stage variable, the formulation includes neither $SOC_{s,t}$ limit constraints (3.3i), nor the charging equation (3.3j) for $t = t + 1$. The system parameters ρ are the different operation limits of the units, such as the ramping rates, maximum and minimum power output, and the ESS efficiencies, and the recourse actions $z_{2t}^{k+1} = [P_{1,t}^{k+1}, \ldots, P_{g,t}^{k+1}, P_{c,t}^{k+1}, P_{sh,t}^{k+1}]^T$. Finally, the result is the uncertainty vector $\delta_{\omega}^{k+1} = [\Delta P_{\omega,t}{}^{k+1}, \ldots, \Delta P_{\omega,t+n}{}^{k+1}]$ which is composed of the individual deviations from the forecast of the RE source ω over the entire look-ahead window; these deviations are more detrimental to the system's performance and generate the most expensive recourse.

The sub-problem (3.3) has a min-max structure, which is a saddle-point type of mathematical problem and in general is non-convex [41]; however, through the dual representation of the recourse, this can be transformed into a max-max formulation that can be easily solved. Thus, the resulting dual mathematical model is as follows:

$$\max_{\substack{\lambda^{k+1},\mu^{k+1},\beta^{k+1},\varepsilon^{k+1},\\ \alpha^{k+1},{\Delta P_{\omega,t}}^{k+1}}} \sum_t \Bigg[\lambda_t^{k+1} \Big[\sum_l P_{l,t} - \sum_\omega P^*_{\omega,t} \Big] + \underbrace{\sum_\omega P^*_{\omega,t} {\Delta P_{\omega,t}}^{k+1} \lambda_t^{k+1}}_{\text{Bi-linear term.}}$$

$$\begin{aligned}
&+ \sum_g \Big[\mu 1_{g,t}^{k+1} P_g^{max} w_{g,t}^k - \mu 2_{g,t}^{k+1} P_g^{min} w_{g,t}^k \\
&\quad + \beta 1_{g,t}^{k+1} (RU_g + u_{g,t}^k P_g^{max}) \\
&\quad + \beta 2_{g,t}^{k+1} (RD_g + v_{g,t}^k P_g^{max}) \Big] \\
&+ \sum_s \Big[\mu 1_{s,t}^{k+1} P_s^{max} w_{s,t}^k - \mu 2_{s,t}^{k+1} P_s^{min} w_{s,t}^k \\
&\quad + \varepsilon 2_{s,t}^{k+1} SOC_s^{max} - \varepsilon 3_{s,t}^{k+1} SOC_s^{min} \\
&\quad - \varepsilon 5_{s,t}^{k+1} P_s^{max} + \varepsilon 6_{s,t}^{k+1} P_s^{max} \Big] \Bigg]
\end{aligned} \tag{3.4a}$$

$$\text{s.t. } \lambda_t^{k+1} + \mu 1_{g,t}^{k+1} - \mu 2_{g,t}^{k+1} + \beta 1_{g,t}^{k+1} - \beta 1_{g,t-1}^{k+1} - \beta 2_{g,t}^{k+1} + \beta 2_{g,t-1}^{k+1} \le C_g^P \qquad \forall t,\ g \tag{3.4b}$$

$$\lambda_t^{k+1} + \mu 1_{s,t}^{k+1} - \mu 2_{s,t}^{k+1} + \beta 1_{s,t}^{k+1} - \beta 1_{s,t-1}^{k+1} - \beta 2_{s,t}^{k+1} + \beta 2_{s,t-1}^{k+1} + \varepsilon 1_{s,t}^{k+1} \le 0 \qquad \forall t,\ s \tag{3.4c}$$

$$\lambda_t^{k+1} \le C_{sh} \qquad \forall t \tag{3.4d}$$

$$\lambda_t^{k+1} \le C_c \qquad \forall t \tag{3.4e}$$

$$[\varepsilon 2_{s,t+1}^{k+1} \quad \varepsilon 3_{s,t+1}^{k+1} \quad \varepsilon 4_{s,t+1}^{k+1}] = E_s^k \qquad \forall s \tag{3.4f}$$

$$\varepsilon 2_{s,t}^{k+1} - \varepsilon 3_{s,t}^{k+1} - \varepsilon 4_{s,t}^{k+1} + \varepsilon 4_{s,t-1}^{k+1} \le 0 \qquad \forall t,\ s \tag{3.4g}$$

$$-\varepsilon 1_{s,t}^{k+1} + \varepsilon 4_{s,t}^{k+1} \frac{1}{\eta_s^{out}} \Delta t \le 0 \qquad \forall t,\ s \tag{3.4h}$$

$$\varepsilon 1_{s,t}^{k+1} - \varepsilon 4_{s,t}^{k+1} \eta_s^{in} \Delta t \le 0 \qquad \forall t,\ s \tag{3.4i}$$

$$\Delta P_{w,t}^{k+1} = {\Delta P_{\omega,t}^+}^{k+1} - {\Delta P_{\omega,t}^-}^{k+1} \qquad \forall t,\ \omega \tag{3.4j}$$

$${\Delta P_{\omega,t}^+}^{k+1} - {\Delta P_{\omega,t}}^{max} \le 0 \qquad \forall t,\ \omega \tag{3.4k}$$

$${\Delta P_{\omega,t}^-}^{k+1} - {\Delta P_{\omega,t}}^{max} \le 0 \qquad \forall t,\ \omega \tag{3.4l}$$

$$\sum_t \left[\frac{{\Delta P_{\omega,t}^+}^{k+1} + {\Delta P_{\omega,t}^-}^{k+1}}{{\Delta P_{\omega,t}}^{max}} \right] - \Gamma \le 0 \qquad \forall \omega \tag{3.4m}$$

where (3.4b) and (3.4c) are the dual equations for the power variables of the dispatchable generation units and the ESS units, respectively. An extra term at the end of (3.4c) is required to include the dual variable from (3.3f), and constraints (3.4g)-(3.4i) represent the dual from the book-keeping model variables for the ESS. Finally, the constraint (3.4f) is added to fix the dual variables of (3.3i) and (3.3j) for $t+1$, since those variables are not solved in the sub-problem.

This procedure introduces bi-linear terms in (3.4a), as reported in the RUC literature (e.g., [40]). Dealing with the bi-linear term is a non-trivial problem; however, in (3.4) the uncertainty set equations (3.4j)-(3.4m) are decoupled from the microgrid model constraints. Since there are no coupling constraints, the bilinear term can be separated, with the uncertainty set constraints being treated as an independent optimization problem as follows:

$$\max_{\Delta P_{\omega,t}^{k+1}} \sum_t \sum_\omega P_{\omega,t}^* {\Delta P_{\omega,t}}^{k+1} \lambda_t^{k+1} \tag{3.5a}$$

$$\text{s.t.} \quad \Delta P_{w,t}^{k+1} = \Delta P_{\omega,t}^{+\,k+1} - \Delta P_{\omega,t}^{-\,k+1} \qquad \forall t,\, \omega \tag{3.5b}$$

$$\Delta P_{\omega,t}^{+\,k+1} - {\Delta P_{\omega,t}}^{max} \leq 0 \qquad \forall t,\, \omega \tag{3.5c}$$

$$\Delta P_{\omega,t}^{-\,k+1} - {\Delta P_{\omega,t}}^{max} \leq 0 \qquad \forall t,\, \omega \tag{3.5d}$$

$$\sum_t \left[\frac{\Delta P_{\omega,t}^{+\,k+1} + \Delta P_{\omega,t}^{-\,k+1}}{{\Delta P_{\omega,t}}^{max}} \right] - \Gamma \leq 0 \qquad \forall \omega \tag{3.5e}$$

where the dual variable of the balance equation (3.3b), λ_t, is regarded as a parameter, given the aforementioned decoupling in the max-max problem. Thus, (3.5) can be reformulated to eliminate the terms ${\Delta P_{\omega,t}}^{k+1} \lambda_t^{k+1}$ from the objective function using the strong duality theory and the KKT conditions as proposed in [79, 86], yielding an equivalent optimization problem which has the following form:

$$\max_{\alpha_\omega^{k+1}, \Delta P_{\omega,t}^{k+1}} \sum_t \left[{\Delta P_{\omega,t}}^{max} (\alpha 2_{\omega,t}^{k+1} + \alpha 3_{\omega,t}^{k+1}) \right] + \Gamma \alpha 4_\omega^{k+1} \tag{3.6a}$$

$$\text{s.t.} \quad \alpha 1_t^{k+1} = \lambda_t^{k+1} \sum_\omega P_{\omega,t}^* \qquad \forall t \tag{3.6b}$$

$$-\alpha 1_{\omega,t}^{k+1} + \alpha 2_{\omega,t}^{k+1} + \frac{\alpha 4_\omega^{k+1}}{{\Delta P_{w,t}}^{max}} = 0 \qquad \forall t,\, \omega \tag{3.6c}$$

$$\alpha 1_{\omega,t}^{k+1} + \alpha 3_{\omega,t}^{k+1} + \frac{\alpha 4_{\omega}^{k+1}}{\Delta P_{w,t}{}^{max}} = 0 \qquad \forall t,\ \omega \qquad (3.6d)$$

$$\Delta P_{w,t}^{k+1} = \Delta P_{\omega,t}^{+\ k+1} - \Delta P_{\omega,t}^{-\ k+1} \qquad \forall t,\ \omega \qquad (3.6e)$$

$$\Delta P_{\omega,t}^{+\ k+1} - \Delta P_{\omega,t}{}^{max} \leq 0 \qquad \forall t,\ \omega \qquad (3.6f)$$

$$\Delta P_{\omega,t}^{-\ k+1} - \Delta P_{\omega,t}{}^{max} \leq 0 \qquad \forall t,\ \omega \qquad (3.6g)$$

$$\sum_{t} \left[\frac{\Delta P_{\omega,t}^{+\ k+1} + \Delta P_{\omega,t}^{-\ k+1}}{\Delta P_{\omega,t}{}^{max}} \right] - \Gamma \leq 0 \qquad (3.6h)$$

$$\alpha 3_{\omega,t}^{k+1} \left[\Delta P_{\omega,t}^{+\ k+1} - \Delta P_{\omega,t}{}^{max} \right] = 0 \qquad \forall t,\ \omega \qquad (3.6i)$$

$$\alpha 2_{\omega,t}^{k+1} \left[\Delta P_{\omega,t}^{-\ k+1} - \Delta P_{\omega,t}{}^{max} \right] = 0 \qquad \forall t,\ \omega \qquad (3.6j)$$

$$\alpha 4_{\omega}^{k+1} \left[\sum_{t} \left[\frac{\Delta P_{\omega,t}^{+\ k+1} + \Delta P_{\omega,t}^{-\ k+1}}{\Delta P_{\omega,t}{}^{max}} \right] - \Gamma \right] = 0 \qquad \forall \omega \qquad (3.6k)$$

where $\alpha 1_{\omega,t}$, $\alpha 2_{\omega,t}$, $\alpha 3_{\omega,t}$, $\alpha 4_{\omega}$ are the dual variables of (3.5b)-(3.5e) for the uncertainty set of each RE unit ω. This eliminates the bi-linear term from the objective function in (3.6), but new bi-linear terms appear in the constraints (3.6i)-(3.6k). However, the KKT conditions can be regarded as a Mathematical Program with Equilibrium Constraints (MPEC) problem and reformulated into an MILP problem using disjunctive constraints [86, 87], which substitutes the conditional terms (3.6i)-(3.6k) with a new set of constraints using integer variables that transform them into linear constraints. Hence, the final sub-problem MILP model used in the iterative process is obtained after substituting (3.6) into (3.4), yielding the following optimization model:

$$
\begin{aligned}
\max_{\substack{\lambda^{k+1},\mu^{k+1},\varepsilon^{k+1},\\ \alpha^{k+1},\beta^{k+1}\\ {\Delta P_{\omega,t}}^{k+1}}} \sum_t \Bigg[& \lambda_t^{k+1}\Big[\sum_l P_{l,t} - \sum_\omega P^*_{\omega,t}\Big] \\
& \underbrace{+\big[{\Delta P_{\omega,t}}^{max}(\alpha 2^{k+1}_{\omega,t} + \alpha 3^{k+1}_{\omega,t})\big] + \Gamma \alpha 4^{k+1}_{\omega}}_{\text{Linear term substitute of the bi-linear}} \\
& + \sum_g \Big[\mu 1^{k+1}_{g,t} P^{max}_g w^k_{g,t} - \mu 2^{k+1}_{g,t} P^{min}_g w^k_{g,t} \\
& \quad + \beta 1^{k+1}_{g,t}(RU_g + u^k_{g,t} P^{max}_g) \\
& \quad + \beta 2^{k+1}_{g,t}(RD_g + v^k_{g,t} P^{max}_g)\Big] \\
& + \sum_s \Big[\mu 1^{k+1}_{s,t} P^{max}_s w^k_{s,t} - \mu 2^{k+1}_{s,t} P^{min}_s w^k_{s,t} \\
& \quad + \varepsilon 2^{k+1}_{s,t} SOC^{max}_s - \varepsilon 3^{k+1}_{s,t} SOC^{min}_s \\
& \quad - \varepsilon 5^{k+1}_{s,t} P^{max}_s + \varepsilon 6^{k+1}_{s,t} P^{max}_s\Big]\Bigg]
\end{aligned} \tag{3.7a}
$$

$$
\text{s.t. } \lambda_t^{k+1} + \mu 1^{k+1}_{g,t} - \mu 2^{k+1}_{g,t} + \beta 1^{k+1}_{g,t} - \beta 1^{k+1}_{g,t-1} - \beta 2^{k+1}_{g,t} + \beta 2^{k+1}_{g,t-1} \le C^P_g \qquad \forall t,\ g \tag{3.7b}
$$

$$
\lambda_t^{k+1} + \mu 1^{k+1}_{s,t} - \mu 2^{k+1}_{s,t} + \beta 1^{k+1}_{s,t} - \beta 1^{k+1}_{s,t-1} - \beta 2^{k+1}_{s,t} + \beta 2^{k+1}_{s,t-1} + \varepsilon 1^{k+1}_{s,t} \le 0 \qquad \forall t,\ s \tag{3.7c}
$$

$$
\lambda_t^{k+1} \le C_{sh} \qquad \forall t \tag{3.7d}
$$

$$
\lambda_t^{k+1} \le C_c \qquad \forall t \tag{3.7e}
$$

$$
[\varepsilon 2^{k+1}_{s,t+1} \quad \varepsilon 3^{k+1}_{s,t+1} \quad \varepsilon 4^{k+1}_{s,t+1}] = E^k_s \qquad \forall s \tag{3.7f}
$$

$$
\varepsilon 2^{k+1}_{s,t} - \varepsilon 3^{k+1}_{s,t} - \varepsilon 4^{k+1}_{s,t} + \varepsilon 4^{k+1}_{s,t-1} \le 0 \qquad \forall t,\ s \tag{3.7g}
$$

$$
-\varepsilon 1^{k+1}_{s,t} + \varepsilon 4^{k+1}_{s,t} \frac{1}{\eta^{out}_s} \Delta t \le 0 \qquad \forall t,\ s \tag{3.7h}
$$

$$
\varepsilon 1^{k+1}_{s,t} - \varepsilon 4^{k+1}_{s,t} \eta^{in}_s \Delta t \le 0 \qquad \forall t,\ s \tag{3.7i}
$$

$$
\alpha 1^{k+1}_t = \lambda^{k+1}_t \sum_\omega P^*_{\omega,t} \qquad \forall t \tag{3.7j}
$$

$$
{\Delta P_{\omega,t}}^{k+1} = {\Delta P^+_{\omega,t}}^{k+1} - {\Delta P^-_{\omega,t}}^{k+1} \qquad \forall t,\ \omega \tag{3.7k}
$$

$$
0 \le \alpha 2^{k+1}_{\omega,t} \le M(1 - b1^{k+1}_{\omega,t}) \qquad \forall t,\ \omega \tag{3.7l}
$$

$$0 \leq -\Delta P_{\omega,t}^{+\ k+1} + \Delta P_{\omega,t}{}^{max} \leq M\ b1_{\omega,t}^{k+1} \qquad \forall t,\ \omega \qquad (3.7\text{m})$$

$$0 \leq \alpha 3_{\omega,t}^{k+1} \leq M(1 - b2_{\omega,t}^{k+1}) \qquad \forall t,\ \omega \qquad (3.7\text{n})$$

$$0 \leq -\Delta P_{\omega,t}^{-\ k+1} + \Delta P_{\omega,t}{}^{max} \leq M\ b2_{\omega,t}^{k+1} \qquad \forall t,\ \omega \qquad (3.7\text{o})$$

$$0 \leq \Delta P_{\omega,t}^{-\ k+1} \leq M(1 - b3_{\omega,t}^{k+1}) \qquad \forall t,\ \omega \qquad (3.7\text{p})$$

$$0 \leq \alpha 1_{\omega,t}^{k+1} + \alpha 3_{\omega,t}^{k+1} + \frac{\alpha 4_{\omega}^{k+1}}{\Delta P_{w,t}{}^{max}} \leq M\ b3_{\omega,t}^{k+1} \qquad \forall t,\ \omega \qquad (3.7\text{q})$$

$$0 \leq \Delta P_{\omega,t}^{+\ k+1} \leq M(1 - b4_{\omega,t}^{k+1}) \qquad \forall t,\ \omega \qquad (3.7\text{r})$$

$$0 \leq -\alpha 1_{\omega,t}^{k+1} + \alpha 2_{\omega,t}^{k+1} + \frac{\alpha 4_{\omega}^{k+1}}{\Delta P_{w,t}{}^{max}} \leq M\ b4_{\omega,t}^{k+1} \qquad \forall t,\ \omega \qquad (3.7\text{s})$$

$$0 \leq \alpha 4_{\omega}^{k+1} \leq M(1 - b5_{\omega}^{k+1}) \qquad \forall \omega \qquad (3.7\text{t})$$

$$0 \leq -\sum_{t} \left[\frac{\Delta P_{\omega,t}^{+\ k+1} + \Delta P_{\omega,t}^{-\ k+1}}{\Delta P_{\omega,t}{}^{max}} \right] + \Gamma \leq M\ b5_{\omega}^{k+1} \qquad \forall \omega \qquad (3.7\text{u})$$

where the bi-linear term in the cost function has been substituted by (3.6a), and disjunctive constraints (3.7l)-(3.7u) are the transformed KKT conditions (3.6i)-(3.6k), with $b1_{\omega,t}$, $b2_{\omega,t}$, $b3_{\omega,t}$, $b4_{\omega,t}$, $b5_{\omega}$ representing integer variables and M being a large constant [87]. Note that there is no generalized formula to define the value of M, and must be selected according to the problem's characteristics. In the proposed RUC model, this constant is chosen as the maximum value of the left hand side of the uncertainty set equations (3.5), similar to what has been suggested in [88].

Master-Problem

The master-problem is the equivalent to the mathematical formulation defined by (2.15) applied to the proposed RUC model. Thus, once the sub-problem yields a solution for the values of the uncertainty vector δ_{ω}^{k+1} for every RE source ω, the result is employed in the iterative process described in Section 2.4.1 to update the solution of the firs-stage variables, which generates a set of cuts duplicating constraints (3.1f)-(3.1n) in the master problem at each iteration k. The MILP formulation for the master-problem is then defined as follows:

$$\min_{\substack{u_{g,t}^{k+1},v_{g,t}^{k+1},w_{g,t}^{k+1}\\ P_{g,t}^{k+1}}} \sum_t \sum_g \left[C_g^u u_{g,t}^{k+1} + C_g^v v_{g,t}^{k+1} + C_g^w w_{g,t}^{k+1}\right] + \theta^{k+1} \tag{3.8a}$$

$$\text{s.t.} \sum_t \left[C_{sh} P_{sh,t}^{k+1} + C_c P_{c,t}^{k+1} + \sum_g C_g P_{g,t}^{k+1}\right] \leq \theta^{k+1} \qquad \forall k \tag{3.8b}$$

$$SOC_{s,t+1}^{k+1} = SOC_s^{fix} \qquad \forall k \tag{3.8c}$$

$$u_{g,t}^{k+1} - v_{g,t}^{k+1} = w_{g,t}^{k+1} - w_{g,t+1}^{k+1} \qquad \forall t,\ g \tag{3.8d}$$

$$v_{g,t}^{k+1} + u_{g,t}^{k+1} \leq 1 \qquad \forall t,\ g \tag{3.8e}$$

$$w_{g,t}^{k+1} - w_{g,t-1}^{k+1} - w_{g,t_u}^{k+1} \leq 0 \qquad \forall t_u : 1 \leq t_u - (t-1) \leq MU_g,\ t,\ g \tag{3.8f}$$

$$w_{g,t-1}^{k+1} - w_{g,t}^{k+1} + w_{g,t_u}^{k+1} \leq 1 \qquad \forall t_u : 1 \leq t_u - (t-1) \leq MD_g,\ t,\ g \tag{3.8g}$$

$$\sum_g {P_{g,t}}^{k+1} + \sum_\omega P_{\omega,t}^* (1 - \Delta {P_{\omega,t}}^{k+1}) - {P_{c,t}}^{k+1} = \sum_l P_{l,t} - {P_{sh,t}}^{k+1} \qquad \forall t,\ k \tag{3.8h}$$

$$P_g^{min} \cdot w_{g,t}^{k+1} \leq {P_g}^{k+1} \leq P_g^{max} \cdot w_{g,t}^{k+1} \qquad \forall t,\ k,\ g \tag{3.8i}$$

$${P_{g,t}}^{k+1} - {P_{g,t-1}}^{k+1} - u_{g,t}^{k+1} \cdot P_g^{max} \leq RU_g \qquad \forall t,\ k,\ g \tag{3.8j}$$

$${P_{g,t-1}}^{k+1} - {P_{g,t}}^{k+1} - v_{g,t}^{k+1} \cdot P_g^{max} \leq RD_g \qquad \forall t,\ k,\ g \tag{3.8k}$$

$${P_{s,t}}^{k+1} = P_{s,t}^{out\,k+1} - P_{s,t}^{in\,k+1} \qquad \forall t,\ k,\ s \tag{3.8l}$$

$$P_{s,t}^{in\,k+1} \leq P_s^{max} \qquad \forall t,\ k,\ s \tag{3.8m}$$

$$P_{s,t}^{out\,k+1} \leq P_s^{max} \qquad \forall t,\ k,\ s \tag{3.8n}$$

$$SOC_s^{min} \leq {SOC_{s,t}}^{k+1} \leq SOC_s^{max} \qquad \forall t,\ k,\ s \tag{3.8o}$$

$${SOC_{s,t+1}}^{k+1} = {SOC_{s,t}}^{k+1} + \left(P_{s,t}^{in\,k+1} \eta_s^{in} - \frac{P_{s,t}^{out\,k+1}}{\eta_s^{out}}\right) \Delta t \qquad \forall t,\ k,\ s \tag{3.8p}$$

where θ is the auxiliary variable of the adversarial problem (3.8a)-(3.8b), that separates the objective function (3.1a) into the terms that are affected and those that are not affected by uncertainty (i.e., first- and second-stage problems, respectively). Additionally, (3.8c) is included in order to force $SOC_{s,t+1}$ to be a first-stage variable by fixing it to the same

value for each k^{th} iteration.

Given that the uncertainty set is defined as a polyhedral, the maximum number of cuts is bounded to the same amount of vertices in the uncertainty set, thus, guaranteeing that convergence can be attained in a finite number of iterations. Note also that the proposed formulations for the master- and sub-problem are MILP problems, and hence can be solved independently by an appropriate method such as branch-and-bound. These two characteristics enable the application of the proposed model to real-time applications as discussed in Chapter 4, sub-section 4.2.1.

3.2 Selection of the uncertainty bounds

The hedging capability of the RUC model depends on the definition of an appropriate uncertainty set. In this thesis, an approach is proposed to select the parameters of the uncertainty set model using the historical performance from the forecasting system. The analysis is performed with the data from previous forecast errors in a way that is consistent with the following affine model herein the RUC to represent the RE-sourced power output:

$$P_{\omega,t} = P^*_{\omega,t}(1 - \Delta P_{\omega,t}) \tag{3.9}$$

where $P^*_{\omega,t}$ represents the RE forecasted power and the error $\Delta P_{\omega,t}$ is the uncertain variable.

The parameters ${\Delta P_{\omega,t}}^{max}$ and Γ in (3.2) define the uncertainty policy, and reflect the decision-maker's preferences regarding risk. It is proposed here that Γ be obtained by an analysis of the forecasting errors based on the error duration curve. For the example depicted in Figure 3.1, using the forecasting data from [43], the curve shows that as ${\Delta P_{\omega,t}}^{max}$ increases, the number of periods Γ decreases; thus, the selection must be coherent with this behavior. Also, since the duration curve represents the average error characteristics, the value of the parameters should be on the right-hand side of the curve in order to be more conservative than average, as shown by the + symbols in Figure 3.1 for this particular set of data.

Another relevant information, that must be selected by the decision-maker, is ${\Delta P_{\omega,t}}^{max}$ depending on the forecast look-ahead time t. These bounds can be obtained from an appropriate forecasting system or by previous performance analysis. For example, Figure 3.2 shows the pattern of the 0.55, 0.60, 0.70, 0.75, and 0.80 percentiles of the absolute error for the same set of data, resulting in different averages over the 24 hour forecast. Note that, for this particular forecasting system, ${\Delta P_{\omega,t}}^{max}$ does not change much with the

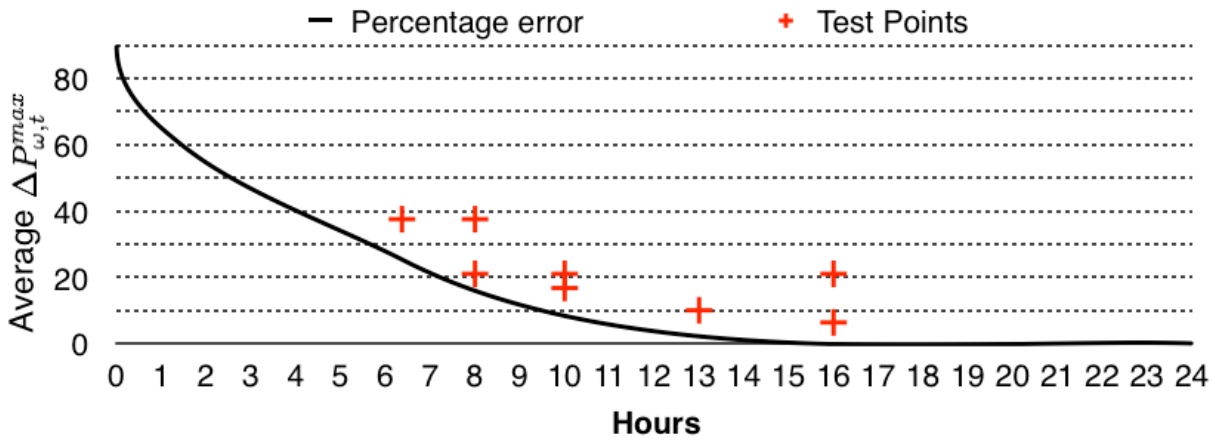

Figure 3.1: Error duration curve.

Table 3.1: Uncertainty policies for testing.

Γ [h]	$\Delta {P_{\omega,t}}^{max}$ [%]
6.37	37.5
8	37.5
10	16.72
16	6.335
8	21
13	10
16	21
10	21

look-ahead time, which may not be the case for other forecasting systems. The average of the forecasting error corresponds to a 21% error; the rest of the curves in Figure 3.2 correspond to percentiles above and below the median. In this research, the RUC is tested considering the uncertainty policies highlighted in Figure 3.1 by the + symbols, and shown in Table 3.1.

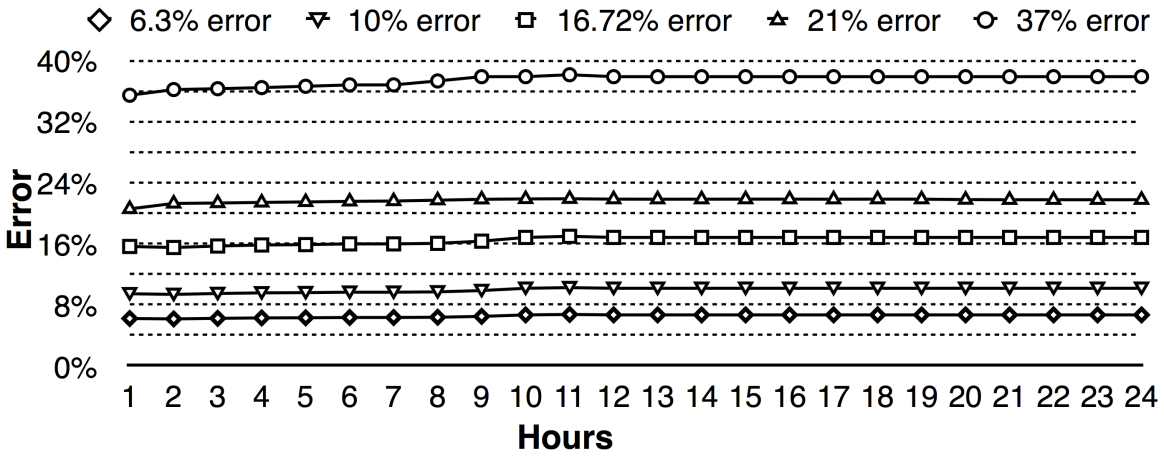

Figure 3.2: Error change in time.

3.3 EMS Architecture

The proposed EMS architecture is based on the requirements for a centralized system discussed in Section 2.1.2, given its advantages for isolated microgrids, such as improved coordination capabilities in the operation [10]. The proposed EMS architecture depicted in Figure 3.3 exploits with more detail the definitions of the recourse model under uncertainty discussed in Section 2.2.2, combining the solution of an RO-based model with a detailed mathematical representation of the system. This is accomplished by using a linear approximation of the microgrid power dispatch problem as the recourse, characterized by the sub-problem dual (3.7) in the RUC, in order to generate the least-favorable forecast mismatch to obtain the hedged solution of the first-stage. Based on the RUC result, the three-phase OPF NLP problem obtains the final recourse decision, thus enabling the controller to yield a hedged final recourse action using a highly detailed model of the microgrid simultaneously.

The calculation sequence is implemented with different time resolutions and levels of detail shown in Figure 3.4, enabling the use of appropriate forecasting techniques depending on the look-ahead window, as described in [89]. Thus, in order to integrate the two stages, different time-step lengths are used for each problem: a 1-hour step (t) is used for the RUC, and a 5-minute step (k_t) is used for the three-phase OPF. Also, different from the approach used in [12] where constant-length look-ahead windows are used, the EMS proposed in this thesis has a variable-size three-phase OPF look-ahead window that shrinks as time gets closer to the next hour, in order to maintain the same frontier condition for the SoC.This

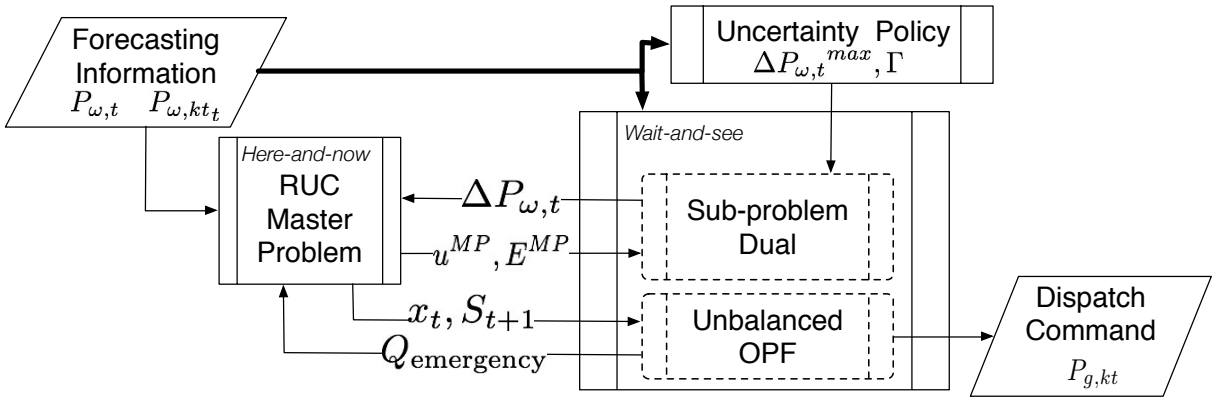

Figure 3.3: EMS architecture.

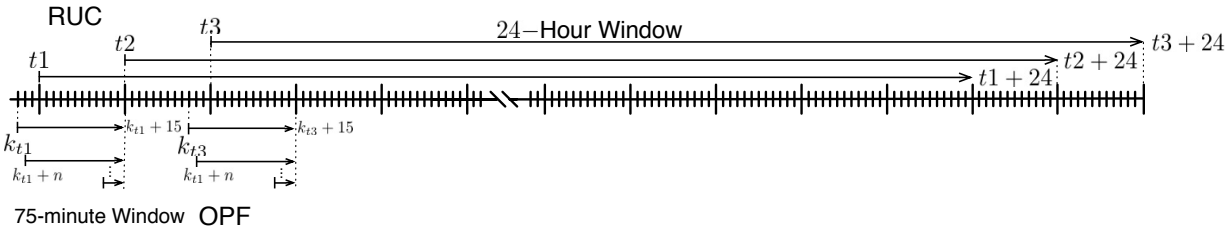

Figure 3.4: EMS horizon variable time-steps.

process can be summarized as follows:

- The RUC is solved for time t with a 24-hour look-ahead window in order to obtain the commitment decisions and the SoC of the storage for time $t+1$, which serves as the boundary condition for the three-phase OPF. The solution is issued 15 minutes ahead of the corresponding time t.
- Based on the RUC solution, the three-phase OPF is executed 15 minutes before time t, providing sufficient time for calculations and emergency actions if required. It starts with an initial 75-minute or 15 5-minute k_t steps look-ahead window, as shown in Figure 3.4, and this window shrinks as time gets closer to the next hour, in order to maintain the same frontier condition. Taking advantage of the RHC approach, the OPF calculates the final dispatch every 5 minutes, and requests corrective actions in case reactive power shortages are detected within its look-ahead window.

The flow diagram depicted in Figure 3.5 summarizes the calculation process and shows

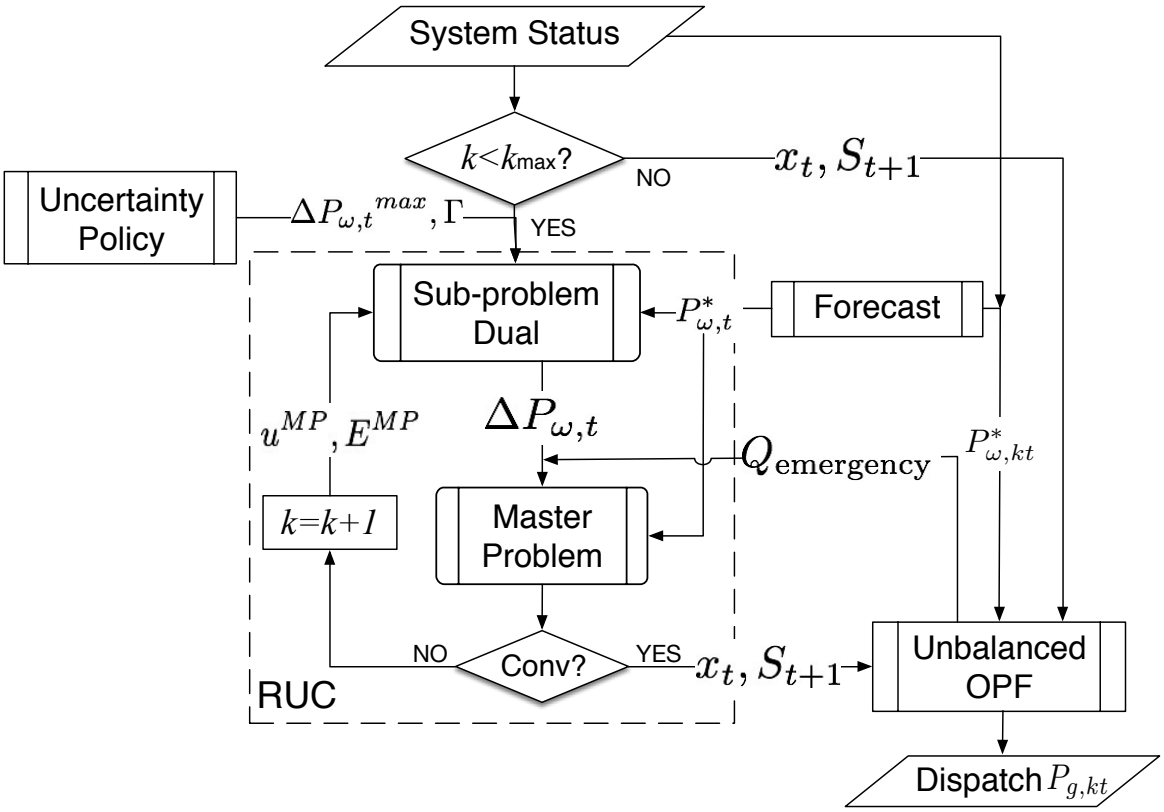

Figure 3.5: EMS implementation flow diagram.

the iterative process of the RUC and the three-phase OPF with feedback. The calculation procedure starts by obtaining the current status of the microgrid; then, the RUC calculation starts solving the sub-problem first. This is a variant from the original version of the primal cutting-planes algorithm, which dictates that a relaxed version of the master-problem is solved first to determine the initial conditions; however, if the current state of the system is available, this realistic starting point should be used to improve convergence. The algorithm then iterates until a solution is obtained or the maximum number of iterations is reached; the result is then communicated to the three-phase OPF, and if a reactive shortage is detected within the 75-minute look-ahead window, the master problem restarts the process increasing the number of units to be committed, as proposed in [12].

In the proposed decomposition framework, the ESS model described by (2.4) should be modified for the three-phase OPF calculations. This is necessary because the SoC is a fixed value at the frontier of the receding horizon of the three-phase OPF, which may result

in load shedding in order to meet the requirement when the system resources are limited. This possible load shedding can be avoided by the inclusion of a positive variable ESS_s^{shed} in the frontier condition of the ESS SoC, in which case the three-phase OPF mathematical model is able to decide not to charge in order to avoid load shedding. This is accomplished by adding the following constraints to the NLP three-phase OPF model proposed in [12]:

$$SOC_{s,kt_{15-n}} = SOC_{s,t+1}^{MP} - ESS_s^{shed} \qquad \forall s \qquad (3.10a)$$

$$ESS_s^{shed}\,(SOC_{s,kt_1} - SOC_{s,kt_{15}}) > 0 \qquad \forall s \qquad (3.10b)$$

$$ESS_s^{shed} < |SOC_{s,kt_1} - SOC_{s,kt_{15}}| \qquad \forall s \qquad (3.10c)$$

3.4 Summary

In this chapter, the mathematical models and the process needed to implement the RUC in the EMS of an isolated microgrid were presented, including a dualization approach and the management of bi-linear terms. Also, the proposed methodology to select the uncertainty policy based on the historical performance of the forecasting was discussed in detail. Finally, the proposed architecture to exploit the RHC principle along with the RO-based recourse actions was presented, including the use of variable look-ahead windows to solve the problem.

Chapter 4

Simulation Results

The performance of the proposed robust EMS described in Section 3.3 is demonstrated and discussed in this chapter for a 24-hour operation cycle on a modified CIGRE test microgrid for different configurations. The results are compared with those of deterministic and SO-based formulations. The algorithm is coded in the high-level optimization modeling language GAMS v2.3.3, using CPLEX v12.1.0 as the solver for the RUC MILP and COIN-IPOPT Library 3.7 to solve the three-phase NLP problem. The simulations are performed in a server, that features an Intel Xeon CPU L7555 at 1.86 GHz (4 processors), and 64 GB of RAM, running on Windows Server 2008 R2 Enterprise 64-bit.

4.1 Test System and Study Cases

The proposed robust EMS is tested on a modified version of the medium-voltage distribution grid used in [90] for DG integration studies, and modified in [12, 51] as an isolated microgrid for EMS benchmarking. Some changes are introduced in order to restrict the available resources in the system operation of the system further, thus bringing out the need to hedge the system against uncertainty. This microgrid test system features 3 diesel units with capacities of 1750 kW, 310 kW and 800 kW, with the two larger ones replacing what was originally a connection to the main grid, as shown in Figure 4.1. The system's total installed capacity is 6,400 kW, including ESS units, intermittent Photovoltaic (PV), Wind Turbine (WT) units, and a Micro-Turbine (MT); the ratings of the DG units are show in Table 4.1. The detailed information of the system model such as generation cost coefficients, transmission line parameters and load levels are provided in the Appendix.

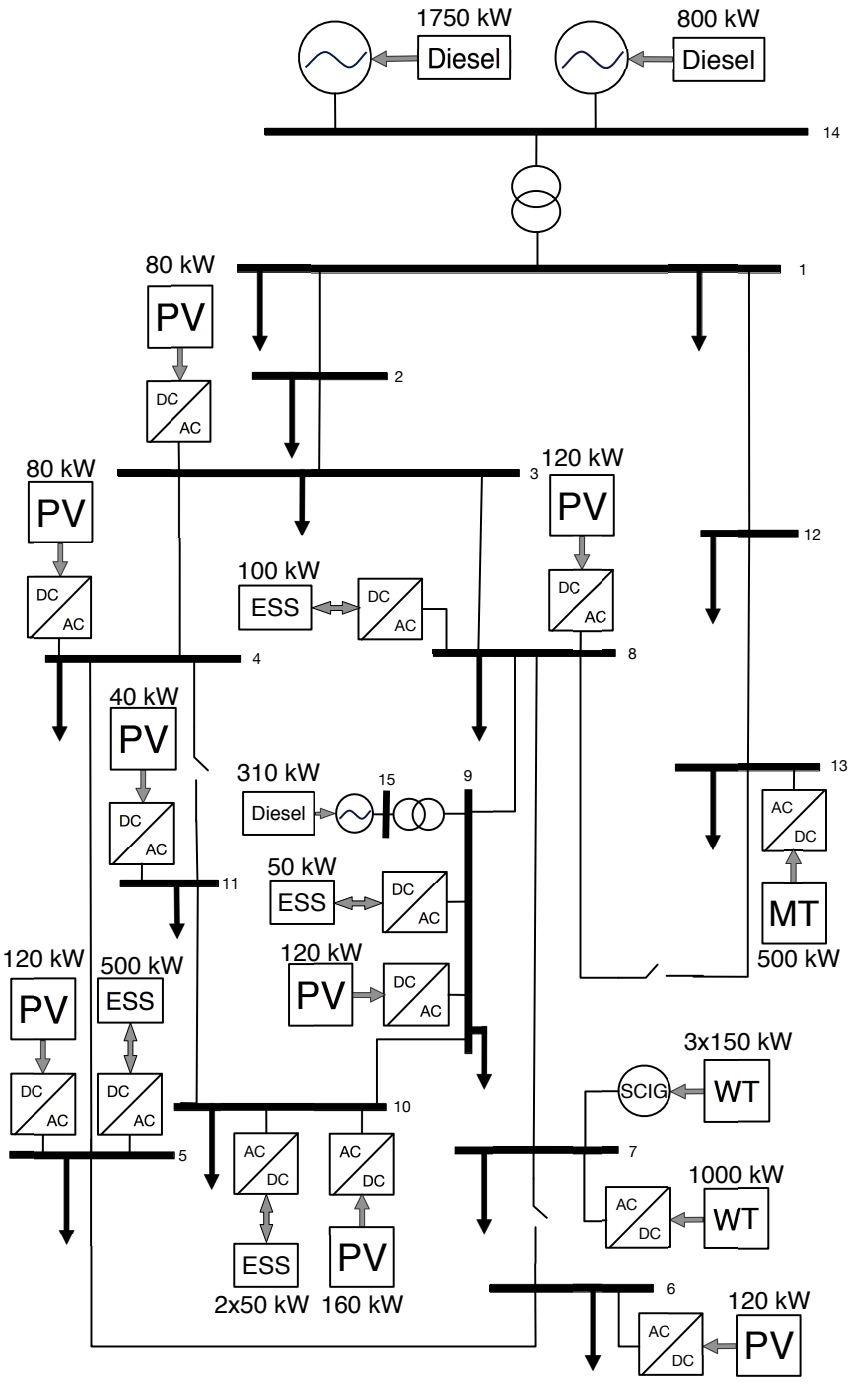

Figure 4.1: Microgrid test system.

Table 4.1: Microgrid DER ratings and locations.

Unit	Node	DER type	$P_g^{max}/P_\omega^{max}/P_s^{max}$ [kW]
G1	N14	Diesel Generator	800
G2	N15	CHP Diesel	310
G3	N14	Diesel Generator	1750
G4	N3	Photovoltaic	80
G5	N4	Photovoltaic	80
G6	N5	Photovoltaic	120
G7	N5	Energy Storage System	500
G8	N6	Photovoltaic	120
G9	N9	Energy Storage System	50
G10	N8	Photovoltaic	120
G11	N8	Energy Storage System	100
G12	N9	Photovoltaic	120
G13	N10	Photovoltaic	160
G14	N10	Energy Storage System	50
G15	N10	Energy Storage System	50
G16	N11	Photovoltaic	40
G17	N13	Gas microturbine	500
G18	N7	Wind turbine (inverter-interfaced)	1000
G19	N16	Wind turbine (SCIG)	150
G20	N16	Wind turbine (SCIG)	150
G21	N16	Wind turbine (SCIG)	150

The microgrid's load is modeled in different ways depending on the stage of the decision making process. In the RUC, the load is modeled as constant power and balanced, and in the three-phase OPF the load is unbalanced with a combination of constant impedance and constant power. In the non-linear model, two types of loads are considered: residential, composed of 80% constant- impedance and 20% constant-power, and commercial, composed of 50% constant-impedance and 50% constant-power. The following phase loading are assumed : phase-a 30%, phase-b 35.7%, and phase-c 34.2% of the total demand. The load profile for the 24-hour period of simulation is shown in Figure 4.2, where the base loading level for all study cases is presented in the Appendix and the peak load is 4.340 MW.

The load and RE forecast information is extracted from [43], which corresponds to

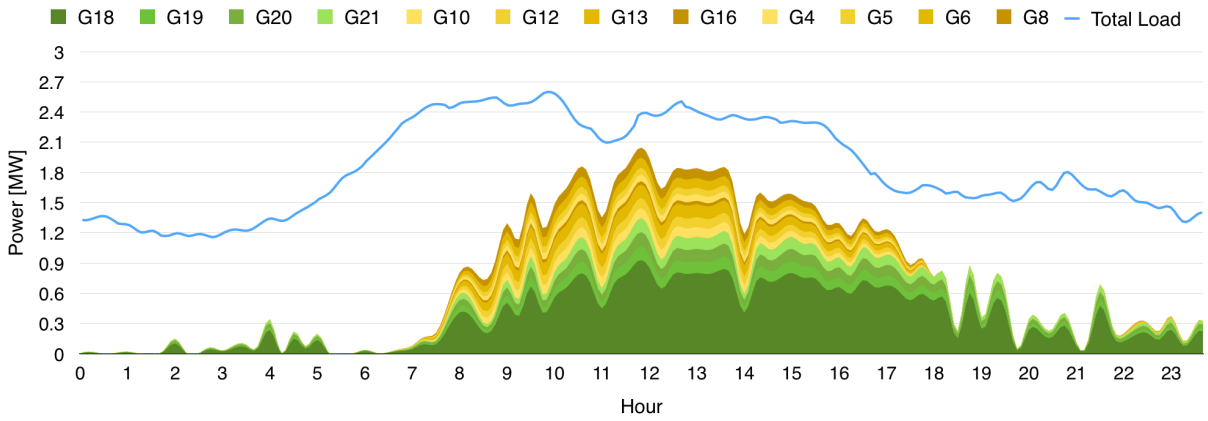

Figure 4.2: RE and load profiles.

data from the microgrid in Huatacondo, Chile. The profiles of the RE sources are shown in Figure 4.2, for both solar and wind power. In this research, the only source of uncertainty considered is the wind power; thus, the wind forecast is the only input parameter subject to unknown mismatches, i.e., $\omega = 1$ and $P_{\omega}^{max} = 1450kW$.

Given that the ESS mathematical model described by (2.4a)-(2.1.2) is appropriate for various technologies, the test system includes different types of units by considering various ratings and efficiencies. In this test system, there is a main ESS unit with high capacity and high efficiency, and smaller ESS units with different capacities and efficiencies distributed throughout the microgrid. The installed ESS units' capacities, ratings, and efficiencies are shown in Table 4.2.

Table 4.2: Microgrid ESS ratings, capacities and efficiencies.

ESS	DG	P_s^{max} [kW]	SOC_s^{max} [kWh]	η^{in}	η^{out}
S1	G7	500	2500	0.96	0.96
S2	G9	50	250	0.85	0.85
S3	G11	100	500	0.95	0.95
S4	G14	50	250	0.8	0.8
S5	G15	50	250	0.87	0.87

In order to test the effectiveness of the recourse models under uncertainty discussed in Sections 2.3 and 2.4, and demonstrate the importance of considering uncertainty in the

EMS for isolated microgrids with and without ESS, different case studies are presented and compared. These cases also demonstrate the main differences between the SO and RO hedging approaches. The following are the study cases considered:

- **Robust Base Case:**

  This case corresponds to the base test system described beforehand, solved using the proposed RUC technique described in Section 3.1. The simulation is performed considering an RUC look-ahead window of 24-hours, corresponding to the profiles of the load and RE sources. The algorithm was tested for eight combinations of uncertainty policy ($\Gamma, \Delta P^{max}_{\omega,t}$) shown in Table 3.1 and previously explained.

- **Deterministic Case:**

  This case corresponds to the deterministic formulation of the EMS, which is implemented here as a special case of the RUC with uncertainty policy $\Gamma = 0$, which implies that the forecast will not have mismatches at any time-step, to be able to compare the look-ahead windows for the same EMS.

- **SUC Case:**

  For the SUC, the process will follow the procedure proposed in [51] and discussed in Section 2.3.1, which uses 100 scenarios updated at each time-step, based on the most recent forecast using a statistic ensembles technique. The SUC horizon is also set to 24 hours as in the deterministic and RUC cases.

- **No-Storage Case**

  Given the current issues with the deployment of ESS in remote microgrids [6], it is relevant to test and compare the effectiveness of the proposed formulations in a context where no ESS is installed. Hence, the ESS is removed from the test system replacing the ESS unit at N5 with a gas microturbine of the 500 kW with the same characteristics as the one installed at N13, in order to provide the system with enough capacity to meet the demand.

4.2 Results

This section presents and discusses the dispatch commands issued for the aforementioned study cases. The different dispatch models are benchmarked, based on the following three criteria:

- Costs, which include the cost of fuel, load shedding, power curtailment and commitment costs over a 24-hour period of operation.
- Reserves, which includes both the average level of total reserves and the change in the instantaneous reserve levels during the 24-hour period. These reserves correspond only to the diesel generators and the micro turbine.
- SoC of the ESS, which corresponds to the total of SoC average and the instantaneous SoC levels over the simulation window, during the 24-hour operating period.

The scheduling of diesel units G1 and G2 (800 kW and 310 kW respectively) is of particular interest, because, given the low cost of the microturbine and the size of G3 (1,750 kW diesel unit), these provide the base load and thus the algorithm always commits them. Hence, the smaller units provide flexibility to the operation of the microgrid, with the uncertainty considerations changing their scheduling depending on the uncertainty policy and the UC model used.

4.2.1 System with Storage

Since the RE units cannot be dispatched, the EMS dispatch signals correspond to the thermal units and ESS. Figure 4.3 depicts an area stacked plot of the dispatch in 5-minute periods for the deterministic formulation, the RUC with the uncertainty policy $(\Gamma, \Delta P_{\omega,t}^{max}) = (10, 21\%)$, and the SUC variant in that order.

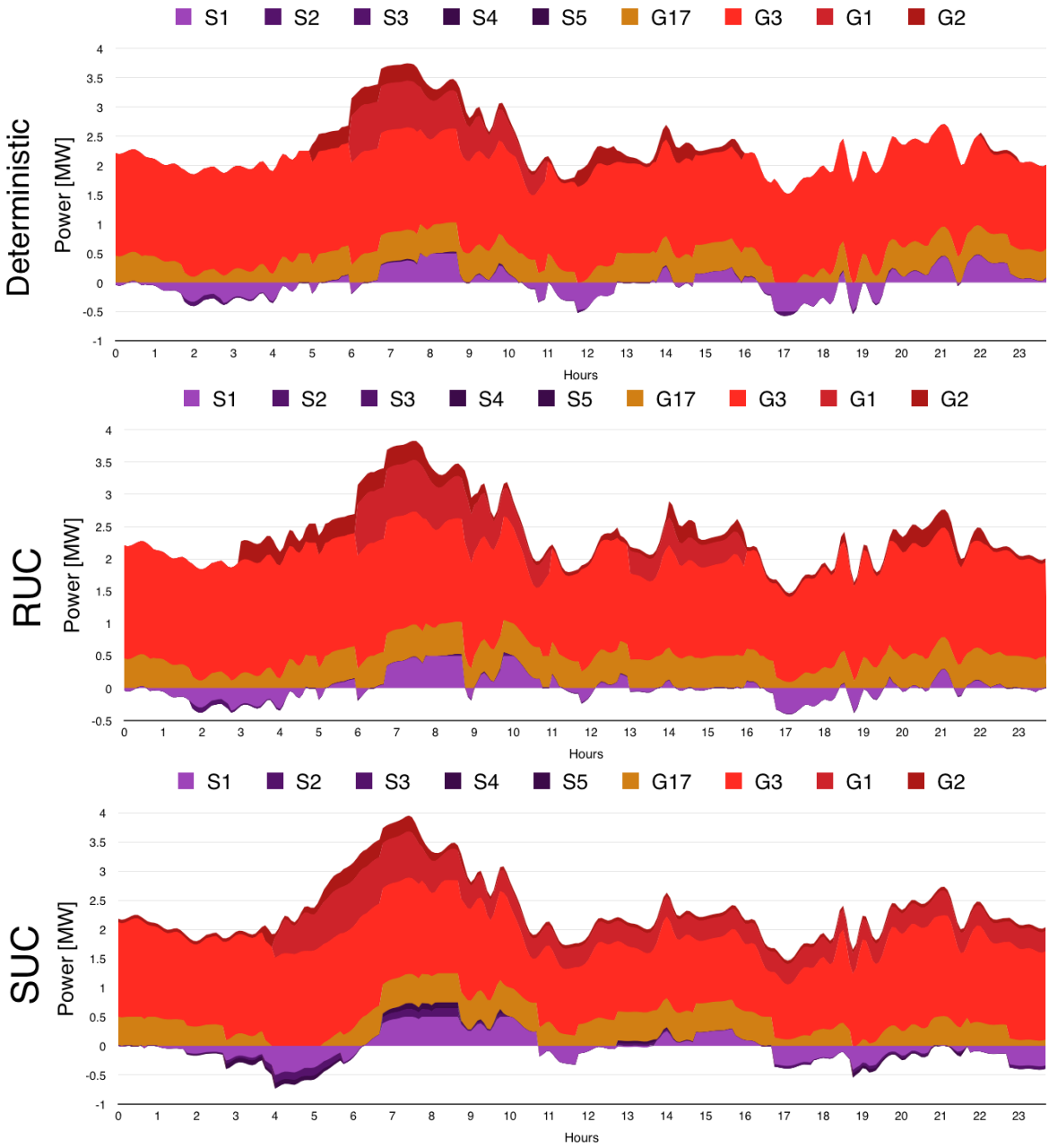

Figure 4.3: Dispatch results for different UC models for base case.

Table 4.3: UC results summary for base case, G1 & G2 (G3 and G21 are always committed).

Case		Hours																							
		g	1	2	3	4	5	6	7	8	9	10	11	12	13	14	15	16	17	18	19	20	21	22	23	24
DET		G1	0	0	0	0	0	0	1	1	1	1	1	0	0	0	0	0	0	0	0	0	0	0	0	0
		G2	0	0	0	0	0	1	1	1	1	1	1	1	1	1	1	1	0	0	0	0	0	0	0	0
SUC		G1	0	0	0	0	1	1	1	1	1	1	1	1	1	1	1	1	1	1	1	1	1	1	1	1
		G2	1	1	1	1	1	1	1	1	1	1	1	1	1	1	1	1	1	1	1	1	1	1	1	1
RUC	(6.3, 37%)	G1	0	0	0	0	0	0	1	1	1	1	1	1	1	1	1	1	0	0	0	0	0	0	0	0
		G2	0	0	0	0	0	1	1	1	1	0	0	0	0	0	0	0	1	1	1	1	1	1	1	1
	(8, 21%)	G1	0	0	0	0	0	0	1	1	1	1	1	0	0	1	1	1	0	0	0	0	0	0	0	0
		G2	0	0	0	0	0	1	1	1	1	1	1	1	1	1	0	0	1	1	1	1	1	1	1	0
	(8, 37%)	G1	0	0	0	0	0	0	1	1	1	1	1	0	0	1	1	1	0	0	0	0	0	0	0	0
		G2	0	0	0	0	0	1	1	1	1	0	0	0	0	0	0	0	1	1	1	1	1	1	1	0
	(10, 21%)	G1	0	0	0	0	0	0	1	1	1	1	1	0	0	1	1	1	0	0	0	0	0	0	0	0
		G2	0	0	0	0	0	1	1	1	1	0	0	0	0	0	0	0	1	1	1	1	1	1	1	1
	(13, 10%)	G1	0	0	0	0	0	0	1	1	1	1	1	0	1	1	0	0	0	0	0	0	0	0	0	0
		G2	0	0	0	0	0	1	1	1	1	1	1	1	1	1	1	1	1	1	1	1	1	1	1	0
	(16, 21%)	G1	0	0	0	0	0	0	1	1	1	1	1	0	0	1	1	1	0	0	0	0	0	0	0	0
		G2	0	0	0	0	0	1	1	1	1	1	1	1	1	1	0	0	1	1	1	1	1	1	1	1
	(16, 6.3%)	G1	0	0	0	0	0	0	1	1	1	1	1	0	0	0	0	0	0	0	0	0	0	0	0	0
		G2	0	0	0	0	0	1	1	1	1	1	1	1	1	1	1	1	1	1	1	1	1	1	1	0

The diesel units are dispatched according to the commitment results shown in Table 4.3. The most relevant difference is between hours 12-24, where the RUC formulation commits more capacity than the deterministic case. However, the number of units committed is less than the SUC case with G2 being committed for the 24 hours of operation.

The ESS units are always committed, and the EMS enforces the charging and discharging commands by means of the SoC level requirements set at the frontier condition for the three-phase OPF. Observe in Figure 4.3 that the ESS units charge during off-peak hours, between hours 0-5 and 17-20, and discharge at the peak hours between hours 7-11 and 20-24 as expected. The main difference between the hedged approaches can be observed in the second peak between hours 17-23, where the SUC variant charges instead of discharging, unlike the deterministic and RUC cases; this difference is due the aforementioned overcommitment of units in the SUC approach.

The results of the UC for different uncertainty policies show how the conservatism level changes depending on the value of $(\Gamma, \Delta P_{\omega,t}^{max})$. In every case, the RUC committed more units than the deterministic variant between hours 17-24, as a result of the uncertain mismatches in those hours, thus forcing the EMS to yield more reserves. Another relevant result can be observed at hours 10-11, where the deterministic problem and variants of the RUC with large levels of Γ commit an extra unit in order to charge the ESS; this difference is due to the interaction of the UC decisions with the management of the ESS SoC in the optimization algorithm.

The effect of the extra commitment and conservatism management are reflected in the total reserve levels for the different uncertainty policies. Thus, the system's average reserve levels are shown in Figure 4.4, where higher levels of reserve are observed in hedged UC variants, yielding more secure system conditions against variations on the availability of RE resources and load. Furthermore, note that the deterministic UC results in the lowest level of reserves, and the SUC produces the highest level. On the other hand, the different RUC uncertainty policies produce values between those of the deterministic and SUC approaches; observe that the cases with a high value of $(\Gamma, \Delta P_{\omega,t}^{max})$ yield increased levels of reserve as expected from the mathematical formulation. This can also be observed in the UC Table 4.3, where the SUC commits all the thermal units for 20 out of the 24 hours while the RUC is less conservative.

The instantaneous levels of reserve during the 24-hour simulation is illustrated in Figure 4.5, showing that the uncertainty policies are able to provide more reserve to the system as compared to the deterministic case at times of high RE generation, considering the wind profiles in Figure 4.2. Note that, during the time window between hours 16-22, the deterministic case does not commit enough units to provide adequate reserves to the system, while the RUC and SUC variants are able to properly hedge the system, with the SUC, providing the highest reserves for every hour.

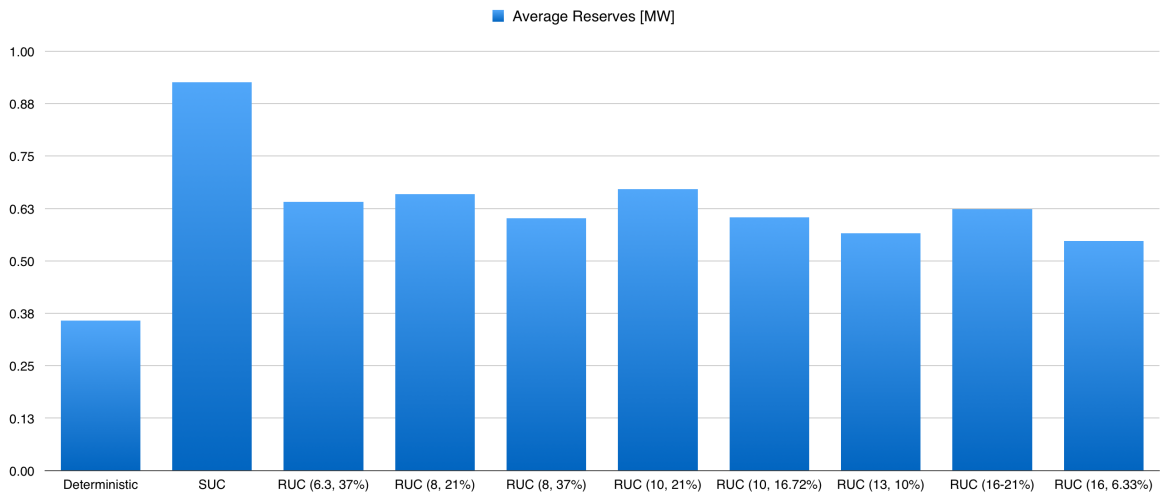

Figure 4.4: Average reserve for base case.

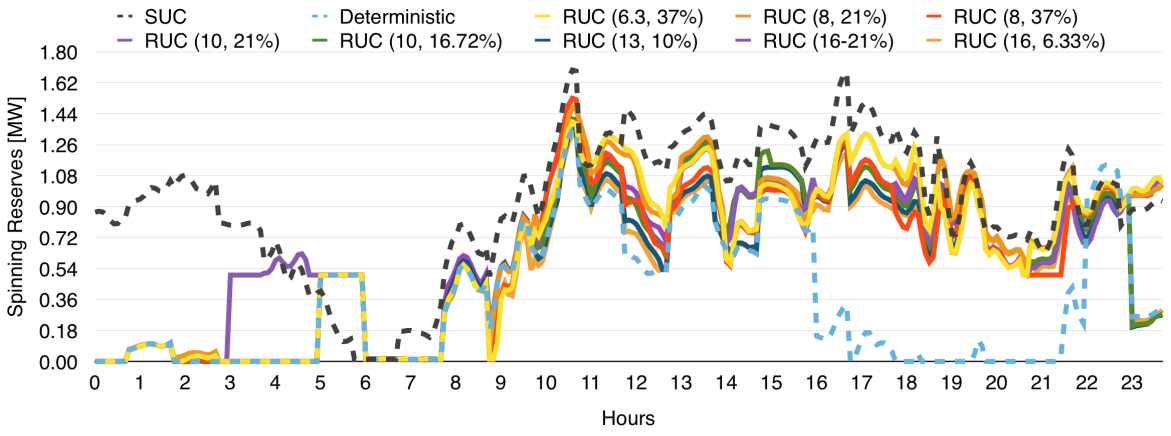

Figure 4.5: Instant reserve for base case.

As the reserves, the level of SoC reflects how much resource the algorithms allocate to compensate for possible deviations in the RE. The average SoC for all the ESS is depicted in Figure 4.6, showing that the deterministic case maintains an average SoC higher than the hedged cases. There are noticeable differences between the UC variants, since the robust formulation leads to a higher utilization of the ESS, and a flatter profile of SoC levels, as shown in Figure 4.7, which is consistent with a more conservative management of the storage resources. These differences can be explained by the fact that the determin-

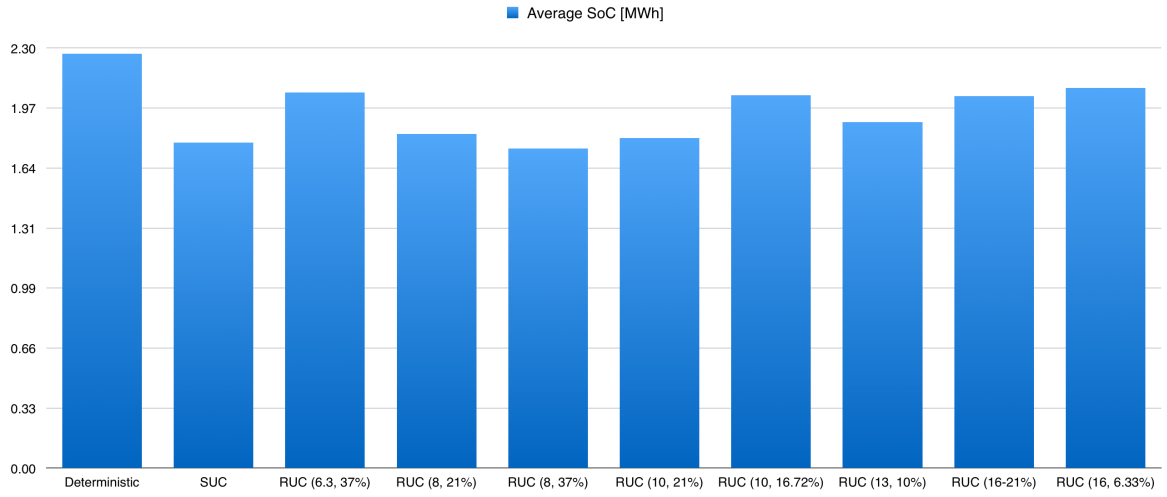

Figure 4.6: Average SoC for base case.

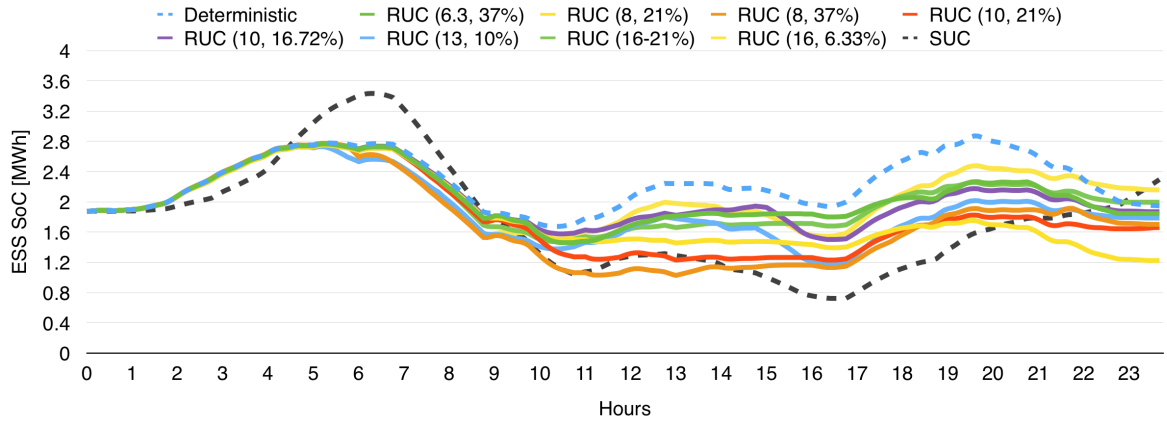

Figure 4.7: Instant SoC for base case.

istic model performs the calculation of the recourse considering a single "optimistic" RE profile, whereas the hedged variants consider more pessimistic scenarios. For the case of the RUC model, the SoC levels are in between those of the deterministic and the SUC, as for the reserves. Moreover, the SUC variant yields more conservative results than any of the the uncertainty policies, to the extent of charging the ESS during the second peak; furthermore, this model produces a more aggressive charging during the first 8 hours causing an overcommitment of units.

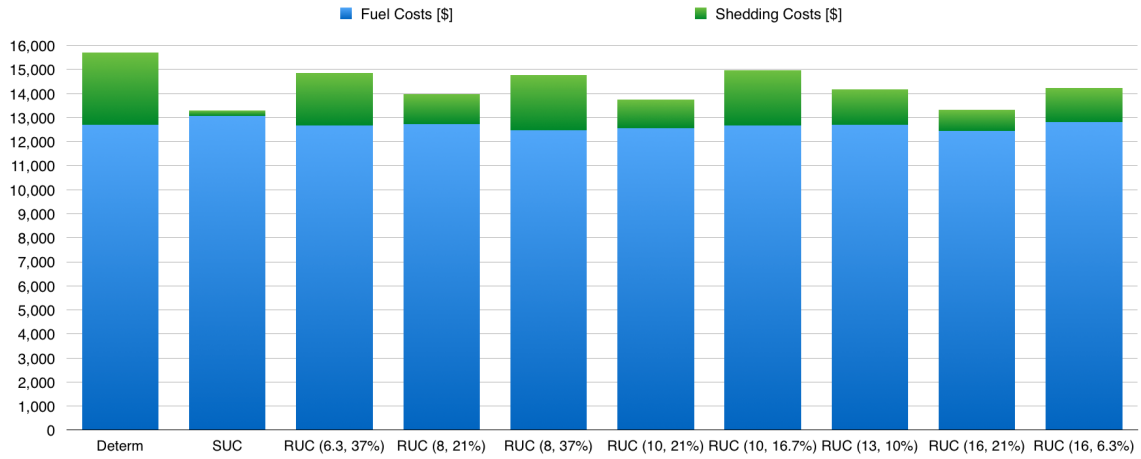

Figure 4.8: Costs for base case.

Finally, there is a reduction in total operating costs when using the RUC model for all the uncertainty policy variants compared to the deterministic case, as shown in Figure 4.8. The savings come primarily due to a reduced level of load shedding in each case, observing a reduction in load shedding between 30% and 40% depending on the selected uncertainty policy. The SUC presents the lowest level of load shedding, with the cost reduction coming from the commitment of all the units 2 hours before the peak (hours 4-6); however, this approach produces the most expensive dispatch in terms of fuel, because the SUC is more conservative than the RUC. Nevertheless, the fuel costs remain practically the same in all UC variants, since this related mostly to the large unit G3; and the other units are comparatively much smaller and lower cost. It should be highlighted that ESS charging/discharging costs are not considered here; these affect the cost results, leading possibly to different conclusions.

4.2.2 System Without Storage

The EMS dispatch signals for the thermal units for the system with no ESS are shown in Figure 4.9; similar to the results of the system with storage, the dispatch is represented as an area stacked plot of the dispatch in 5-minute periods. The illustrated results correspond to the deterministic formulation, the RUC with the uncertainty policy $(\Gamma, \Delta P^{max}_{\omega,t}) = (10, 21\%)$, and the SUC variant. In this case, the microturbine G7 that replaces the main ESS unit is committed for the entire operation period.

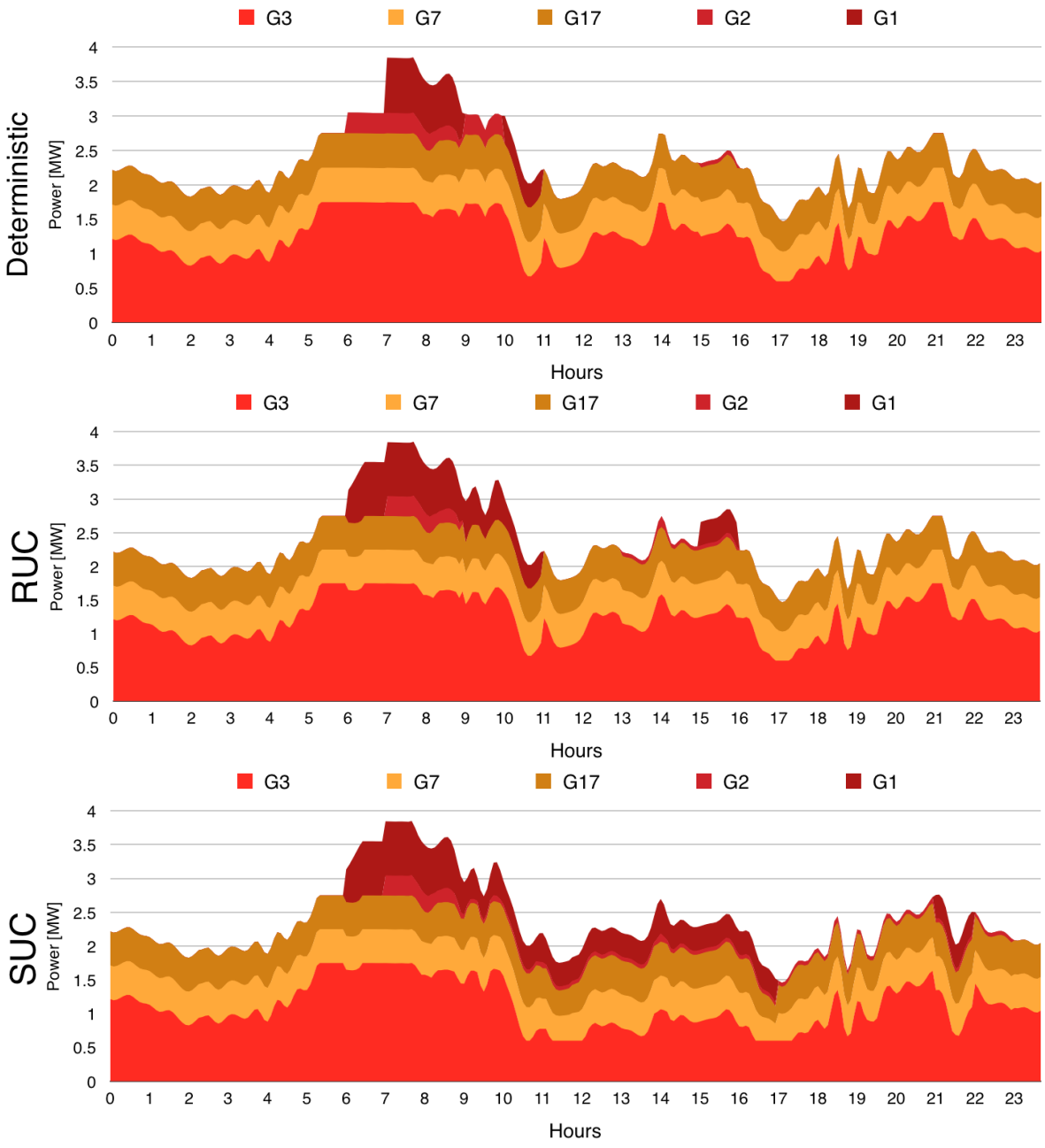

Figure 4.9: Dispatch results for different UC models, for the system with no storage.

Table 4.4: UC results summary for no-ESS system, G1 and G2 (G3, G7 and G17 are always committed).

Case		Hours																							
		g	1	2	3	4	5	6	7	8	9	10	11	12	13	14	15	16	17	18	19	20	21	22	23	24
DET		G1	0	0	0	0	0	0	0	1	1	0	1	0	0	0	0	0	0	0	0	0	0	0	0	0
		G2	0	0	0	0	0	0	1	1	1	1	0	0	0	0	0	1	0	0	0	0	0	0	0	0
SUC		G1	0	0	0	0	0	0	1	1	1	1	1	1	1	1	1	1	1	0	0	0	0	1	0	0
		G2	0	0	0	0	0	0	0	1	1	1	1	1	1	1	1	1	1	1	1	1	1	1	1	0
RUC	(6.3, 37%)	G1	0	0	0	0	0	0	0	1	1	0	0	0	0	1	1	1	0	0	0	0	0	0	0	0
		G2	0	0	0	0	0	0	1	1	1	1	1	0	0	0	0	1	0	0	0	0	0	0	0	0
	(8, 21%)	G1	0	0	0	0	0	0	0	1	1	0	0	0	0	1	1	1	0	0	0	0	0	0	0	0
		G2	0	0	0	0	0	0	1	1	1	1	1	0	0	0	0	0	0	0	0	0	0	0	0	0
	(8, 37%)	G1	0	0	0	0	0	0	0	1	1	1	0	0	0	1	1	1	0	0	0	0	0	0	0	0
		G2	0	0	0	0	0	0	1	1	1	1	1	0	0	0	0	1	0	0	0	0	0	0	0	0
	(10, 21%)	G1	0	0	0	0	0	0	0	1	1	0	0	0	0	1	1	1	0	0	0	0	0	0	0	0
		G2	0	0	0	0	0	0	1	1	1	1	1	0	0	0	0	0	0	0	0	0	0	0	0	0
	(13, 10%)	G1	0	0	0	0	0	0	0	1	1	0	0	0	0	0	0	0	0	0	0	0	0	0	0	0
		G2	0	0	0	0	0	0	1	1	1	1	1	0	0	0	0	1	0	0	0	0	0	0	0	0
	(16, 21%)	G1	G	0	0	0	0	0	0	0	1	1	0	0	0	0	1	1	1	0	0	0	0	0	0	0
		G2	G	0	0	0	0	0	0	1	1	1	1	1	0	0	0	0	0	0	0	0	0	0	0	0
	(16, 6.3%)	G1	0	0	0	0	0	0	0	1	1	0	1	0	0	0	0	0	0	0	0	0	0	0	0	0
		G2	0	0	0	0	0	0	1	1	1	1	0	0	0	0	0	1	0	0	0	0	0	0	0	0

The commitment results of diesel units G1 and G2 are shown in Table 4.4, where the differences between the approaches are mainly observed in hours 6-11 and 15-16; note that the RUC commits more capacity than the deterministic UC case. Observe also that the UC results in the hours 18-23 are the same for both formulations, reflecting that additional hedging is not required in those hours. The overcommitment of the SUC formulation can be observed again in Figure 4.9, where G1 is dispatched in hours 11-15, even when the system does not really need an extra unit on-line.

The RUC average levels of reserve are only marginally higher than the deterministic case, as shown in Figure 4.10. Nevertheless, in hours 6-10 in Figure 4.11 it is clear that the algorithm allocates the reserves properly when the RE output is higher, as observed in the RE profiles in Figure 4.2. On the other hand, the SUC results are more conservative than

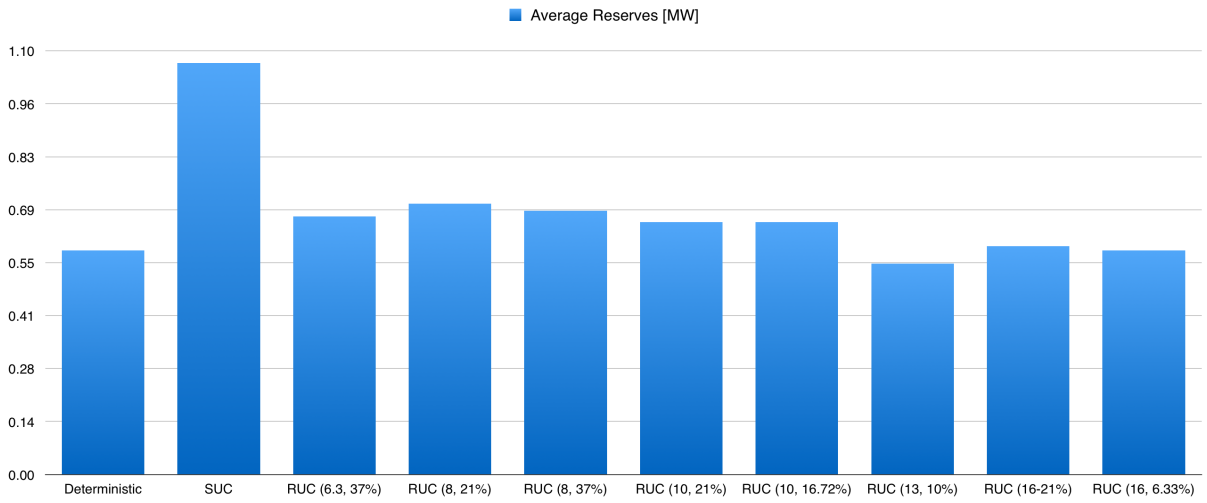

Figure 4.10: Average reserves for the system with no ESS.

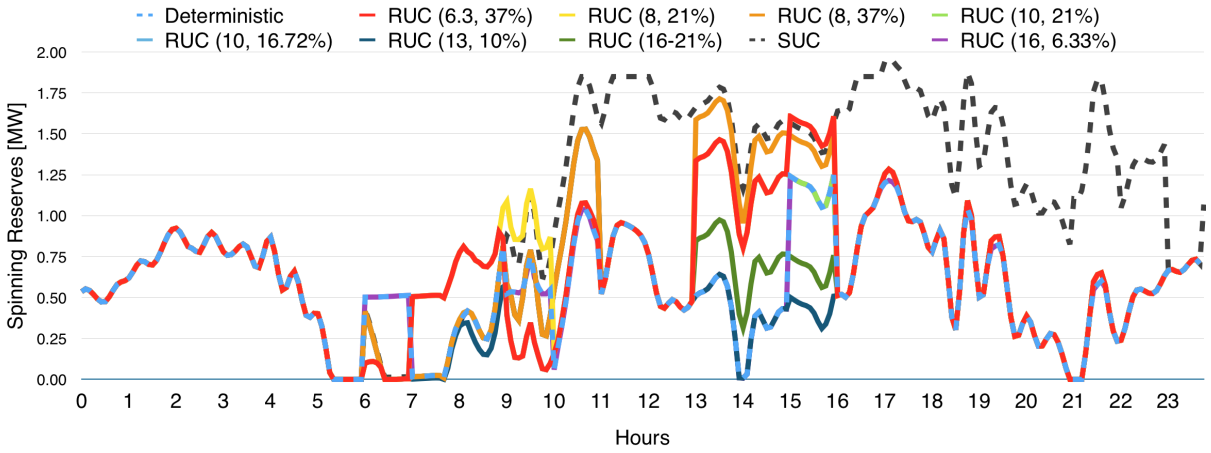

Figure 4.11: Instant reserves results for system with no ESS.

the RUC results, providing the system with the highest average reserve; however, note in Figure 4.9 that the overcommitment in the SUC model results in the diesel units operating at minimum power in the valley periods, which is detrimental to the fleet performance and hence is an unwanted outcome. In this case, in order to accommodate the high amount of power in the system, the units operate at reduced generation levels, to the extent that G2 operates at minimum power for 13,16 hours.

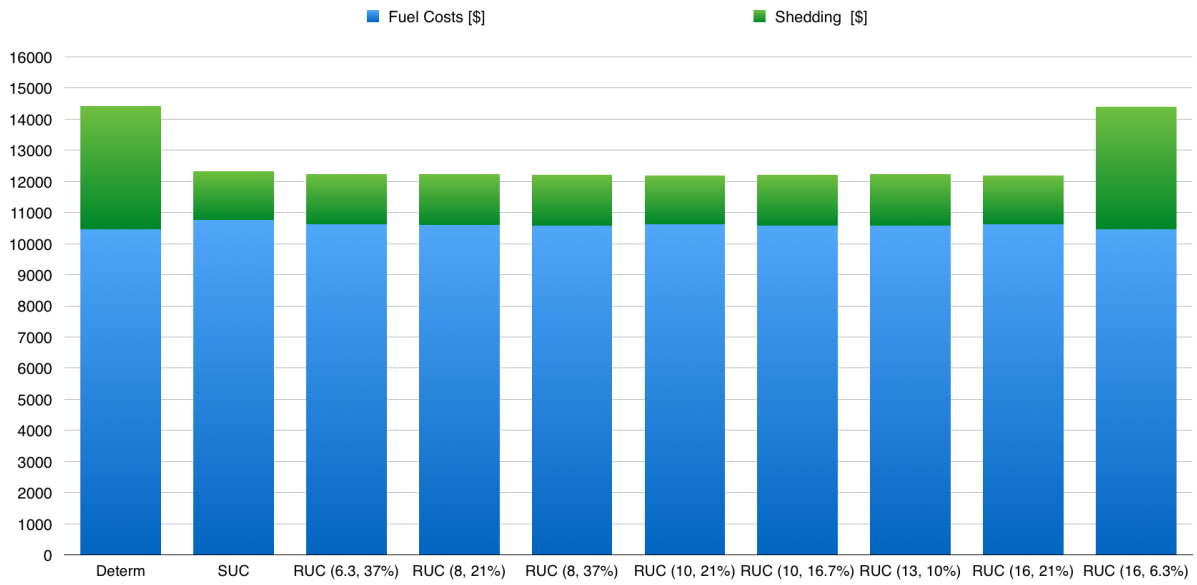

Figure 4.12: Costs for system with no storage.

Finally, there is a similar reduction of total operating costs for all the RUC variants and the SUC, as shown in Figure 4.12. This is due to a reduction in load shedding of 60% when comparing most of the RUC results with those of the deterministic case, except for the case when the $\Delta P_{\omega,t}^{max}$ is small (i.e., $\Delta P_{\omega,t}^{max} = 6.33\%$) which yields similar results as in the deterministic formulation. Note that the fuel costs are practically the same in all UC variants, since this is related mostly to the large unit G3; and the other units are comparatively much smaller and run at lower cost.

4.2.3 Computational Performance

One of the main concerns in EMS algorithm development is their appropriateness for real-time operation; hence, as discussed in Section 1.2, the computational complexities of uncertainty-aware formulations may hinder their performance in real-time application. Thus, it is relevant to discuss the computational performance of the RUC model.

From the perspective of computational performance, some simulations were run with overly conservative polices (e.g. $\Gamma = 16$, $\Delta P_{\omega,t}^{max} = 37\%$). This arises from the fact that a 37% change in a 16 time steps out of the 24-hour look-ahead window is too drastic, resulting in many possible solutions at the same cost. The cases reported here are for the

Table 4.5: Iteration count per hour of the RUC algorithm for different uncertainty policies.

Γ	$\Delta P_{\omega,t}^{max}$	Base System		No-Storage	
		Min iteration	Max iteration	Min iteration	Max iteration
6.37	37.5	1	4	2	5
8	37.5	1	3	2	5
10	16.72	1	3	2	4
16	6.335	1	3	1	3
8	21	1	4	2	4
13	10	1	3	1	3
16	21	1	3	2	3
10	21	1	4	1	3
10	37	No convergence after 10 iterations			
16	30	No convergence after 10 iterations			
16	37	No convergence after 10 iterations			

policies that maintain the relationship depicted in Fig. 3.1, yielding solution times below 60 CPU seconds per iteration, for the number of iterations provided in Table 4.5 for each uncertainty policy used, over the the 24 hour simulation window.

Note that if the uncertainty set is oversized the mathematical problem is unable to find an appropriate solution to the worst realization since there are many scenarios that result in the same recourse. As the levels of conservatism are increased, some uncertainty policies produce solutions of the sub-problem that have the same cost function value with different $\Delta P_{\omega,t}$ results in the RUC sub-problem (3.7), thus slowing down the convergence speed; on the other hand, there are uncertainty policies too conservative to converge in the maximum number of iterations. Furthermore, given that the models use the current system information to calculate the commitment and the most pessimistic RE profile, unless the prediction changes drastically from one hour to the next, the algorithm will not be required to perform many iterations to obtain a new set of results; hence, the convergence of the algorithm in suitable time is accomplished by selecting uncertainty policies coherent with the actual performance of the forecasting system.

It is important to note that the number of iterations required for the RUC to converge is affected by the optimality criterion of the MILP solver and the convergence criterion of the primal cutting-planes. In this case, CPLEX defines the relative tolerance of the branch-and-bound solving algorithm on the gap between the best integer objective and

the objective of the best remaining node [91]. If this tolerance is too high, as the default value in GAMS of 10%, the primal cutting-planes algorithm is unable to converge in a reasonable number of iterations. For this reason, the gap criteria has been set to 0 (e.g., `OPTION OPTCR=0`). On the other hand, the convergence tolerance for the cutting-planes algorithm is set at 0.1%, with the objective of testing the proposed model with strict convergence criteria.

4.3 Summary

In this chapter, the proposed RUC model and EMS architecture were tested on a modified CIGRE test system under different configurations, considering a system with storage and without storage. The results were compared with those of a deterministic formulation and the SUC, demonstrating the benefits of hedging the UC solutions against uncertainty. The models were compared on the basis of reserve and ESS SoC management, costs, dispatch and UC.

The results demonstrated that through a proper selection of the uncertainty policy, an improved performance and a more secure operation can be obtained. It is shown that the economic performance of the EMS depends on the selection of the uncertainty policy. Overall, even though the fuel costs for the different RUC variants show only marginal reduction, there is an important improvement in the security of the microgrid given by the additional reserves and better management of the ESS. Furthermore, the RUC is able to produce hedged UC results without considering any probabilistic information from the forecasting system and within reasonable computational times.

Chapter 5

Conclusions and Future Work

5.1 Summary

The focus of this thesis has been on the mathematical formulation of an uncertainty-aware EMS for isolated microgrids using an RO approach. The microgrid concept was first introduced and an overview of the current research trends of uncertainty management in power systems, and particularly in microgrid dispatch, was presented along with the research objectives. The control requirements and structures appropriate for isolated microgrids were also discussed, and the bases for the proposed mathematical model of the RUC were laid out. Moreover, the concepts and mathematical tools to manage uncertainties in control problems were presented, introducing and formalizing the technique, and including a discussion on implementation, advantages and disadvantages of its application to EMS. The recourse formulation of problems under uncertainty was also discussed along with the general mathematical model for SO, and the SUC model applied to microgrid EMS was presented. Finally, the RO-based recourse model was presented including a detailed description of the algorithm used to solve the RUC problem and hedge the system against uncertainty, with limited probabilistic information from the forecast.

The aforementioned mathematical models were then exploited to develop the proposed RUC suitable for EMS of isolated microgrids. A detailed discussion of the mathematical procedures to maintain the problem tractability as an MILP, including a dualization approach and the management of bi-linear terms was then presented. Also, the proposed methodology to select the uncertainty policies based on the historical performance of the forecasting was discussed in detail. The proposed architecture that exploits the RHC principle along with the RO-based recourse actions was presented as well, including the use of

variable look-ahead windows to solve the problem.

The concepts and algorithms proposed in this thesis were finally tested under different system configuration conditions for a realistic isolated microgrid based on the benchmark MV CIGRE system, and the results were presented and discussed. The results demonstrated that through a proper selection of the uncertainty policy, an improved performance and a more secure operation could be obtained. It was shown that the economic performance of the EMS for various uncertainty policies depended on the selection of the uncertainty policy. Overall, even though the fuel costs for the different RUC variants show only marginal reduction, there is an important improvement in the security of the microgrid given by the additional reserves and better management of the ESS. Furthermore, the RUC is able to produce hedged UC results without considering any probabilistic information from the forecasting system and within reasonable computational times.

5.2 Contributions

The main contributions of the research presented in this thesis are:

- A novel and comprehensive mathematical model that combines RHC and two-stage recourse actions with a robust optimization framework is proposed. This architecture utilizes an RUC model within a two-stage decision making process appropriate for EMS development, yielding the least-cost dispatch while complying with uncertainty and ESS management requirements. The improvement in the results with respect to a deterministic case are obtained without requiring probabilistic information from the forecast.

- New master- sub-problem models to solve the RUC problem using a primal cutting-planes algorithm are presented. The models are formulated as MILP problems, enabling the application of RO to hedge the EMS while maintaining processing times that allow the implementation in the real-time operation of isolated microgrids.

- A suitable and novel framework for the sizing of the uncertainty set according to the historical performance of the forecasting system is proposed and tested. This practical approach provides the decision maker with a coherent approach to manage the level of conservatism of the RUC model in a comprehensive fashion.

- A comprehensive comparison between the SO- and RO-based approaches to hedge the isolated microgrid against uncertainty is presented and discussed. The comparative analysis was performed within proper theoretical and practical frameworks

demonstrating the adequacy of the RUC to make the system immune to uncertainty without requiring detailed scenario representations.

5.3 Future Work

Possible areas of future research are the following:

- Further testing of the algorithm for longer operation periods, e.g., a year of operation. This testing will allow to make better comparisons between the RUC and SUC models.
- The actual implementation of the proposed microgrid EMS architecture in a realistic test bed in order to test the feasibility and capabilities of the algorithm, computational performance, and determine the hardware and software requirements.
- A more detailed modeling of the ESS must be explored; some of the computational challenges in the the problem formulation can be overcome by using a better model of the recourse constraints.
- Extend the formulation and tests combining different sources of uncertainty such as solar powered DERs and loads, including mathematical formulations to relate the different sources in order to avoid over-conservatism.
- Enhance the proposed EMS to include more resources in the recourse model such as demand response mechanisms.

APPENDIX

System Data

Table 1: Cost Functions, Start-up and Shut-down Costs of Generators.

Unit No.	a $[US\$/kWh^2]$	b $[US\$/kWh]$	c $[US\$]$	C_{Sup} $[US\$]$	C_{Sdn} $[US\$]$
1	0	0.2781	7.5	15	5.3
2	0	0.2876	0	7.35	1.44
3	0.00001	0.224	45.5	95	15.3
17	0	0.053	3.1	3	0.5

*Cost functions are based on a diesel price of US$3.78/gal and a gas price of US$5/MBTu

Table 2: Transformers Parameters.

TF No	Node from-to	X [pu]	*Type*	V from [kV]	V to [kV]	S_{rated} [kVA]
1	14-1	0.05	$\Delta - Y_g$	0.48	12.47	5,000
2	15-9	0.05	$\Delta - Y_g$	0.48	12.47	500
3	16-7	0.05	$\Delta - Y_g$	0.48	12.47	700

Table 3: Line Parameters.

Line No	Node from-to	R_{ph} [Ω]	X_{ph} [Ω]	B_{ph} [μS]	R_0 [Ω]	X_0 [Ω]	B_0 [μS]
1	1-2	0.208	0.518	4.596	0.421	2.160	1.884
2	2-3	0.173	0.432	3.830	0.351	1.800	1.570
3	3-4	0.106	0.264	2.336	0.214	1.098	0.958
4	4-5	0.097	0.242	2.145	0.197	1.008	0.879
5	5-6	0.266	0.665	5.898	0.541	2.772	2.418
6	6-7	0.042	0.104	0.919	0.084	0.432	0.377
7	7-8	0.289	0.721	6.396	0.586	3.006	2.622
8	8-9	0.055	0.138	1.226	0.112	0.576	0.502
9	9-10	0.133	0.333	2.949	0.270	1.386	1.209
10	10-11	0.057	0.143	1.264	0.116	0.594	0.518
11	11-4	0.085	0.212	1.877	0.172	0.882	0.769
12	3-8	0.225	0.562	4.979	0.456	2.340	2.041
13	1-12	0.846	2.112	18.729	1.716	8.802	7.677
14	12-13	0.517	1.292	11.452	1.049	5.382	4.694
15	13-8	0.346	0.864	7.660	0.702	3.600	3.140

Table 4: Load Parameters.

Node	Apparent Power [kVA]						Power Factor	
	Phase A		Phase B		Phase C			
	Res	Com	Res	Com	Res	Com	Res	Com
1	344.00	80.00	172.00	180.00	200.00	180.00	0.90	0.80
2	100.00	200.00	50.00	200.00	0.00	200.00	0.95	0.85
3	0.00	80.00	200.00	80.00	50.00	80.00	0.90	0.80
4	200.00	0.00	100.00	0.00	100.00	0.00	0.90	1.00
5	200.00	50.00	172.00	200.00	0.00	50.00	0.95	0.85
6	50.00	0.00	100.00	0.00	172.00	0.00	0.95	1.00
7	0.00	100.00	100.00	100.00	0.00	100.00	0.95	0.95
8	100.00	0.00	150.00	0.00	0.00	200.00	0.90	0.90
9	100.00	0.00	150.00	0.00	100.00	0.00	0.95	1.00
10	150.00	0.00	100.00	0.00	250.00	0.00	0.90	1.00
11	50.00	150.00	50.00	150.00	0.00	150.00	0.95	0.85
12	0.00	145.00	0.00	145.00	0.00	145.00	0.95	0.85
13	0.00	90.00	0.00	90.00	172.00	90.00	0.90	0.90

Table 5: Directly-Connected Synchronous Generators Parameters.

Unit No.	S_{base} [kVA]	V_{base} [kV]	P_{max} [kW]	P_{min} [kW]	x_d [pu]	x''_d [pu]	x''_q [pu]	x_0 [pu]
1	1000	0.48	800	350	3.05	0.134	0.153	0.051
2	390	0.48	310	60	3.5	0.142	0.166	0.038
3	2000	0.48	1750	1000	3.05	0.134	0.153	0.051

Table 6: Inverter-interfaced DERs Parameters.

	DER				Inverter		
Unit No.	P_{max} [kW]	P_{min} [kW]	η_{in} [%]	η_{out} [%]	S_{max} [kVA]	η @ P_{max} [%]	η @ 20%P_{max} [%]
4	20	0	-	-	250	91%	95%
5	20	0	-	-	250	91%	95%
6	30	0	-	-	375	91%	95%
7	500	-500	96%	96%	625	91%	95%
8	30	0	-	-	38	91%	95%
9	50	-50	85%	85%	63	91%	95%
10	30	0	-	-	38	91%	95%
11	100	-100	95%	95%	63	91%	95%
12	30	0	-	-	38	91%	95%
13	40	0	-	-	50	91%	95%
14	50	-50	80%	80%	63	91%	95%
15	50	-50	87%	87%	63	91%	95%
16	40	0	-	-	50	91%	95%
17	500	100	-	-	625	91%	95%
18	1000	0	-	-	1250	91%	95%

Table 7: Directly-connected SCIG Parameters.

Unit No.	S_{base} [kVA]	V_{base} [kV]	P_{max} [kW]	P_{min} [kW]	r_s [pu]	x_s [pu]	r'_r [pu]	x'_r [pu]	x_m [pu]
19	190	0.48	150	0	0.007	0.15	0.0072	0.15	2.95
20	190	0.48	150	0	0.007	0.15	0.0072	0.15	2.95
21	190	0.48	150	0	0.007	0.15	0.0072	0.15	2.95

Table 8: Ramping Limits and Minimum Up-, Down-times.

Unit No.	R_{up} [kW/min]	R_{dn} [kW/min]	M_{up} [hr]	M_{dn} [hr]
1	16	16	2	1
2	6.2	6.2	3	2
3	28	28	2	1
4	50	50	3	2
5	4	4	0	0
6	4	4	0	0
7	6	6	0	0
8	120	120	0	0
9	6.6	6.6	1	1
10	6	6	1	1
11	6	6	0	0
12	10	10	1	1
13	6	6	0	0
14	40	40	1	1
15	6	6	0	0
16	42.4	42.4	1	1
17	8	8	0	0
18	40	40	0	0
19	2.8	2.8	1	1
20	2	2	0	0
21	10	10	2	2
22	200	200	0	0
23	30	30	0	0
24	30	30	0	0
25	30	30	0	0

References

[1] H. Farhangi, "The path of the smart grid," *IEEE Power and Energy Magazine*, vol. 8, no. 1, pp. 18–28, January 2010.

[2] IEA, "World energy outlook 2013," Tech. Rep. [Online]. Available: http://www.oecd-ilibrary.org/energy/world-energy-outlook_20725302

[3] T. Mohn, "It takes a village: Rural electrification in east africa," *IEEE Power and Energy Magazine*, vol. 11, no. 4, pp. 46–51, July 2013.

[4] R. Panora, J. Gehret, M. Furse, and R. Lasseter, "Real-world performance of a certs microgrid in manhattan," *IEEE Trans. on Sustainable Energy*, vol. PP, no. 99, pp. 1–1, 2014.

[5] S. Van Broekhoven, N. Judson, S. Nguyen, and W. Ross, "Microgrid study: Energy security for dod installations," No. MIT-LL-TR-1164. MIT Lexington Lincoln Laboratory, Tech. Rep., 2012.

[6] M. Arriaga, C. Canizares, and M. Kazerani, "Renewable energy alternatives for remote communities in northern Ontario, Canada," *IEEE Trans. on Sustainable Energy*, vol. 4, no. 3, pp. 661–670, July 2013.

[7] G. Mendes, J. Von Appen, and C. Ioakimidis, "Integrated energy microgrids for community-scale systems: Case study research in the azores islands," in *8th International Conference on the European Energy Market*, May 2011, pp. 382–387.

[8] D. Ton, W. Wang, and W. Wang, "Smart Grid R&D by the U.S. Department of Energy to optimize distribution grid operations," in *IEEE PES General Meeting*, July 2011, pp. 1–5.

[9] N. Hatziargyriou, H. Asano, R. Iravani, and C. Marnay, "Microgrids," *IEEE Power and Energy Magazine*, vol. 5, no. 4, pp. 78–94, 2007.

[10] IEEE PES TF in Microgrid Control, D. Olivares, A. Mehrizi-Sani, A. Etemadi, C. Canizares (Chair), R. Iravani, M. Kazerani, A. Hajimiragha, O. Gomis-Bellmunt, R. Saeedifard, M. Palma-Behnke (Secretary), A. Jimenez-Estevez, and N. Hatziargyriou, "Trends in microgrid control," *IEEE Trans. Smart Grid*, vol. 6, no. 4, pp. 1905–1919, July 2014.

[11] R. Hunter and G. Elliot, *Wind-diesel systems: a guide to the technology and its implementation*. Cambridge University Press, 1994.

[12] D. Olivares, C. Canizares, and M. Kazerani, "A centralized energy management system for isolated microgrids," *IEEE Trans. on Smart Grid*, vol. 5, no. 4, pp. 1864–1875, July 2014.

[13] C. Colson, M. Nehrir, and S. Pourmousavi, "Towards real-time microgrid power management using computational intelligence methods," in *IEEE Power and Energy Society General Meeting*, July 2010, pp. 1–8.

[14] S. Conti, R. Nicolosi, S. Rizzo, and H. Zeineldin, "Optimal dispatching of distributed generators and storage systems for mv islanded microgrids," *IEEE Trans. Power Delivery*, vol. 27, no. 3, pp. 1243–1251, 2012.

[15] A. Parisio and L. Glielmo, "A mixed integer linear formulation for microgrid economic scheduling," in *IEEE Int. Conf. Smart Grid Communications*, 2011, pp. 505–510.

[16] L. Xiaoping, D. Ming, H. Jianghong, H. Pingping, and P. Yali, "Dynamic economic dispatch for microgrids including battery energy storage," in *2nd IEEE Int. Symposium on Power Electronics for Distributed Generation Systems*, 2010, pp. 914–917.

[17] C. A. Hernandez-Aramburo, T. C. Green, and N. Mugniot, "Fuel consumption minimization of a microgrid," *IEEE Trans. Industry Applications*, vol. 41, no. 3, pp. 673–681, 2005.

[18] Z. Dinghuan, Y. Rui, and G. Hug-Glanzmann, "Managing microgrids with intermittent resources: A two-layer multi-step optimal control approach," in *North American Power Symposium*, Sept 2010, pp. 1–8.

[19] Q. Jiang, M. Xue, and G. Geng, "Energy management of microgrid in grid-connected and stand-alone modes," *IEEE Trans. Power Systems*, vol. 28, no. 3, pp. 3380–3389, 2013.

[20] P. Ruiz, C. Philbrick, E. Zak, K. Cheung, and P. Sauer, "Uncertainty management in the unit commitment problem," *IEEE Trans. Power Systems*, vol. 24, no. 2, pp. 642–651, 2009.

[21] Q. Wang, Y. Guan, and J. Wang, "A chance-constrained two-stage stochastic program for unit commitment with uncertain wind power output," *IEEE Trans. Power Systems*, vol. 27, no. 1, pp. 206–215, 2012.

[22] H. Zhang and P. Li, "Chance constrained programming for optimal power flow under uncertainty," *IEEE Trans. on Power Systems*, vol. 26, no. 4, pp. 2417–2424, Nov 2011.

[23] P. Pinson, "Wind energy: Forecasting challenges for its operational management," *Preprint Statistical Science*, 2013.

[24] J. Birge and F. Louveaux, *Introduction to Stochastic Programming*, 2nd ed., ser. Springer Series in Operations Research and Financial Engineering. Springer Verlag, 2011.

[25] S. Takayuki and J. Birge, "Stochastic unit commitment problem," *Int. Trans. in Operational Research*, vol. 11, no. 1, pp. 19–32, 2004.

[26] A. Papavasiliou, S. Oren, and R. O'Neill, "Reserve requirements for wind power integration: A scenario-based stochastic programming framework," *IEEE Trans. Power Systems*, vol. 26, no. 4, pp. 2197–2206, 2011.

[27] F. Bouffard and F. Galiana, "Stochastic security for operations planning with significant wind power generation," *IEEE Trans. Power Systems*, vol. 23, no. 2, pp. 306–316, 2008.

[28] M. Parvania and M. Fotuhi-Firuzabad, "Demand response scheduling by stochastic SCUC," *IEEE Trans. on Smart Grid*, vol. 1, no. 1, pp. 89–98, June 2010.

[29] L. Wu, M. Shahidehpour, and T. Li, "Stochastic security-constrained unit commitment," *IEEE Trans. Power Systems*, vol. 22, no. 2, pp. 800–811, 2007.

[30] C. C. Caroe and R. Schultz, "A two-stage stochastic program for unit commitment under uncertainty in a hydro-thermal power system," in *Report SC 98-11, Konrad-Zuse-Zentrum fur Informationstechnik*, 1998, pp. 98–113.

[31] P. Xiong and P. Jirutitijaroen, "A stochastic optimization formulation of unit commitment with reliability constraints," *IEEE Trans. on Smart Grid*, vol. 4, no. 4, pp. 2200–2208, Dec 2013.

[32] P. Pinson, H. Madsen, H. A. Nielsen, G. Papaefthymiou, and B. Klöckl, "From probabilistic forecasts to statistical scenarios of short-term wind power production," *Wind Energy*, vol. 12, no. 1, pp. 51–62, 2009.

[33] A. Papavasiliou and S. Oren, "A comparative study of stochastic unit commitment and security-constrained unit commitment using high performance computing," in *European Control Conference*, July 2013, pp. 2507–2512.

[34] A. Nemirovski, "Lectures on robust convex optimization," *class notes, Georgia Inst. of Technol., Fall*, 2009.

[35] D. Bertsimas, E. Litvinov, X. Sun, J. Zhao, and T. Zheng, "Adaptive robust optimization for the security constrained unit commitment problem," *IEEE Trans. Power Systems*, vol. 28, no. 1, pp. 52–63, 2013.

[36] C. Zhao, J. Wang, J. Watson, and Y. Guan, "Multi-stage robust unit commitment considering wind and demand response uncertainties," *IEEE Trans. Power Systems*, vol. PP, no. 99, pp. 1–10, 2013.

[37] R. Jiang, J. Wang, M. Zhang, and Y. Guan, "Two-stage minimax regret robust unit commitment," *IEEE Trans. on Power Systems*, vol. 28, no. 3, pp. 2271–2282, Aug 2013.

[38] Q. Wang, J. Watson, and Y. Guan, "Two-stage robust optimization for N-k contingency-constrained unit commitment," *IEEE Trans. on Power Systems*, vol. 28, no. 3, pp. 2366–2375, Aug 2013.

[39] L. Baringo and A. J. Conejo, "Offering strategy via robust optimization," *IEEE Trans. on Power Systems*, vol. 26, no. 3, pp. 1418–1425, August 2011.

[40] J. Morales, A. J. Conejo, P. Madsen, H. Pinson, and M. Zugno, *Integrating Renewables in Electricity Markets*, 1st ed., ser. Springer International Series in Operations Research & Management Science. Springer US, 2014, vol. 205.

[41] A. Thiele, T. Terry, and M. Epelman, "Robust linear optimization with recourse," *Rapport technique*, pp. 4–37, 2010.

[42] J. Ma, F. Yang, Z. Zhao Li, and S. Qin, "A renewable energy integration application in a microgrid based on model predictive control," in *IEEE PES General Meeting*, July 2012, pp. 1–6.

[43] R. Palma-Behnke, C. Benavides, F. Lanas, B. Severino, L. Reyes, J. Llanos, and D. Saez, "A microgrid energy management system based on the rolling horizon strategy," *IEEE Trans. Smart Grid*, vol. 4, no. 2, pp. 996–1006, 2013.

[44] P. Varaiya, F. Wu, and J. Bialek, "Smart operation of smart grid: Risk-limiting dispatch," *Proceedings of the IEEE*, vol. 99, no. 1, pp. 40–57, Jan 2011.

[45] Y. Zhang, N. Gatsis, V. Kekatos, and G. B. Giannakis, "Risk-aware management of distributed energy resources," in *18th Int. Conference on Digital Signal Processing*, July 2013, pp. 1–5.

[46] B. Zhao, Y. Shi, X. Dong, W. Luan, and J. Bornemann, "Short-term operation scheduling in renewable-powered microgrids: A duality-based approach," *IEEE Trans. on Sustainable Energy*, vol. 5, no. 1, pp. 209–217, Jan 2014.

[47] A. Hooshmand, M. Poursaeidi, J. Mohammadpour, H. Malki, and K. Grigoriads, "Stochastic model predictive control method for microgrid management," in *IEEE PES Innovative Smart Grid Technologies*, Jan 2012, pp. 1–7.

[48] H. Bludszuweit, J. Dominguez-Navarro, and A. Llombart, "Statistical analysis of wind power forecast error," *IEEE Trans. on Power Systems*, vol. 23, no. 3, pp. 983–991, Aug 2008.

[49] Z.-S. Zhang, Y.-Z. Sun, D. Gao, J. Lin, and L. Cheng, "A versatile probability distribution model for wind power forecast errors and its application in economic dispatch," *IEEE Trans. on Power Systems*, vol. 28, no. 3, pp. 3114–3125, Aug 2013.

[50] W. Su, J. Wang, and J. Roh, "Stochastic energy scheduling in microgrids with intermittent renewable energy resources," *IEEE Trans. on Smart Grid*, vol. PP, no. 99, pp. 1–9, 2013.

[51] D. Olivares, J. Lara, C. Canizares, and M. Kazerani, "Stochastic-predictive energy management system for isolated microgrids," *Submitted to IEEE Trans. Smart Grid*, pp. 1–8, May 2014.

[52] A. A. Thatte, L. Xie, D. E. Viassolo, and S. Singh, "Risk measure based robust bidding strategy for arbitrage using a wind farm and energy storage," *IEEE Trans. on Smart Grid*, vol. 4, no. 4, pp. 2191–2199, Dec 2013.

[53] W. Wu, J. Chen, B. Zhang, and H. Sun, "A robust wind power optimization method for look-ahead power dispatch," *IEEE Trans. on Sustainable Energy*, vol. 5, no. 2, pp. 507–515, April 2014.

[54] M. Burger, G. Notarstefano, and F. Allgower, "A polyhedral approximation framework for convex and robust distributed optimization," *IEEE Trans. on Automatic Control*, vol. 59, no. 2, pp. 384–395, Feb 2014.

[55] Y. Zhang, N. Gatsis, and G. B. Giannakis, "Robust energy management for microgrids with high-penetration renewables," *IEEE Trans. on Sustainable Energy*, vol. 4, no. 4, pp. 944–953, Oct 2013.

[56] A. H. Hajimiragha and M. R. D. Zadeh, "Research and development of a microgrid control and monitoring system for the remote community of bella coola: Challenges, solutions, achievements and lessons learned," in *IEEE International Conference on Smart Energy Grid Engineering*. IEEE, 2013, pp. 1–6.

[57] E. Planas, A. Gil-de Muro, J. Andreu, I. Kortabarria, and I. Martínez de Alegría, "General aspects, hierarchical controls and droop methods in microgrids: A review," *Renewable and Sustainable Energy Reviews*, vol. 17, no. 0, pp. 147 – 159, 2013.

[58] A. Bidram and A. Davoudi, "Hierarchical structure of microgrids control system," *IEEE Trans. on Smart Grid*, vol. 3, no. 4, pp. 1963–1976, Dec 2012.

[59] J. Jimeno, J. Anduaga, J. Oyarzabal, and A. G. de Muro, "Architecture of a microgrid energy management system," *European Transactions on Electrical Power*, vol. 21, no. 2, pp. 1142–1158, 2011.

[60] J. Pecas Lopes, C. Moreira, and A. Madureira, "Defining control strategies for microgrids islanded operation," *IEEE Trans. Power Systems*, vol. 21, no. 2, pp. 916–924, 2006.

[61] F. Katiraei and C. Abbey, "Diesel plant sizing and performance analysis of a remote wind-diesel microgrid," in *IEEE Power Engineering Society General Meeting*, June 2007, pp. 1–8.

[62] B. Lasseter, "Microgrids [distributed power generation]," in *Proc. IEEE-PES Winter Meeting*, vol. 1, Jan. 2001, pp. 146 –149.

[63] B. Zhao, X. Zhang, J. Chen, C. Wang, and L. Guo, "Operation optimization of standalone microgrids considering lifetime characteristics of battery energy storage system," *IEEE Trans. on Sustainable Energy*, vol. 4, no. 4, pp. 934–943, Oct 2013.

[64] M. Korpas and A. Holen, "Operation planning of hydrogen storage connected to wind power operating in a power market," *IEEE Trans. Energy Conversion*, vol. 21, no. 3, pp. 742 –749, Sept. 2006.

[65] J. Mattingley, Y. Wang, and S. Boyd, "Receding horizon control," *IEEE Control Systems Magazine*, vol. 31, no. 3, pp. 52–65, June 2011.

[66] F. Allgower, R. Findeisen, and Z. K. Nagy, "Nonlinear model predictive control: From theory to application," *Journal-Chinese Institute of Chemical Engineers*, vol. 35, no. 3, pp. 299 – 315, 2004.

[67] G. B. Dantzig, "Linear programming under uncertainty," *Management science*, vol. 1, no. 3-4, pp. 197–206, 1955.

[68] J. Higle, "Stochastic programming: Optimization when uncertainty matters," *Tutorials in Operations Research INFORMS*, pp. 30–53, 2005.

[69] J. R. Birge, "The value of the stochastic solution in stochastic linear programs with fixed recourse," *Mathematical programming*, vol. 24, no. 1, pp. 314–325, 1982.

[70] K. Høyland and S. W. Wallace, "Generating scenario trees for multistage decision problems," *Management Science*, vol. 47, no. 2, pp. 295–307, 2001.

[71] J. L. Higle and S. Sen, "Stochastic decomposition: An algorithm for two-stage linear programs with recourse," *Mathematics of Operations Research*, vol. 16, no. 3, pp. 650–669, 1991.

[72] P. Kall and J. Mayer, *Stochastic Linear Programming Models, Theory, and Computation*, ser. International Series in Operations Research and Management Science. Springer Verlag, 2011, vol. 156.

[73] A. L. Soyster, "Convex programming with set-inclusive constraints and applications to inexact linear programming," *Operations research*, vol. 21, no. 5, pp. 1154–1157, 1973.

[74] A. Ben-Tal, L. El Ghaoui, and A. Nemirovski, *Robust optimization*. Princeton University Press, 2009.

[75] D. Bertsimas and M. Sim, "The price of robustness," *Operations research*, vol. 52, no. 1, pp. 35–53, 2004.

[76] Z. Bo and Z. Long, "Solving two-stage robust optimization problems using a column-and-constraint generation method," *Operations Research Letters*, vol. 41, no. 5, pp. 457 – 461, 2013.

[77] A. Ben-Tal, A. Goryashko, E. Guslitzer, and A. Nemirovski, "Adjustable robust solutions of uncertain linear programs," *Mathematical Programming*, vol. 99, no. 2, pp. 351–376, 2004.

[78] A. Ben-Tal, D. Den Hertog, A. De Waegenaere, B. Melenberg, and G. Rennen, "Robust solutions of optimization problems affected by uncertain probabilities," *Management Science*, vol. 59, no. 2, pp. 341–357, 2013.

[79] M. Zugno and A. J. Conejo, "A robust optimization approach to energy and reserve dispatch in electricity markets," Tech. Rep., 2013.

[80] A. M. Geoffrion, "Generalized benders decomposition," *Journal of optimization theory and applications*, vol. 10, no. 4, pp. 237–260, 1972.

[81] G. B. Dantzig and P. Wolfe, "Decomposition principle for linear programs," *Operations research*, vol. 8, no. 1, pp. 101–111, 1960.

[82] A. J. Conejo, E. Castillo, R. Minguez, and R. Garcia-Bertrand, *Decomposition Techniques in Mathematical Programming: Engineering and Science Applications*. Springer, 2006.

[83] Z. Long and Z. Bo, "Robust unit commitment problem with demand response and wind energy," in *IEEE PES General Meeting*, July 2012, pp. 1–8.

[84] J. E. Kelley, "The cutting-plane method for solving convex programs," *Journal of the Society for Industrial & Applied Mathematics*, vol. 8, no. 4, pp. 703–712, 1960.

[85] D. Bertsimas and J. N. Tsitsiklis, *Introduction to linear optimization*. Athena Scientific Belmont, MA, 1997.

[86] S. A. Gabriel, A. J. Conejo, J. D. Fuller, B. F. Hobbs, and C. Ruiz, *Complementarity Modeling in Energy Markets*, ser. International Series in Operations Research & Management Science. Springer, 2012. [Online]. Available: http://books.google.com/books?id=Lu1L5wUea8IC

[87] J. Fortuny-Amat and B. McCarl, "A representation and economic interpretation of a two-level programming problem," *Journal of the operational Research Society*, vol. 32, no. 9, pp. 783–792, 1981.

[88] S. A. Gabriel and F. U. Leuthold, "Solving discretely-constrained MPEC problems with applications in electric power markets," *Energy Economics*, vol. 32, no. 1, pp. 3 – 14, 2010.

[89] S. Soman, H. Zareipour, O. Malik, and P. Mandal, "A review of wind power and wind speed forecasting methods with different time horizons," in *Proc. North American Power Symposium (NAPS)*, 2010, pp. 1–8.

[90] CIGRE Task Force C6.04, K. Strunz, E. Abbasi, C. Abbey, C. Andrieu, U. Annakkage, S. Barsali, R. Campbell, R. Fletcher, F. Gao, T. Gaunt, A. Gole, N. R. Hatziargyriou, R. Iravani, G. Joos, H. Konishi, M. Kuschke, E. Laverkvi, C. Liu, S. Mahseredjian, F. Mosallat, D. Muthumuni, A. Orths, S. Papathanassiou, K. Rudion, Z. Styczynski, and S. Verma, "Benchmark systems for network integration of renewable and distributed energy resources," *CIGRE Technical Report*, May 2013.

[91] CPLEX, IBM ILOG, "V12. 1: User's manual for cplex," *International Business Machines Corporation*, vol. 46, no. 53, p. 157, 2009.